Příloha A:

Svoboda J., Bláha M., Sedláček J., Vohlídal J., Balcar H., Mav-Golež I., Žigon M.: *New Approaches to the Synthesis of Pure Conjugated Polymers,* Acta Chimica Slovenica 53 (4): 407-416, **2006**.

Minireview

New Approaches to the Synthesis of Pure Conjugated Polymers

Jan Svoboda[1], Michal Bláha[1], Jan Sedláček[1], Jiří Vohlídal[1], Hynek Balcar[2], Ida Mav-Golež[3], Majda Žigon[3]

[1] *Department of Physical and Macromolecular Chemistry, Faculty of Science, Charles University, Hlavova 8/2030, CZ-128 40 Prague 2 – Albertov, Czech Republic, vohlidal@natur.cuni.cz*

[2] *J. Heyrovský Institute of Physical Chemistry, Academy of Sciences of the Czech Republic, Dolejškova 3, CZ-182 23, Prague 8, Czech Republic*

[3] *Laboratory for Polymer Chemistry and Technology, National Institute of Chemistry, Hajdrihova 19, POB 660, SI-1001 Ljubljana, Slovenia; ida.mav@ki.si*

Received 06-01-2006

Abstract

This short-review article is based on the lecture presented at the 13th Conference on Materials and Technology held in Portorož, October 10–12, 2005 and summarizes our recent results obtained in the investigation and development of polymerization methods aimed at the synthesis of high-purity conjugated polymers, polyacetylenes and polyanilines in particular. *Part 1. Introduction* provides a survey of main procedures currently used in synthesis of conjugated polymers; *Part 2. Catalytic chain polymerizations in two-phase systems* contains a brief information on the liquid-liquid systems but mainly it deals with a preparation of mesoporous polymerization catalysts and their use and effectivness in the synthesis of high-purity polyacetylenes. The catalyst systems obtained by anchoring of soluble, catalytically active transition-metal complexes on mesoporous supports such as polybenzimidazole beads, all-siliceous molecular sieves MCM 41, MCM 48, and SBA 15, and the sieves with inner pores modified by linkers with $-NH_2$, $-PPh_2$ and $-N(PPh_2)_2$ end groups are discussed as to their activity, stereoselectivity, re-use and transport limitations for guest macromolecules. *Part 3. Transformation of stoichiometric polymerizations to catalytic processes* mainly deals with the polymerization of aniline and its derivatives with the catalytic system Fe^{3+}/H_2O_2. Quality of polyanilines prepared by catalytic and stoichiometric procedures are compared and new results are presented, according to which both active species present in the reaction mixture, Fe^{3+} ions and $HO^{\bullet}$ radicals, participate in the overall mechanism, creating a synergic system. Concluding *Part 4. Conclusions, limitations and perspectives* provides a summary of results obtained including advances and limitations of these synthesis approaches and perspectives of their use and development.

Keywords: catalytic oxidative polymerization, coordination polymerization, conjugated polymers, functional polymers, hydrogen peroxide, immobilized catalysts, iron trichloride, mesoporous polymerization catalysts, mesoporous molecular sieves, metathesis, polyacetylenes, polyanilines, polybenzimidazole, polyvinylenes.

1. Introduction

For almost three decades, conjugated polymers and oligomers have been under intensive research and development as new functional materials for electronics, photonics, advanced coatings, and related applications.[1,2] Some conjugated polymers such as polypyrrole and polyaniline have already found practical applications in the construction of capacitors, analytical sensors, antistatic films and coatings, materials for electrostatic discharge protection, electrochromic windows, anticorrosion paints, etc. More advanced applications of conjugated polymers in the construction of electronic devices, photovoltaic cells and actuators are anticipated; the first all-polymeric printed circuits and displays have recently been presented. Neat conjugated polymers are insulators or semiconductors, which, however, become conductive upon partial oxidation or reduction, also referred to as doping; in the case of polyaniline, protonation (proton doping) is also necessary.[3] The doping processes allow the properties of these polymers to tune from insulators to metallic conductors.

The properties of conjugated polymers important for their application in electronics are remarkably sensitive to the presence of impurities, which might act as uncontrolled dopants, traps of charge carriers, quenchers of excited states, etc. Catalyst residues

and side-products from polymer synthesis are typical contaminants of conjugated polymers and are mostly removed by repeated precipitation or by adsorption to silica or alumina or other sorbents. Both of these techniques are time consuming, of limited efficiency and, to a great extent, empirical because the chemical structure of catalyst residues is often unknown. Production of high amounts of waste solvents is another important disadvantage of this approach. Therefore, the development of new preparation procedures giving pure conjugated polymers almost free of catalyst residues and other polymerization side products is highly desirable.

There are about six types of procedures used for the preparation of conjugated polymers:

1. **Homogeneous coordination polymerization (catalytic chain polymerization)** of the insertion or metathesis type, mainly used for syntheses of polyvinylenes (polyacetylenes), polyphenylenevinylenes and related polymers,[4] for example:

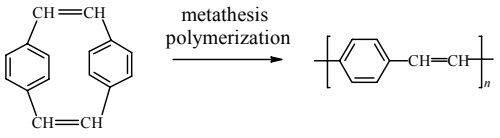

1(1,4),4(1,4)-dibenzena-cyclohexapha-2,5-diene — poly(1,4-phenylenevinylene)

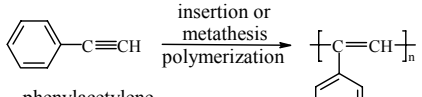

phenylacetylene — poly(phenylacetylene)

2. **Chemical (stoichiometric) polymerization**, typically an oxidation or dehalogenation polymerization,[3] in which a monomer or mixture of monomers react with the stoichiometric equivalent of a coupling agent giving the corresponding polymer and a high amount of side products. Chemical polymerization has already found applications in industrial production of polyanilines and polythiphenes, for example:

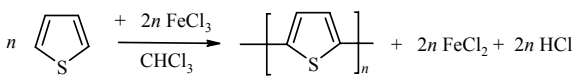

thiophene — polythiophene

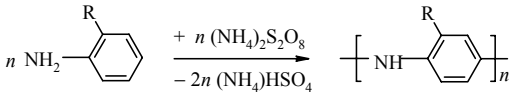

alkylaniline — polyalkylaniline

3. **Catalytic versions** of chemical polymerization, such as Suzuki-Miyaura, Heck and Sonogashira couplings, are frequently used to prepare polyaryleneethynylenes and fluorene polymers and copolymers.[5]

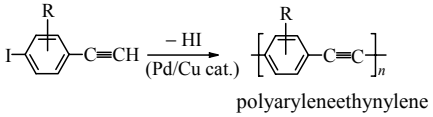

polyaryleneethynylene

Sonogashira coupling

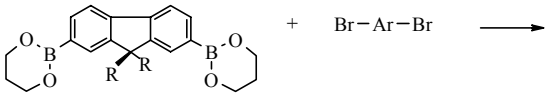

Suzuki - Miyaura coupling

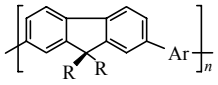

4. **Chemical transformation of a precursor polymer**, such as the transformation of poly{(5,6-bis(trifluoromethyl)bicyclo[2,2,2]octa-5,7-dienevinylene} to poly(vinylene), also known as "Durham polyacetylene" by the retro-Diels-Alder reaction (see, e.g., chapter 13 in ref.[4b]):

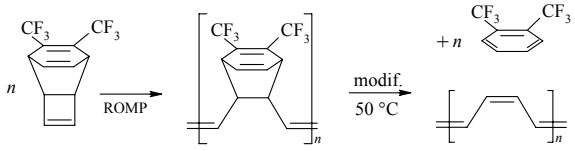

"Durham polyacetylene"

5. **Electrochemical polymerization** of monomers such as aniline, pyrrol or thiophene, yielding a conducting polymer film deposited on the anode material.[3] This method is useful for the preparation of conducting polymer films for electronic devices such as electro-analytical sensors composed of a receptor for a particular compound anchored on a conducting polymer film. On the other hand, electropolymerization is not regarded as a method suitable a the large-scale production of conducting polymers.

6. **Photochemical polymerization**, which is typically used for the polymerization of diacetylenes assembled in Langmuir-Blodget films[6], for example:

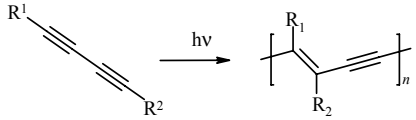

diacetylene — polydiacetylene

The first two preparative methods have the highest innovation potential:

- homogeneous chain polymerizations can be transformed into reactions in two phase systems, allowing easy and effective separation of the catalyst residues from the polymer formed;
- stoichiometric oxidative polymerizations can be transformed into catalytic processes yielding acceptable side products.

In this contribution, we present the state of the art and our own recent results obtained in these two fields.

2. Catalytic Chain Polymerizations in Two-Phase Systems

A homogeneous catalytic polymerization can be transformed into a two-phase process by: *(i)* dissolving the catalyst in a liquid of poor miscibility with both the polymer formed and the solvent in which the polymer is dissolved, or *(ii)* using heterogeneous polymerization catalysts, mostly originally homogeneous catalyst anchored on a solid support.

The first approach is usually accomplished by using an *ionic liquid* to form the catalytic phase of the system. To achieve an effective catalyst separation from the polymer phase, catalyst species should be ionic or ionizable and the polymer formed should be soluble in a non- or low-polarity solvent. These conditions are well fulfilled, e.g., in the polymerization of phenylacetylene and its derivatives with rhodium complexes.[7] The ionic liquid must be properly chosen since the polymerization activity of Rh catalysts is sensitive to the structure of both the cation and anion of the ionic liquid.

A use of *fluorocarbons* (perfluorinated hydrocarbons), which are immiscible with the majority of other solvents, represents another possibility of implementing two-phase polymerization processes of the liquid-liquid class. However, the use of fluorocarbons as solvents for the catalyst phase is much more complicated because only catalysts comprising highly fluorinated ligands are well soluble in fluorocarbons. This thermodynamic requirement makes this approach difficult since complexes bearing perfluorinated ligands are rather rare and knowledge about their catalytic activity is still quite poor.[8] In addition, fluorinated ligands are expensive, not easily available, and they must be selected carefully in order not to quench the activity of the catalyst.

Anchored catalysts. This approach consists in anchoring a homogeneous catalyst on a suitable organic or inorganic support that is easily separable from the polymer solution. Microporous supports widely used in chemical industry cannot be applied for these purposes because micropores (diameter up to ca 1.5 nm) are too narrow to allow the macromolecules formed to escape into the surrounding solution and make active species free for a formation of further macromolecules. This was clearly demonstrated in attempts to polymerize various acetylenes with H-zeolites and Co^{II} and Ni^{II} exchanged zeolites. Evidence of polymer formation was obtained from Raman spectra, however, the polymers formed remained caged in zeolites and attempts to isolate them by dissolving the supports in hydrofluoric acid were unsuccessful, yielding products of the polymer hydrolysis and hydrofluorination.[9]

The use of mesoporous (pore diameters up to ca 50 nm) or macroporous catalyst supports can eliminate the above-mentioned transport limitations because the nanopores are large enough to enable the formed polymer molecules to escape from the support into a surrounding solution by a reptation and/or diffusion. We used this approach in the synthesis of high-purity, stereoregular polymers of substituted acetylenes. Air-stable dinuclear Rh^{I}(diene) complexes, which are known to polymerize substituted acetylenes to *cis-transoid* polyacetylenes,[4] were anchored on mesoporous supports of two kinds: *(i)* mesoporous polybenzimidazole (PBI) beads[10a] with high population of pores of the diameter from 10 to 20 nm (ca. 650 m^2/g),[10b,c] and *(ii)* all-siliceous mesoporous molecular sieves with practically uniform pore diameter *d* differing in the pore architecture: MCM-41 (hexagonal pore packing, d = 3.4 nm), MCM-48 (cubic pore packing, d = 3.2 nm), SBA-15 (hexagonal pore packing, d = 6.8 nm).[11] So obtained catalysts were found to polymerize various substituted acetylenes (Scheme 1) and to exhibit the same, i.e., *cis-transoid* stereoselectivity as non anchored catalysts.

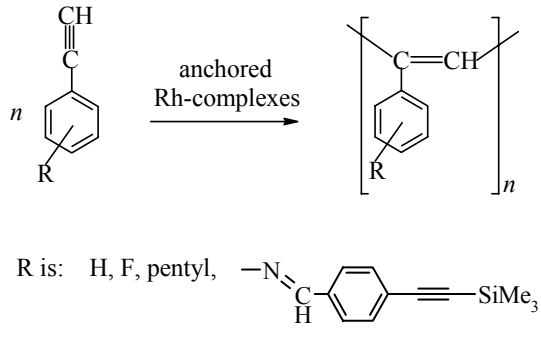

Scheme 1. Polymerizations studied with a use of anchored rhodium-based catalysts.

Preparation of mesoporous polymerization catalysts. Anchoring of Rh complexes was accomplished by the direct adsorption of the complexes from THF or CH_2Cl_2 solutions. Since Rh complexes are colored, a

course of anchoring can be easily monitored by UV/vis spectroscopy. In addition, the content of Rh in the resulting supported catalysts was determined by ICP mass spectrometry. The ICP MS method was also used to determine contamination of the prepared polymers with Rh residues as well as leaching of Rh species into the surrounding solution during the experiment (via analysis of the supernatant upon isolation of the polymer).

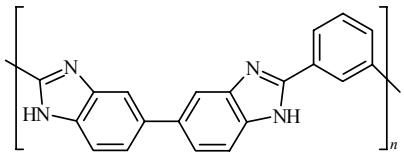

Scheme 2. Chemical structure of PBI beads

Commercially available catalytically active $[\{Rh(cod)\}_2(\mu\text{-}Cl)_2]$ and $[\{Rh(nbd)\}_2(\mu\text{-}Cl)_2]$ complexes (cod and nbd stand for η^2:η^2-coordinated cyclooctadiene and norbornadiene, respectively) are easily anchored onto neat mesoporous PBI beads; practically 100% anchoring is achieved at 3% loading (weight of Rh/weight of PBI).[10a] Analysis of the liquid phase remaining upon anchoring has shown that no compound is released into the liquid phase during the anchoring process. Consistently, the ESCA analysis of the supported catalyst has shown that chlorine atoms remain bound to the anchored Rh species. These observations indicate that, during anchoring, dinuclear Rh species are transformed into the mononuclear ones, which are then bound onto the support via the nitrogen groups of PBI. Rh complexes with μ-methoxo bridge ligands do not anchor onto PBI.

Molecular sieves exhibit anchoring behavior different from that of PBI. Commercially available μ-chloro Rh(diene) complexes do not anchor onto neat molecular sieves at all. On the other hand, rhodium μ-methoxo complex $[\{Rh(cod)\}_2(\mu\text{-}OMe)_2]$ is smoothly, practically totally anchored onto tested neat, all-siliceous mesoporous molecular sieves under the elimination of methanol to the liquid phase. This indicates that this anchoring proceeds via MeO – SiO ligand exchange.[11a]

In order to exploit easily available μ-chloro Rh complexes in designing new mesoporous catalysts, we modified inner pores of molecular sieves by reaction with compounds such as $(CH_3O)_3Si\text{-}(CH_2)_3\text{-}NH_2$, $(C_2H_5O)_3Si\text{-}(CH_2)_2\text{-}PPh_2$ and $(CH_3O)_3Si\text{-}(CH_2)_3\text{-}N(PPh_2)_2$. In this way we introduced ligands coordinating to Rh species onto pore walls. The pore modification proceeds under the liberation of the corresponding alcohol (methanol or ethanol) into the liquid phase, while the following catalyst anchoring proceeds without a release of any byproduct.[11b,c] Typical loading of the molecular-sieve-supported catalysts that we used in our experiments was 1%. It should be mentioned here that the alcohol liberation is not quantitative, most probably owing to the sorption of a part of formed alcohol on the support pores. Solid-state NMR analyses of the resulting hybrid catalysts show that, on average, 0.7 to 0.8 of OCH_3 groups per one linker molecule remain unreacted.[11c] This indicates the following structures of catalyst species formed by anchoring an Rh μ-chloro complex onto a modified molecular sieve:

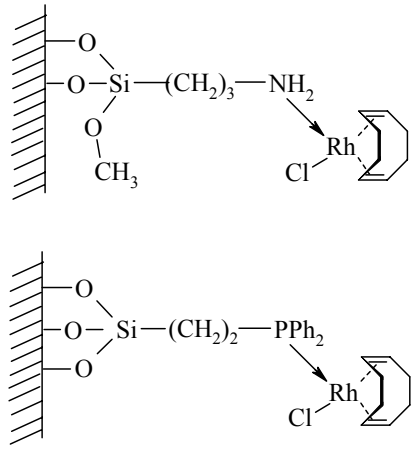

Scheme 3. Assumed structures of Rh catalysts with modified molecular-sieves supports.

Summary of results of polymerization experiments. The polymerizations of substituted acetylenes (phenylacetylene and its 4-pentyl-, 2-fluoro-, 4-fluoro- and 4-($Me_3Si\text{-}C{\equiv}C\text{-}C_6H_4CH{=}N$-) derivatives) to readily isolable *cis-transoid* polyvinylenes were performed in batch reactors. The course of the reaction was monitored by size exclusion chromatography (SEC) of the liquid phase sampled from the reaction mixture upon short centrifugation. Catalyst leaching was monitored by the mass-spectrometry (ICP-MS) analysis of both the used supported catalyst and the isolated polymer (obtained by pouring a centrifuged reaction mixture into a twenty-fold excess of methanol). The supernatant from the polymer isolation was also analyzed for rhodium content. In addition, experiments were done to examine whether the polymerization really proceeds in the catalyst pores and does not proceed in the liquid phase: an already reacting polymerization mixture was, upon short centrifugation, split into two parts of equal volume – that containing all the supported catalyst and that free of the supported catalyst. The further course of polymerization in both mixtures was then monitored. Typically, polymerization continued in the system with the supported catalyst only, which proves that the reaction takes only part in the supported-catalyst species. Exceptionally, the polymerization also took place in the system without supported catalyst, which points to leaching of active species from the heterogeneous catalyst.

Rh(cod) complexes immobilized on mesoporous PBI, non-modified molecular sieves, and molecular sieves modified with $(CH_3O)_3Si$-$(CH_2)_3$-NH_2 spacers exhibit good polymerization activity and provide high-*cis-transoid* polyacetylenes, same as the corresponding complexes used as homogeneous catalysts.[11] This proves that anchoring does not alter the product stereoselectivity of rhodium catalysts. The polymers formed, including that with 4-(Me_3Si-C≡C-C_6H_4CH=N-) ring substituents, are continuously released from the hybrid catalyst to the surrounding solvent, which allows easy polymer separation from the catalyst. Molecular weight of so prepared polymer ($<M>_w$ typically ranges from $1 \cdot 10^5$ to $3 \cdot 10^5$) is equal to or higher than that of the corresponding polymer prepared homogeneously. According to molecular dimensions recently determined[12a] for poly(phenylacetylene) and calculated[12b] for polyvinylene chains of various configurations, diameters of macromolecules formed exceed diameter of the host mesoporous channels mainly in the case of catalysts supported on the MCM-41 and MCM-48 molecular sieves (free-pore diameter 3.4 and 3.2 nm, respectively). This shows that the reptation mode (snake-like movement) plays important role in releasing macromolecules from pores.

The immobilized catalysts give high-purity neat polymers containing from 0.00002 to 0.0001 wt.% of Rh, which represents 0.002 – 0.015% of the catalyst used. Reference polymers prepared by corresponding homogeneous processes under comparable conditions contain from 0.01 – 0.1 wt.% of Rh (1 – 15% of the catalyst used). This means that the transformation of homogeneous processes to heterogeneous ones brings about thousand-fold reduction in the neat polymer contamination with catalyst residues. In addition, a formation of oligomers, typical side products of the polymerization of substituted acetylenes with rhodium catalysts, is also significantly reduced although not completely eliminated on anchored catalysts (vide infra).

Unlike the preceding systems, Rh(cod) complexes anchored on molecular sieves modified with $(C_2H_5O)_3Si$-$(CH_2)_2$-PPh_2 do not provide effective polymerization catalysts, most probably owing to too high concentration of -PPh_2 groups in the vicinity of the active sites. Namely, it is known that triaryl phosphines help to control homogeneous polymerization processes induced with Rh catalysts if they are applied in the equimolar amount with respect to the catalyst, and that they disturb the polymerization when used in higher amounts.[4e, 13] The phosphine-linker-anchored Rh catalysts can be activated towards polymerization by organic amines, which, however, also promote significant leaching of anchored rhodium species to the solvent phase, so counteracting the target intended by the catalyst anchoring.

The above-described successful results obtained with anchored Rh(cod) complexes have not been achieved with anchored Rh(nbd) complexes. Surprisingly, the last gave considerably lower polymer yields although the parent Rh(nbd) complexes, when applied as homogeneous catalysts, show higher activity than the corresponding Rh(cod) ones. This might be explained in two ways. First, Rh(nbd) complexes are known to induce, under proper conditions, living stereoregular polymerization of substituted acetylenes,[13] in which kinetic-chain transfer is practically absent. Therefore, it can happen that the polymer chains formed on the anchored Rh(nbd) catalysts remain bound to active polymerization centers and thus cannot be released from the catalyst pores into the surrounding solution. However, in our experiments, we did not use reaction conditions needed for living polymerization. Another explanation consists in a formation of insoluble, so called columnar forms of polyphenylacetylenes inside pores.[14a,b] Molecules of substituted polyacetylenes behave as random coils in solutions,[12] however, if practically stereoregular, *cis-transoid* macromolecules are rapidly formed in a restricted volume element inside pores and they do not have time to undergo a partial isomerization,[14c] a formation of insoluble forms can be promoted.

Another key point of the development of heterogeneous polymerization catalysts is obtaining robust, recyclable catalysts for environmentally friendly and economical processes. Unfortunately, the new catalysts developed so far show a slow but continuous decrease in polymerization activity when used repeatedly.[10,11] The ESCA method has revealed a change in the chemical structure of anchored Rh species upon polymerization,[11] interpretation of which, however, is still uncertain.

Mesoporous molecular sieves MCM-41 have also been used as a support for anchoring Mo Schrock carbene complexes Mo(=$CHCMe_2Ph$)(=N-2,6-*i*-$Pr_2C_6H_3$)$(OR)_2$, where OR = $OCMe_3$ or $OCMe(CF_3)_2$, via a ligand exchange reaction with OH groups of MCM-41 by the elimination of the corresponding alcohol.[15a] The Mo/MCM-41 heterogeneous metathesis catalysts were found active in ROMP of cyclooctene and norbornene, as well as in metatheses of alkenes and cross-metatheses of alkenes and cycloalkenes. In the case of ROMP of cycloalkenes, chain transfer agents such as hept-1-ene or hexen-5-yl acetate can efficiently regulate the polymer molecular weight. The catalyst was found to be Mo-leaching resistant and to keep its activity unchanged upon addition of a new dose of substrate. However, a decrease in the catalytic activity was observed upon catalyst recycling, which should be ascribed to contaminants entering pores during this operation. Nevertheless, the results obtained show that such a catalyst can be effectively used for the preparation of pure soluble polymers by metathesis polymerization as well as for other metathesis reactions. Ruthenium-based mesoporous catalysts prepared by other authors showed better stability.[15b]

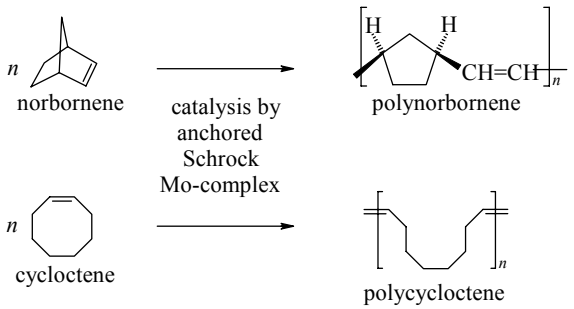

Scheme 4. Metathesis polymerizations studied with a use of anchored Schrock complexes.

3. Transformation of Chemical Polymerizations to Catalytic Processes

The replacement of chemical polymerization by a catalytic process is of potential importance mainly in the case of oxidative polymerization of anilines, pyrroles, and thiophenes, since this approach can considerably reduce contamination of neat polymers. Polyaniline (PANI) and its derivatives are routinely prepared by the stoichiometric oxidative polymerization of aniline (ANI), which gives a high amount of side products.[3] The most frequently used oxidant for polymerization of ANIs is ammonium peroxodisulphate, which is transformed into ammonium hydrogensulphate. Although this side product does not deteriorate properties of formed PANIs, its removal from neat PANI represents about half of cost of this product.[3a] We currently use this oxidant in our research of homo- and co-polymerization of various anilines carried out in the last years, in particular 2- and 3-aminobenzenesulfonic acids,[16a-f] 2-methoxyaniline,[16c-g] and 2- and 3-aminobenzoic acids.[16e,f] Nevertheless, it is clear that a replacement of the stoichiometric process by the catalytic one should bring about substantial improvement in the production of polyanilines and related polymers. Such process can be based on catalytic oxidation, in which the main inorganic oxidant is present in a catalytic amount and is continuously re-oxidized by a supporting oxidant such as molecular oxygen or ozone or hydrogen peroxide which itself is ultimately transformed into water during the polymerization, as depicted below for a system with H_2O_2 as supporting oxidant (Scheme 5).

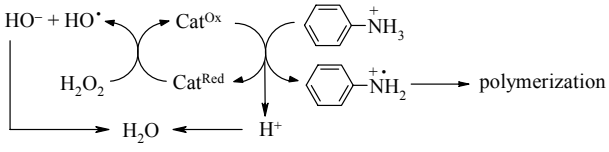

Scheme 5. Assumed catalytic cycle for a catalytic oxidative polymerization of ANI with a use of H_2O_2.

ANI has already been polymerized catalytically with (i) Cu^{2+}/O_2[3a] and Fe^{3+}/ozone[3a, 17] systems, which both show rather low polymerization activity, (ii) enzyme-based systems H_2O_2/peroxidase[18], which is too expensive, and (iii) Fe^{3+}/H_2O_2 and Ru^{3+}/H_2O_2 systems[19]. So far, the best results have been obtained using the Fe^{3+}/H_2O_2 system, which has been used in polymerizations of aniline and its 2-ethyl and 2-propyl derivatives[19] to yield the corresponding polyanilines even at an Fe/aniline molar ratio of 1:500 (this ratio should be 2.5 when the half-oxidized form of polyaniline, so-called emeraldine form, is synthesized by stoichiometric chemical polymerization). Sun et al.[19c,d] have observed that the polymerization of aniline could also be induced by hydrogen peroxide alone at temperatures above 60 °C. Hence they proposed that, in the Fe^{3+}/H_2O_2 system, iron ions induce decomposition of H_2O_2 into $HO^\bullet$ radicals, which indeed polymerize ANI. However, there are still other possible mechanisms of this reaction: (i) ANI might be polymerized with Fe^{3+} ions and the formed Fe^{2+} ions reoxidized by H_2O_2 (Scheme 3), or (ii) both reaction modes can take part in the overall reaction (vide infra).

To obtain a better insight into this reaction system, we have examined activity of the $FeCl_3/H_2O_2$ and $CuCl_2/H_2O_2$ systems in the polymerization of ANI, 2-methoxyaniline (OMA), and 2-chloroaniline (CANI). We found that the $FeCl_3/H_2O_2$ system applied in aqueous HCl (1 M) smoothly polymerizes all studied monomers at room temperature as well as at 5 °C giving high isolated polymer yields (70 - 90%) comparable to those obtained by the stoichiometric process even at an $FeCl_3$/aniline molar ratio of 1 : 1 000. On the other hand, the $CuCl_2/H_2O_2$ system, which also decomposes H_2O_2 to $HO^\bullet$ radicals, as well as H_2O_2 by itself, is practically inactive at room temperature. This clearly indicates that the presence of Fe^{3+} species in the reaction mixture is essential for the oxidative polymerization of aniline and aniline derivatives, i.e., that Fe^{3+} ions are key oxidants in this process.

Although results of catalytic polymerization experiments are very promising, quality of so prepared polymers is lower than that of polyanilines prepared by stoichiometric processes. Typical UV/vis spectra of PANIs prepared using various oxidation systems (Fig. 1) show that the $FeCl_3/H_2O_2$ system polymerizes ANI and CANI to the emeraldine forms, which, however, show lower intensity of the Q-band (band at ca 600 nm assigned to quinoid units)[16b,20] compared to that observed for PANIs prepared stoichiometrically. Consistently, also conductivity of the polymers prepared with the Fe^{3+}/H_2O_2 system reaches only 10% to 50% ($\sigma \approx 0.5$ S/cm) of that observed for stoichiometrically prepared polymers.[3d]

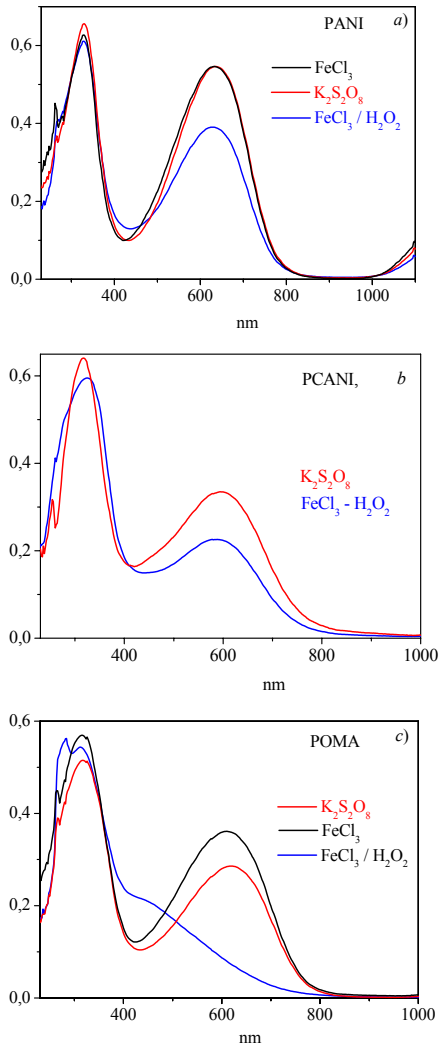

Figure 1. UV/vis spectra of: a) PANI, b) PCANI and c) POMA samples prepared by various procedures

Characteristics of catalytically prepared poly(OMA) (POMA) are still worse: (i) the Q-band is not developed in its UV/vis spectrum (Fig. 1*c*), and (ii) POMA does not become conductive upon doping with HCl ($\sigma \approx 10^{-11}$ S/cm). Surprisingly, no principal difference can be observed between both FTIR and FT Raman spectra of POMA samples prepared by the catalytic and stoichiometric procedures, respectively. However, broadening of the signal of aromatic protons in the ^{1}H NMR spectrum of POMA prepared using the $FeCl_3/H_2O_2$ system indicates the presence of more than three types of benzene rings and a broad signal at 3.7 ppm indicates the presence of free amino groups and oxymethylene units in this polymer. These observations can be explained by the partial oxidation of CH_3 groups of the monomer molecules and transformation of the oxidized monomer molecules into $–O-CH_2-O-C_6H_4-$ units incorporated in POMA chains. Such units interrupt the main chain conjugation, which is consistent with the deteriorated conductivity of this polymer. It is quite probable that such units are formed through oxidation of the methyl groups induced by hydroxyl radicals formed as a side product in the reoxidation of the main oxidant (see Scheme 5).

The above observations indicate that PANIs prepared catalytically contain relatively high number of structure defects deteriorating their functional properties, and that the amount of these defects is a function of the ring substituents of PANI chains. Unsubstituted PANI and PCANI with electron-withdrawing chlorine substituent contain substantially lower number of structure defects compared to POMA carrying electron-donating $-OCH_3$ substituents. Also it is notable that POMA prepared by stoichiometric polymerization with $FeCl_3$ exhibits the Q-band intensity higher than POMA prepared with peroxodisulphate, which is also well known initiator of radical reactions. This fact supports the hypothesis that side reactions of free HO$^\bullet$ radicals are responsible for creation of defects deteriorating functional properties of catalytically prepared PANIs.

Valuable information can be drawn from the found stoichiometry of the catalytic polymerization. For ANI to be polymerized to the emeraldine form, 2.5 equivalents of the oxidant per one ANI equivalent are needed.[3c] The $[H_2O_2]/[ANI]$ mole ratio equal to 1.25 was found to be sufficient to accomplish total polymerization of ANIs with $FeCl_3/H_2O_2$ system. It means that HO$^\bullet$ radicals formed as side product of the reoxidation of Fe^{2+} ions (see Scheme 1) really participate as oxidant species in the overall polymerization process. The above-stated observation that neither H_2O_2 by itself nor $CuCl_2/H_2O_2$ polymerize ANI at temperatures up to 20 °C indicates that the presence $FeCl_3$ is essential for starting the polymerization, i.e., it is essential for the oxidation of anilinium ions (Scheme 3). Hence it can be suggested that HO$^\bullet$ radicals act as oxidant in further steps of ANI polymerization, most probably in the dehydrogenation of the intermediate formed in the combination of two anilinium or anilinium and polyanilinium cation-radicals (Scheme 6).

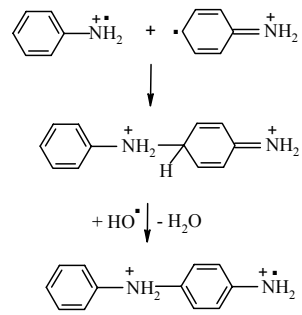

Scheme 6. Possible role of H_2O_2 in the catalytic polymerization of ANI with the system Fe^{3+}/H_2O_2.

Another notable observation is that at temperatures about 5 °C a stoichiometric polymerization with $FeCl_3$ gives only about 3% yield of PANI (MW = 6 000) and about 20% yield of POMA (MW = 8 000) within two days, whereas the catalytic polymerization with $FeCl_3$/H_2O_2 gives the yield about 80% for both polymers (MW is 31 000 for PANI and 3 200 for POMA). This suggests that, at lowered temperatures, the ability of Fe^{3+} ions to eliminate ring-hydrogen from the last-inbuilt monomeric unit is insufficient (Scheme 4). This is most probably the reason of the low to negligible polymerization activity of $FeCl_3$ observed at lowered temperatures.[3a] It can be concluded that Fe^{3+} ions and $HO^{\bullet}$ radicals actually form a synergic system, in which iron ions are key component in the first stage and $HO^{\bullet}$ radicals in the second stage of the incorporation of an ANI unit into a PANI chain.

4. Conclusions, Limitations and Perspectives

There is no doubt that purity is one of the most important factors for obtaining conjugated polymers with desired functional properties. It is also clear that a decrease in a contamination of crude, as synthesized polymers is perhaps the most effective way toward high-purity final materials. Results of recent investigations summarized in this paper points to possibilities as well as limitations of two advanced preparative approaches to the synthesis of pure conjugated polymers, which are based on transformations of (i) homogeneous catalytic processes into heterogeneous ones, and (ii) stoichiometric (chemical) processes into catalytic ones.

Heterogeneous processes based on the transformations ad (i) provide polymers that are almost free of catalyst residues and enable easy separation of the catalyst from the polymer formed. On the other hand, this method has limitations summarized below:

a) It is applicable for the synthesis of soluble polymers only.

b) It requires a use of mesoporous supports for anchoring the active catalyst to eliminate transport limitations of bulky macromolecules inside pores. Nevertheless, a diameter of the support pores needs not be as high as the static diameters of formed macromolecules because the reptation of macromolecules participates in their release from the pores.

c) In some cases also a chemical modification of inner pore walls is needed to make anchoring of catalyst species possible. On the other hand, such modification can be exploited as a method of tuning the chemical surroundings of active species towards their more effective function as well as increased long-time stability.

d) The method cannot be used for a design of living polymerization systems in which growing polymer chains are solidly linked to active species.

e) Besides, this method is not favorable for the preparation of highly stereoregular polymers, which can undergo a rapid crystallization in restricted volume elements inside pores.

Polymerizations with anchored catalysts can be potentially applied not only for the synthesis of high-purity polyacetylenes but also for syntheses of other high-purity polymers, maybe for polymers with applications in medicine and pharmacology, too. However, such an application requires further detailed study in which a fulfillment of pharmacological limits for contaminants of various kinds needs to be examined.

Relatively low attention has been paid to the catalytic oxidative polymerization of ANI despite that this process is known for ca. fourteen years[19]. As a result, the contemporary knowledge on this process is rather poor. Although it is not mentioned in published papers, PANIs prepared by catalytic processes exhibit worse quality compared to polymers prepared by stoichiometric reactions, mainly evidenced by the lowered conductivity, lowered intensity of Q-band in UV/vis spectra and increased content of structure defects, at least according to our observations. It seems clear that roots of these defects lie in side reactions of the catalytic oxidation, the mechanism of which is yet not well understood.

Our observations collected till now point to high complexity of the catalytic reaction. It is obvious that both kinds of oxidant species present in the reaction mixture, Fe^{3+} ions and $HO^{\bullet}$ radicals, participate in the overall mechanism, creating a synergic reaction system. As to the roles of individual oxidants, Fe^{3+} ions are crucial for starting the polymerization (oxidation of anilinium ions) while $HO^{\bullet}$ radicals seems to be highly active mainly at the dehydrogenation of intermediates formed in the combination of ion-radicals. Unfortunately, $HO^{\bullet}$ radicals most probably enter yet not well-recognized side reactions leading to structure defects deteriorating functional properties of PANIs. Better knowledge on the fate of $HO^{\bullet}$ and other radicals occurring in the reaction system should open a way to a desired improvement of properties of catalytically prepared PANIs.

As we have found, the content of structure defects in catalytically prepared PANIs is a function of the ring substituent; this content is low in unsubstituted PANI and CPANI carrying electron-withdrawing Cl substituent, whereas it is high in POMA with electron-donating $-OCH_3$ substituents. Taking into account

requirements for diverse applications of PANI, it can be concluded that the quality of catalytically prepared PANI is acceptable for its applications in the fields of anticorrosion and perhaps also antistatic coatings, whereas it is insufficient for more advanced applications in the field of electronics. Nevertheless, there is a space for improvement of the already known catalytic polymerization procedures toward lowering the undesirable reactions of radicals to an acceptable level and/or introduction of new, low-cost catalytic systems for oxidative polymerization of ANIs. Advances in these fields might bring about a breakthrough in this area of science of steadily increasing practical importance.

5. Acknowledgements

Financial support of the Czech Science Foundation (projects 104/06/1087 and 203/05/2194), the Ministry of Higher Education, Science and Technology of the Republic of Slovenia and Slovenian Research Agency (program P2-145), and the Czech-Slovenian program Kontakt (18/2005-06) is greatly acknowledged. Co-authors J. Svoboda and M. Bláha are indebted to the Czech Science Foundation for the fellowship (project 203/03/H140).

6. References

1. a) G. Hadziioannou, P. F. van Hutten (Eds.) *Semiconducting Polymers, Chemistry, Physics and Engineering,* Wiley-VCH, Weinheim, **2000**; b) R. Farchioni, G. Grosso, G. (Eds.) *Organic Electronic Materials; Conjugated Polymers and Low Molecular Weight Organic Solids,* Springer Series in Materials Science. Vol. 41, Berlin, **2001.**
2. a) B. Z. Tang, J. W. Y. Lam, *Acc. Chem. Res.* **2005**, *38*, 745–754 b) J. L. Bredas, D. Beljonne, V. Coropceanu, J. Cornil, *Chem. Rev*. **2004**, *104*, 4971–5003; c) Y.S. Gal, S.H. Jin, H.S. Lee, S.Y. Kim, *Macromol. Res.* **2005,** *13*, 491–498;.
3. a) N. Toshima, S. Hara, *Prog. Polym. Sci.* **1995,** *20,* 155–183; b) J. Stejskal, P. Kratochvíl, A. D. Jenkins, *Collect. Czech. Chem. Commun.* **1995,** *60,* 1747–1755; c) A. G. MacDiarmid, *Angew. Chem., Int. Ed.* **2001,** *40,* 2581–2590; d) J. Stejskal, R. G. Gilbert, *Pure Appl. Chem.* **2002,** *74,* 857–867.
4. a) Shirakawa H., Masuda T., Takeda K.: in S. Patai, ed., *The Chemistry of Tripple-Bonded Functional Groups*, Supplement C2, Wiley, New York, 1994, Chapter 17, pp. 945–1016; b) K. J. Ivin, J. C. Mol *Olefin Metathesis and Metathesis Polymerization,* Academic Press, San Diego, 1997; c) U. H. F. Bunz, *Chem. Rev.* **2000,** *100,* 1605–1644; d) J. Vohlídal, J. Sedláček, M. Žigon, *Kovine Zlitine Tehnol.* **1997,** *31,* 581–586; e) J. Sedláček, J. Vohlídal, *Collect. Czech. Chem. Commun.* **2003,** *68*, 1745–1790; f) M. G. Mayershofer, O. Nuyken, *J. Polym. Sci. Part A: Polym. Chem.* **2005,** *43,* 5723–5747.
5. a) A. Kraft, A. C. Grimsdale, A. B. Holmes, *Angew. Chem., Int. E*d. **1998**, *3*7, 402; b) M. J. Leclerc, *J. Polym. Sci. Part A: Polym. Chem.* **2001**, *39*, 2867–2873; c) O. Lavastre, S. Cabioch., P.H. Dixneuf, J. Vohlídal, *Tetrahedron,* **1997,** *53,* 7595–7604.
6. a) A. Sarkar, S. Okada, H. Matsuzawa, H. Matsuda, H. Nakanishi. *J. Mater. Chem.* **2000,** *10,* 819–828; b) Y. M. Zhao, K. Campbell, R. R. Tykwinski, *J. Org. Chem.* **2002,** *67,* 336–344; c) R. R. Tykwinski, Y. M. Zhao, *Synlett* **2002,** 1939–1953.
7. a) P. Mastrorilli, C. F. Nobile, V. Gallo, G. P. Suranna, G. Farinola, *J. Mol. Cat. A-Chem.* **2002**, *184*, 73–78; b) A. M. Trzeciak, J. J. Ziolkowski, *Appl. Organometal. Chem*. **2004**, *18*, 124–129.
8. a) J. Čermák, K. Auerová, H. T. T. Nguyen, V. Blechta, P. Vojtíšek, J. Kvíčala, *Collect. Czech. Chem. Commun.* **2001,** *66*, 381–396; b) J. Čermák, L. Sťastná, J. Sýkora, I. Císařová, J. Kvíčala, *Organometallics* **2004,** *23,* 2850–2854.
9. a) P. K. Dutta, M. Puri, *J. Catal.* **1988**, *111*, 453–456; b) S. D. Cox, G. D. Stucky, *J. Phys. Chem.* **1991**, *95*, 710–720; c) S. Bordiga, G. Ricchiardi, G. Spoto, D. Scarano, L. Carnelli, A. Zecchina, C. O. Areán, *J. Chem. Soc. Faraday Trans.* **1993**, *89*, 1843–1855; d) C. Pereira, G. T. Kokotailo, R. J. Gorte, *J. Phys. Chem.* **1991**, *95*, 705–709.
10. a) J. Sedláček, M. Pacovská, D. Rédrová, H. Balcar, A. Biffis, B. Corain, J. Vohlídal, *Chem. Eur. J.* **2002**, *8*, 366–371; b) A. D'Archivio, L. Galantini, A. Biffis, K. Jeřábek, B. Corain, *Chem. Eur. J.* **2000**, *6,* 794–799; c) D. C. Sherrington, C. Olason, *React. Funct. Polym.* **1999**, *42,* 163–172.
11. a) H. Balcar, J. Sedláček, J. Čejka, J. Vohlídal, *Macromol. Rapid Commun.* **2002**, *23*, 32–37; b) H. Balcar, J. Čejka, J. Sedláček, J. Svoboda, J. Zedník, Z. Bastl, V. Bosáček, J. Vohlídal, *J. Mol. Catal. A-Chem.* **2003**, *203*, 287–298; c) H. Balcar, J. Sedláček, J. Svoboda, N. Žilková, J. Vohlídal, M. Pacovská, *Collect. Czech. Chem. Commun.* **2003**, *68*, 1861–1876.
12. a) D. Rédrová, J. Sedláček, M. Žigon, J. Vohlídal, *Collect. Czech. Chem. Commun.* **2005,** *70,* 1787–1798; b) J. Vohlídal, *Macromol. Chem. Phys.* **2006,** *207,* 224–230.
13. a) Y. Kishimoto, P. Eckerle, T. Miyatake, M. Kainosho, A. Ono, T. Ikariya, R. Noyori, *J. Am. Chem. Soc.* **1999,** *121,* 12035–12044; b) M. Isomura, Y. Misumi, T. Masuda, *Polym. Bull.* **2000,** *45,* 335–339; c) M. Miyake, Y. Misumi, T. Masuda, *Macromolecules* **2000,** *33,* 6636–6639; d) A. Nakazato, I. Saeed, T. Katsumata, M. Shiotsuki, T. Masuda, J. Zedník, J. Vohlídal, *J. Polym. Sci. Polym. Chem.* **2005,** *43,* 4530–4536.
14. a) W. Yang, M. Tabata , S. Kobayashi, K. Yokota, A. Shimizu, *Polym. J.* **1991,** *23,* 1135–1138; b) Y. Mawatari, M. Tabata, T. Sone, K. Ito, Y. Sadahiro, *Macromolecules,* **2001,** *34,* 3776–3782; c) V. Percec, J. G. Rudick, P. Nombel,

W. Buchowicz, *J. Polym. Sci. Polym. Chem.* **2002,** *40,* 3212–3220.

15. a) H. Balcar, N. Žilková, J. Sedláček, J. Zedník, *J. Mol. Catal. A-Chem.* **2005**, *232*, 53–58; b) B. De Clercq, F. Lefebvre, F. Verpoort, *Appl. Catal. A-General* **2003,** *247,* 345–364.
16. a) I. Mav, M. Žigon, A. Šebenik, *Synth. Met.* **1999,** *101,* 717–718; b) I. Mav, M. Žigon, A. Šebenik, J. Vohlídal, *J. Polym. Sci. Polym. Chem.,* **2000,** *38,* 3390–3398; c) I. Mav, M. Žigon, *Polym. Bull.* **2000,** *45*, 61–68; d) I. Mav, M. Žigon, *J. Polym. Sci. Polym. Chem.,* **2001,** *39,* 2482–2493; e) I. Mav, M. Žigon, *Synth. Met.* **2001,** *119*, 145–146; f) I. Mav, M. Žigon, *Polym. Int.* **2002,** *51*, 1072–1078; g) I. Mav, M. Žigon, *J. Polym. Sci. Polym. Chem.,* **2001,** *39,* 2471–2481.
17. a) N. Toshima, H. Yan, M. Kajita, Y. Honda, N. Ohno, *Chem. Lett.* **2000,** 1428–1429; H. Yan, M. Kajita, N. Toshima, *Macromol. Mater. Eng.* **2002,** *287,* 503–508.
18. a) W. Liu, J. Kumar, S. Tripathy, J. Senecal, L. Samuelson, *Synth. Met.* **1999,** *100,* 71–78; b) R. Nagarajan, S. Tripathy, J. Kumar, F. F. Bruno, L. Samuelson, *Macromolecules* **2000,** *33,* 9542–9547; c) I. Y. Sakharov, A. C. Vorobiev, J. J. C. Leon, *Enzyme Microb. Tech.* **2003**, *33,* 661; c) A. V. Caramyshev, E. G. Evtushenko, V. F. Ivanov, A. R. Barcel, M. G. Roig, V. L. Shnyrov, R. B. van Huystee, I. N. Kurochkin, A. K. Vorobiev, I. Y. Sakharov, *Biomacromolecules* **2005,** *6,* 1360–1366; d) Z. Jin, Y. X. Su, Y. X. Duan, *Synth. Met.* **2001,** *122,* 237–242; e) S. Alvarez, S. Manolache, F. Denes, *J. Appl. Polym. Sci.* **2003,** *88,* 369–379; f) S. Takamuku, Y. Takeoka, M. Rikukawa, *Synth. Met*. **2003,** *135*, 331–332.
19. a) D. K. Moon, K. Osakada, T. Maruyama, T. Yamamoto, *Makromol. Chem.* **1992,** *193,* 1723–1728; b) C. F. Liu, D. K. Moon, T. Maruyama, T. Yamamoto, *Polym. J.* **1993,** *25,* 775–779; c) Z. Sun, Y. Geng, J. Li, X. Jing, F. Wang, *Synth. Met.* **1997,** *84,* 99–100; d) Z. Sun, Y. Geng, J. Li, X. Jing, F. Wang, *J. Appl. Polym. Sci.* **1999,** *72,* 1077–1084; e) P. K. Tandon, R. Baboo, A. K. Singh, G. Purwar, M. Purwar, *Appl. Organomet.Chem.* **2005,** *19* 1079–1082.
20. a) J. E. Albuquerque, L. H. C. Mattoso, D. T. Balogh, R. M. Faria, J. G. Masters, A. G. MacDiarmid, *Synth. Met.* **2000**, *113,* 19–24; b) I. Mav, M. Žigon, J. Vohlídal, *Macromol. Symp.* **2004,** *212,* 307–315.

Povzetek

Vsebina kratkega preglednega članka je bila tematika predavanja na 13. konferenci o materialih in tehnologijah v Portorožu, 10.-12. oktobra 2005, in povzema dosežke naših laboratorijev na področju raziskav in razvoja sinteze konjugiranih polimerov visoke čistote, predvsem poliacetilenov in polianilinov. V uvodu je podan pregled pomembnejših postopkov, ki se trenutno uporabljajo za sintezo konjugiranih polimerov. Poglavje o katalitski verižni polimerizaciji v dvofaznih sistemih podaja jedrnato informacijo o sistemih tekoče-tekoče s poudarkom na pripravi mezoporoznih katalizatorjev ter njihovi uporabi in učinkovitosti za sintezo poliacetilenov visoke čistote. Za katalitske sisteme, ki so bili pripravljeni z imobilizacijo topnih, katalitsko aktivnih kompleksov kovin prehoda na mezoporoznih nosilcih, je bila raziskana katalitska učinkovitost, stereoselektivnost, ponovna uporaba in omejitve pri transportu makromolekul. Za nosilce so bili uporabljeni polibenzimidazol, molekularna sita iz silicijevega dioksida MCM 41, MCM 48 in SBA 15 in molekularna sita, pri katerih je bila notranjost por modificirana s spojinami s končnimi skupinami $–NH_2$, $–PPh_2$ in $–N(PPh_2)$. Poglavje pretvorbe stehiometričnih polimerizacij v katalitske procese obravnava predvsem polimerizacijo anilina in njegovih derivatov s katalitskim sistemom Fe^{3+}/H_2O_2. Podana je primerjava lastnosti polianilinov, pripravljenih po katalitski in stehiometrični polimerizaciji. Glede na rezultate je razvidno, da so aktivne zvrsti v reakcijski mešanici ioni Fe^{3+} in radikali $HO^{\bullet}$, ki v sinergiji sodelujejo pri polimerizaciji. V zaključnem delu je podan povzetek rezultatov naših raziskav z nakazanimi prednostmi in omejitvami sinteznih pristopov ter perspektive za njihovo uporabo in nadaljnji razvoj.

Příloha B:

Bláha M., Riesová M., Zedník J., Anžlovar A., Žigon M., Vohlídal J.: *Polyaniline synthesis with iron(III) chloride–hydrogen peroxide catalyst system: Reaction course and polymer structure study*, Synthetic Metals 161 (13-14): 1217-1225, **2011**.

Synthetic Metals 161 (2011) 1217–1225

Contents lists available at ScienceDirect

Synthetic Metals

journal homepage: www.elsevier.com/locate/synmet

Polyaniline synthesis with iron(III) chloride–hydrogen peroxide catalyst system: Reaction course and polymer structure study

Michal Bláha[a,*], Martina Riesová[a], Jiří Zedník[a], Alojz Anžlovar[b], Majda Žigon[b], Jiří Vohlídal[a]

[a] Charles University in Prague, Faculty of Science, Department of Physical and Macromolecular Chemistry, Hlavova 2030, CZ-128 40 Prague, Czech Republic
[b] National Institute of Chemistry, Laboratory of Polymer Chemistry and Technology, Hajdrihova 19, SI-1000 Ljubljana, Slovenia

ARTICLE INFO

Article history:
Received 15 October 2010
Received in revised form 28 March 2011
Accepted 11 April 2011
Available online 10 May 2011

Keywords:
Catalytic oxidative polymerization
Conducting polymer
Hydrogen peroxide
Iron(III) chloride
Polyaniline

ABSTRACT

We report on the catalytic polymerization of aniline (ANI) with $FeCl_3/H_2O_2$ system, which can considerably lower contamination of neat polyanilines (PANIs) by side-products characteristic of stoichiometric polymerization. However, catalytically prepared PANIs exhibit reduced conductivity related most probably to side reactions involving radicals generated as integral components of the $FeCl_3/H_2O_2$ system. Catalytic polymerization of ANI with $FeCl_3/H_2O_2$ system was found to be the reaction of approximately 2nd order with respect to ANI and gives PANIs of a good quality only when $[H_2O_2]$ in the reaction mixture was kept low, i.e., at under-stoichiometric ratios $[H_2O_2]/[ANI]$. At over-stoichiometric ratio $[H_2O_2]/[ANI]$, PANIs of lowered conductivity, worse spectroscopic characteristics and increased size of PANI nanostructures were obtained; nevertheless, these PANIs were not over-oxidized to pernigraniline state. The reaction-time profiles of the open-circuit potential of reaction mixtures exhibited an inflection related to the H_2O_2 depletion from the system. Total consumption of H_2O_2 exceeded its consumption necessary on ANI polymerization, which proves partial decomposition of H_2O_2 by Fe ions. UV/vis and resonance Raman spectra indicate incomplete deprotonization of PANIs prepared with $FeCl_3/H_2O_2$ system and subsequently treated with aqueous ammonia, which proves partial self-doping of these PANIs. However, IR and NMR spectra indicate rather low extent of self-doping. It has been proposed that self-doping of PANI involves phenolic OH groups originated from side reactions involving radical species formed from H_2O_2.

1. Introduction

Polyaniline (PANI) and ring-substituted PANIs are well-known conducting functional polymers [1,2] that are routinely prepared by the stoichiometric oxidative polymerization of aniline (ANI) and its derivatives with ammonium peroxodisulfate (APS) [3,4]. This reaction gives, in addition to PANI in the emeraldine salt (ES) state, a high amount of ammonium hydrogensulfate (2.5 mol/1 mol of reacted ANI) as byproduct [4–6]. Though this byproduct does not deteriorate functional properties of PANI, its removal from neat PANI represents about one half of the PANI cost [7]. Therefore, the development of preparative processes that can reduce contamination of formed PANI with byproducts is of importance, since it can potentially bring about considerable savings.

A replacement of APS with H_2O_2, which ideally gives water as the side product, was found to be ineffective. H_2O_2 did not polymerize ANI at 0 °C; it gave a very low PANI yield at room temperature [8,9] and, at 60 °C, the polymerization was fast but gave PANI of very poor quality [10]. The ANI polymerization in a saturated NaCl solution gave PANI of acceptable quality but in a low yield and, of course, contaminated with NaCl [11] (that polymerization was started at 50 °C and the reaction mixture was cooled down to room temperature upon addition of H_2O_2). Catalytic processes giving water as byproduct are more promising. Catalytic ANI polymerization (partly reviewed in Ref. [12]) was accomplished with catalytic systems such as Cu^{2+}/O_2 [7,13], Fe^{3+}/O_3 [7,14,15], Fe^{3+}/H_2O_2 [9,10,16–21], Ru^{3+}/H_2O_2 [22], Cu(II) scorpionate/H_2O_2 [23,24] and various peroxidase/H_2O_2 systems [25–32]. From these systems $Fe^{2+(3+)}/H_2O_2$ exhibits top efficiency. It polymerizes ANI even at the Fe/ANI molar ratio below 1/500 (note that Fe^{3+}/ANI ratio of 2.5 is needed for an ideal ANI transformation to PANI ES with stoichiometric polymerization with Fe^{3+} ions).

Concerning the mechanism of PANI polymerization with Fe^{3+}/H_2O_2 system, Sun et al. suggested that HO• radicals formed by decomposition of H_2O_2 with iron ions are real oxidants in this polymerization [10,16]. However, there are at least two other possible explanations: (i) real oxidants are Fe^{3+} ions that are permanently restored by oxidation of Fe^{2+} ions with H_2O_2 or HO• radicals, and (ii) both Fe^{3+} ions and HO• radicals are active oxidants (Scheme 1). Comparative study of the catalytic (with $FeCl_3/H_2O_2$ and $CuCl_2/H_2O_2$) and stoichiometric (with $FeCl_3$ and H_2O_2) ANI polymerization has shown that Fe^{3+} ions and HO• radicals form

* Corresponding author. Tel.: +420 221 951 311; fax: +420 2 2491 9752.
E-mail address: Michal.Blaha@csop.cz (M. Bláha).

0379-6779/$ – see front matter © 2011 Elsevier B.V. All rights reserved.
doi:10.1016/j.synthmet.2011.04.008

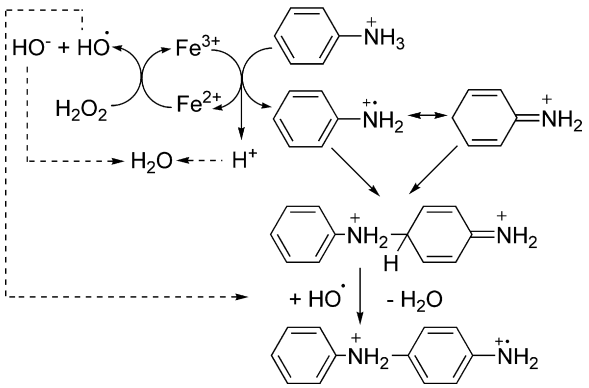

Scheme 1. Scheme proposed for ANI polymerization with Fe^{3+}/H_2O_2 system.

a synergic system in which Fe^{3+} ions most probably play a key role in the oxidation of ANI molecules to radical-cations, whereas HO• radicals significantly contribute mainly in later stage of an ANI molecule incorporation into a PANI chain (Scheme 1) [9]. This means that H_2O_2 ideally acts as a two-electron oxidant in ANI polymerization [9] (Scheme 1); therefore, the ideal stoichiometric molar ratio H_2O_2/ANI: $r = 1.25$ provided that radicals HO• do not undergo a side reaction.

PANIs prepared with Fe^{3+}/H_2O_2 exhibit not only lower conductivity but also lower UV/vis absorbance ratio A_Q/A_B (for Q-band and B-band see Section 3.3) compared to a standard PANI prepared with APS [20]. Zhu et al. [20] attributed the lowered ratio A_Q/A_B to an over-oxidation of PANIs prepared with Fe^{3+}/H_2O_2. In a more general sense, a decrease in the ratio A_Q/A_B indicates the presence of some structure defects and/or proton self-doping of PANI [33–37]. Structure defects present in a catalytically prepared PANI should be closely related to the catalytic polymerization process. Therefore, we carried out a more detailed study on ANI polymerization with the $FeCl_3/H_2O_2$ system in order to get an insight into the course of this process and to get new information on the character and origin of structural defects in so prepared PANIs. The results obtained are reported in this paper.

2. Experimental

2.1. Chemicals

Aniline (p.a.), hydrogen peroxide (p.a., 30% aq.), hydrochloric acid (37%) and lithium chloride were purchased from Lach Ner (Czech Republic). Aniline was purified by vacuum distillation before a use. Concentration of H_2O_2 was determined by manganometric titration. Iron(III) chloride hexahydrate (97%, A.C.S. reagent), ammonium peroxodisulfate (APS), dimethylformamide (DMF), triethylamine (TEA), *N*-methylpyrrolidinon (NMP) and dimethylsulfoxide (DMSO) (all Sigma–Aldrich) were used as supplied.

2.2. Polymerizations

Reference sample: PANI(APS) was prepared by ANI polymerization with APS using the standard procedure [6]. Catalytic polymerizations of ANI were done in the following way: Measured volumes of ANI (2.30 mL, 25 mmol) and $FeCl_3$(aq) (1 M, 250 μL, 0.25 mmol of $FeCl_3$) were dissolved in HCl(aq) (2 M, 25 mL, 50 mmol of HCl), the solution was cooled to 0 °C, diluted with cool distilled water (10.06–22.28 mL) and kept under stirring at 0 °C for 30 min. Then a measured volume (0.165–12.38 mL) of aqueous H_2O_2 (9.49 M, i.e., 1.56–117.5 mmol of H_2O_2) was added to begin polymerization. Total volume of the resulting polymerization mixture was always 50 mL, $[ANI]_0 = 0.5$ M, $[HCl]_0 = 1$ M, and

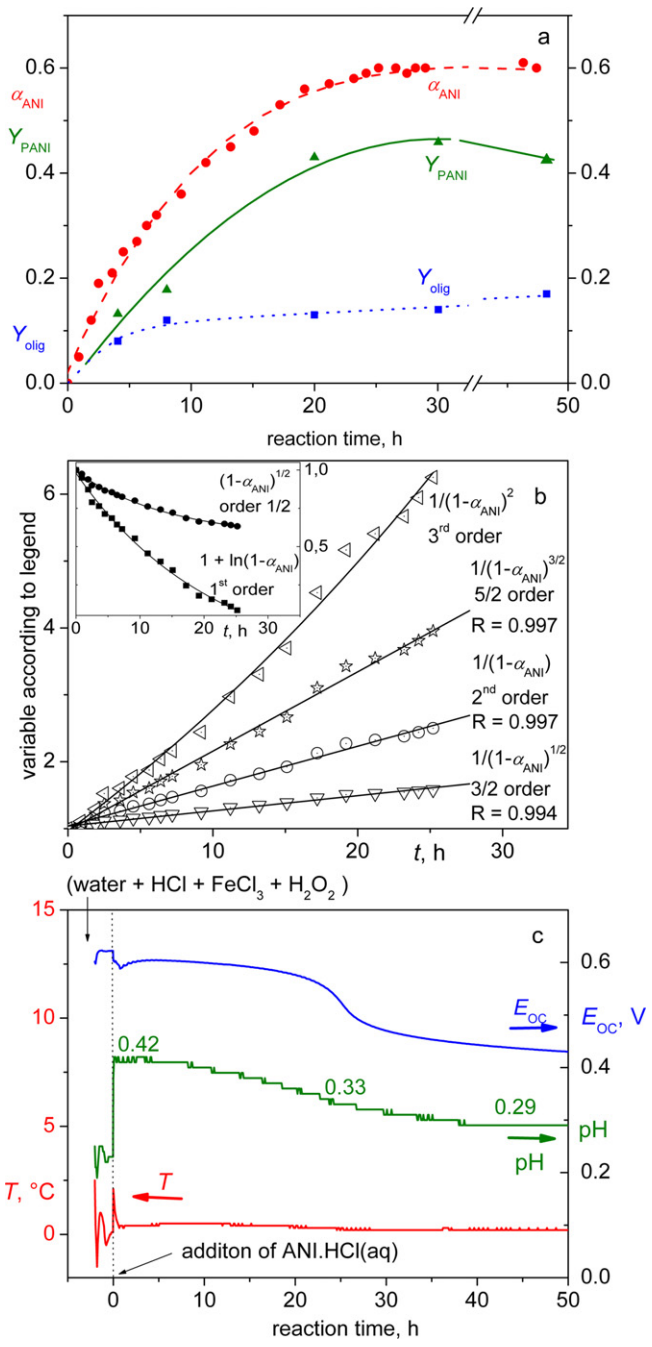

Fig. 1. Graphical data on the course of catalytic polymerization of ANI: (a) conversion curves based on the degree of ANI conversion, α_{ANI}, and isolated yields of PANI, Y_{PANI}, and oligomers of ANI, Y_{olig}. (b) Fits of integral equations for reactions of the reaction order from 1/2 to 3 to the above α_{ANI} conversion curve. (c) Reaction-time profiles of the temperature, *T*, pH and open circuit potential, E_{OC}, of polymerization mixture. Reaction conditions: $[ANI{\cdot}HCl]_0 = 0.5$ M; $[HCl]_0 = 0.5$ M; $[FeCl_3]_0 = 0.005$ M; $r = 0.75$.

$[FeCl_3]_0 = 0.005$ M; $[H_2O_2]_0$ was varied from 0.03125 M to 2.30 M, which corresponds to the molar ratio H_2O_2/ANI = *r*, from 0.0625 to 4.6. The reaction mixture was allowed to react under monitoring the open-circuit potential, E_{OC}, temperature, *T*, and pH of the reaction mixture till the end of a drop in E_{OC} (see Section 3.1). Polymerizations at $r = 3.4$ and 4.6 were done without monitoring the above quantities and were stopped after 24 h. The formed PANI ES was isolated by centrifugation, washed with 0.1 M HCl (3× 50 mL), water (2× 50 mL), and acetone (50 mL), dried under a stream of air in a hood and then in a desiccator above P_2O_5. Collected filtrates

4 anilinium ions $\xrightarrow[-\ 10\ H_2O]{+\ 5\ H_2O_2}$ ideal PANI ES tetrade + 2 H^+

Scheme 2. Stoichiometry of ANI polymerization (for both half-reactions see Supporting Info).

from PANI ES isolation were evaporated to determine their gravimetric yield further dubbed as the yield of ANI oligomers, Y_{olig}. Emeraldine base (EB) of a PANI was gained by treating PANI ES with sixfold stoichiometric excess of aqueous ammonia (0.2 M). PANI EB samples were intensively washed with water and dried as described above.

2.3. Measurements

Open-circuit potential, E_{OC}, temperature, T, and pH of a reaction mixture were measured using a PHM 220 (Radiometer Copenhagen) instrument connected to a data station, a Pt-wire working electrode and a saturated calomel reference electrode for E_{OC}, a glass electrode for pH and a sensor T 201 (Radiometer Analytical) for T. Capillary Zone Electrophoresis (CZE) analyses were done on a ^{3D}CE/diode array detector (Agilent Technologies) instrument using a bare fused silica capillary: 50 μm internal and 363 μm external diameter, total length of 50.3 cm, inlet-to-detector distance of 41.8 cm (Polymicro Technologies, Phoenix, USA) embedded in a cartridge thermostated to 25 °C, and the ChemStation software. New capillary was conditioned by consecutive flushing with water (5 min), 0.1 M NaOH (10 min), water (5 min) and background

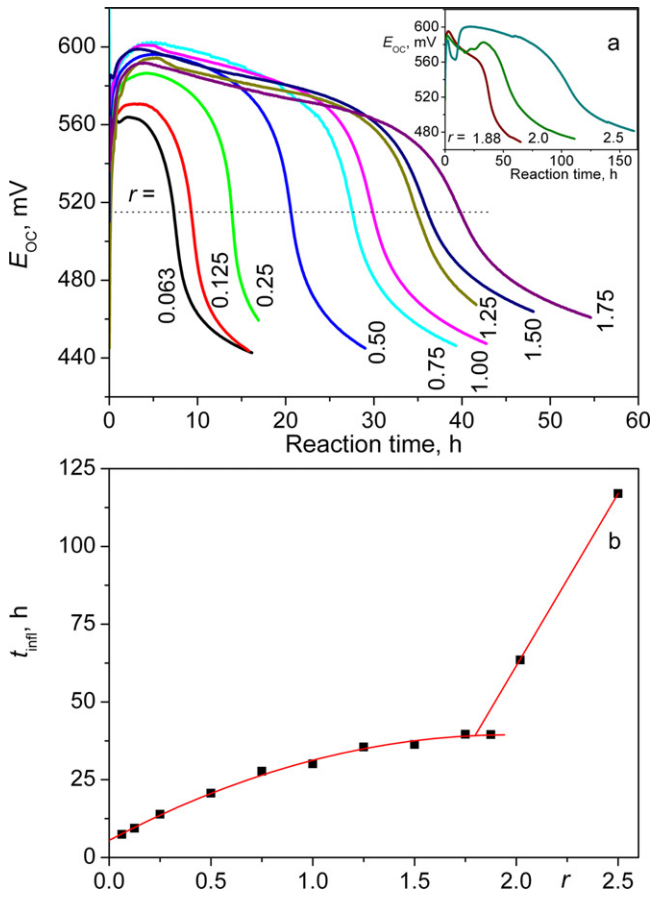

Fig. 2. (a) Reaction-time profiles of the open circuit potential, E_{OC}, for polymerization mixtures of various starting stoichiometry r; (b) time of the inflection point, t_{infl}, on the reaction-time profile of E_{OC} as a function of r. T = 0.3 °C, others conditions as in Fig. 1.

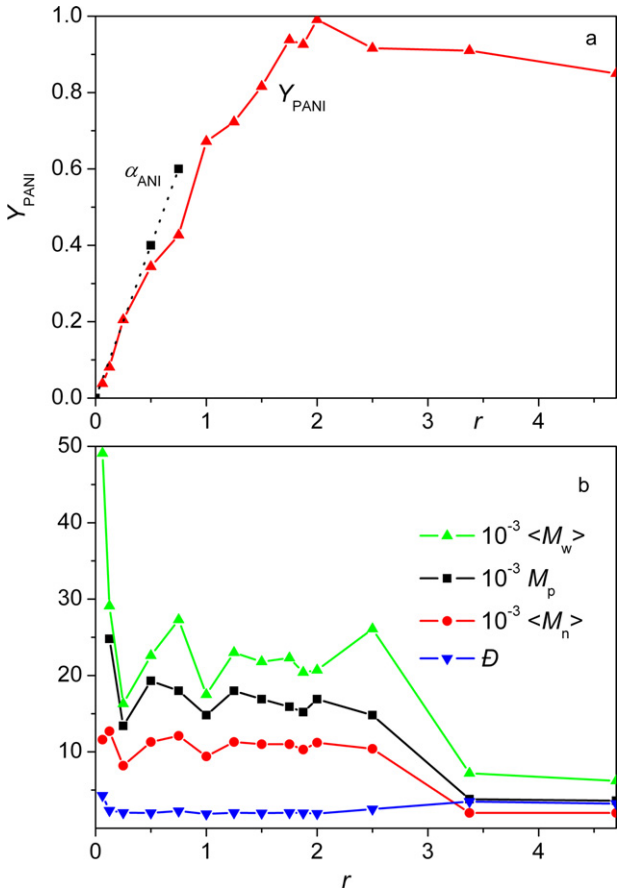

Fig. 3. Isolated relative yield, Y_{PANI} (a) and molecular-weight characteristics (b) of PANI as a function of r. M_w is the weight-average and M_n the number-average molecular weight of PANI (relative to PMMA standards), M_p molecular weight pertaining to the apex of SEC record and $Đ$ dispersity of PANI. Reaction conditions same as in Fig. 2.

electrolyte (25 mM LiOH and 50 mM formic acid; pH 3.5, 20 min). Prior to each analysis, the capillary was rinsed with the running background electrolyte for 4.5 min. Separation voltage of +25 kV and hydrodynamic injection of 30 mbar for 5 s was applied in all experiments. Imidazole was used as an internal standard to control reproducibility of the injected amount and the calibration curve method was applied to determine the concentration of ANI in the liquid phase of a reaction mixture. Gas chromatography analyses were done on a Shimadzu GC-2010 instrument. SEM Micrographs of PANIs were obtained on a Scanning Electron Microscope Zeiss Supra35VP instrument. SEC analyses were done on a TSP (Thermo Separation Product, Florida, USA) chromatograph equipped with an RI and UV/vis detectors (310 nm) and mixed C column (Polymer Laboratories, UK) using DMF with 0.5%$_{vol}$ of TEA (for PANI deprotonation) and 0.5%$_{weight}$ of LiCl (to prevent aggregation) as the eluent (flow rate 0.7 mL/min). The column system was calibrated with PMMA standards.

UV/vis spectra were recorded on a Shimadzu UV-2401 and HP 8452 instruments using PANI solutions (ca. 0.02 mg/mL) in NMP with 0.5%$_{vol}$ of TEA and quartz cuvettes. Spectra were normalized to the absorbance at the isosbestic point (310 nm) [36–38]. Raman spectra were recorded on a DXR Raman microscope (Thermo Scientific) using excitation at 532, 633 and 780 nm (usual laser power at the sample 0.1–0.2 mW) and undiluted samples, and on a Dimension P1 XL Raman spectrometr (Lambda Solutions) using KBr diluted samples and excitation at 785 nm (laser power 7 mW). FT IR spectra were recorded on a Nicolet Magma IR 760 spectrometer using the diffusion reflectance method and KBr diluted samples.

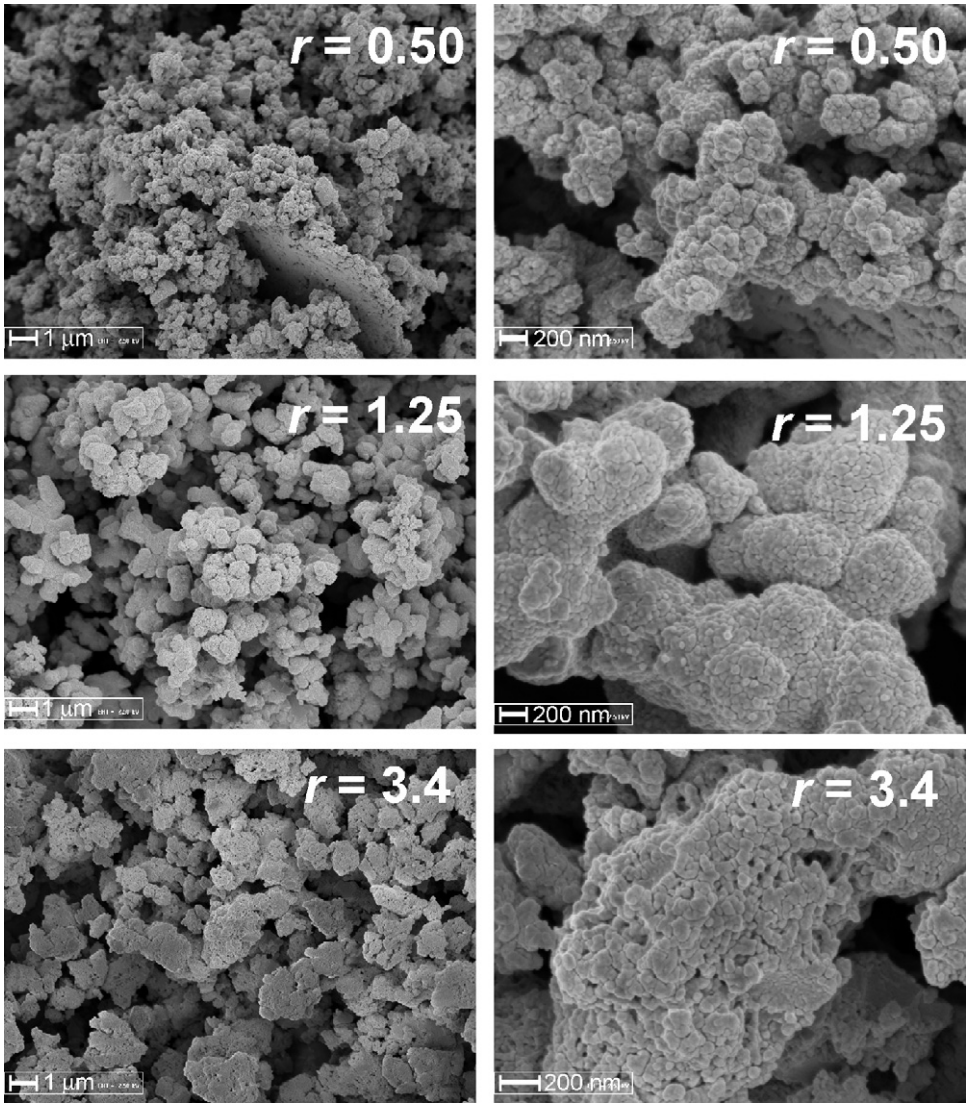

Fig. 4. SEM images of PANIs prepared using different ratios *r*. For reaction conditions see Fig. 2.

^{1}H NMR spectra were measured on a Bruker Avance III 600 MHz spectrometer. Conductance of PANI ES samples was measured by the four-point van der Pauw method on pellets 13 mm in diameter compressed at 700 MPa with a manual hydraulic press (density of pellets was 1.35 ± 0.04 g cm^{-3}) using a current source SMU Keithley 237 and a Multimeter Keithley 2010 voltmeter with a 2000 SCAN 10-channel scanner card.

3. Results and discussion

3.1. Course of polymerization

Conversion curves for the degree of ANI conversion, α_{ANI}, yield of PANI, Y_{PANI}, and yield of ANI oligomers, Y_{olig}, for the catalytic polymerization carried out at $r = 0.75$ (molar ratio H_2O_2/ANI) are shown in Fig. 1a. The observed systematic inequality: $Y_{PANI} < \alpha_{ANI}$ is owing to washing ANI oligomers out during isolation of PANI as evidenced by the reaction-time dependence of Y_{olig}. The final (limiting) value of $\alpha_{ANI} = 0.6$ is in accord with the applied value $r = 0.75$. Correctness of limiting α_{ANI} values determined by CZE was verified by the determination of the content of non-reacted ANI in supernatants from isolation of PANI. A supernatant was neutralized with $NaHCO_3$ to pH 8, ANI was extracted with chloroform, the extract was dried with $MgSO_4$ and, upon filtration, $CHCl_3$ was evaporated and the remaining liquid was azeotropically dried with ethanol. Isolated red-brownish ANI was weighed and its purity (95–98%) was checked by ^{1}H NMR and GC analyses. A good agreement between isolated amounts of ANI and limiting α_{ANI} values was found.

To obtain an insight into the kinetics of catalytic polymerizations, we examined fits of the α_{ANI} conversion curves with integral equations for reactions of the half to third order of reaction with respect to ANI. Best fits were obtained with equations for reactions of the order from 3/2 to 5/2 (Fig. 1b). However, meanwhile this is only interesting empirical knowledge that cannot be reliably

Table 1
Dependence of the conductivity, σ, on *r* for ES forms of PANIs. Reaction conditions same as in Fig. 2.

r	σ (S cm^{-1})
0.25	1.07
1.00	0.81
1.25	0.38
1.50	0.58
1.75	0.46
2.5	8.6×10^{-2}
4.6	1.3×10^{-7}

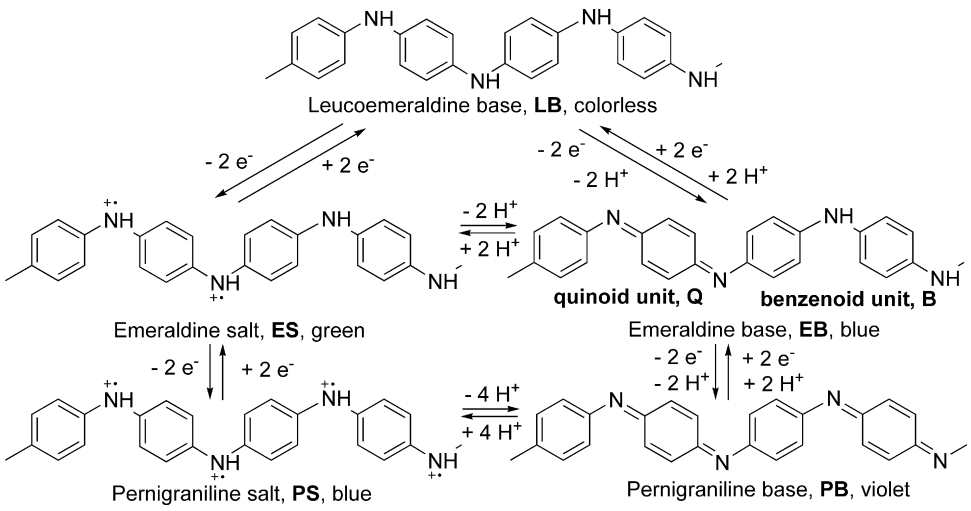

Scheme 3. Redox and protonization states of a regular PANI chain.

interpreted in terms of a plausible mechanism since polymerizations of ANI are strongly affected by continuous aggregation and precipitation of both growing and dead PANI chains, which makes any reliable kinetic analysis extremely difficult.

The reaction-time profiles of T, pH and E_{OC} (open-circuit potential) of the polymerization mixture with $r = 0.75$ are shown in Fig. 1c. As can be seen, temperature kept nearly constant during the whole polymerization, most probably because it is relatively slow. The reaction-time profile of pH (Fig. 1c) showed steady decrease in pH during the polymerization and even for some time also after ANI depletion, which can be due to slow establishing of protolytic equilibrium in the resulting heterogeneous system and/or contamination of electrode surfaces with PANI. In the experiment characterized in Fig. 1c, pH of the mixture decreased from the initial value of 0.42 to value of 0.33 at t_{infl} (see next paragraph) and to 0.29 at the end of monitoring. Respective activities of

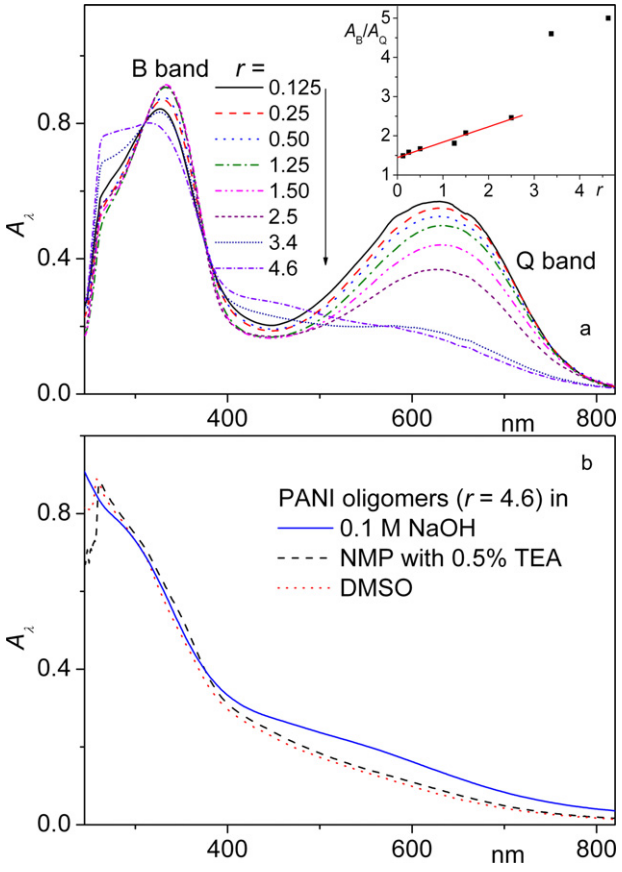

Fig. 5. (a) UV/vis spectra of PANI EBs as a function of the H_2O_2/ANI ratio r; inset: the B/Q band-intensity ratio, A_B/A_Q, as a function of r. (b) UV/vis spectra of the fraction of soluble and/or solubilized species obtained from the supernatant from isolation of PANI($r = 4.6$).

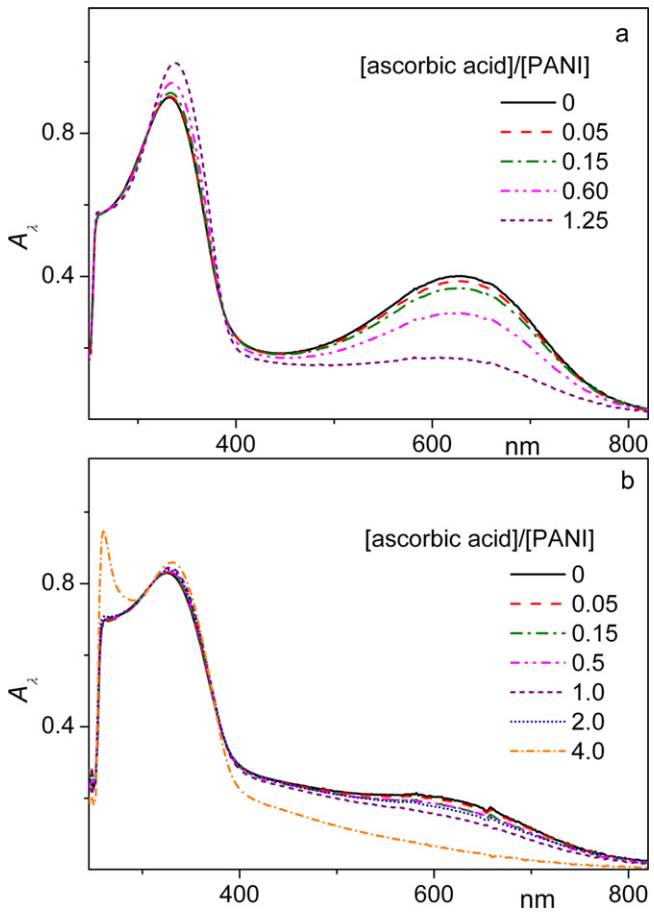

Fig. 6. UV/vis spectra of PANI EB forms upon treatment with various stoichiometric amounts of ascorbic acid: (a) $r = 2.5$; (b) $r = 3.4$.

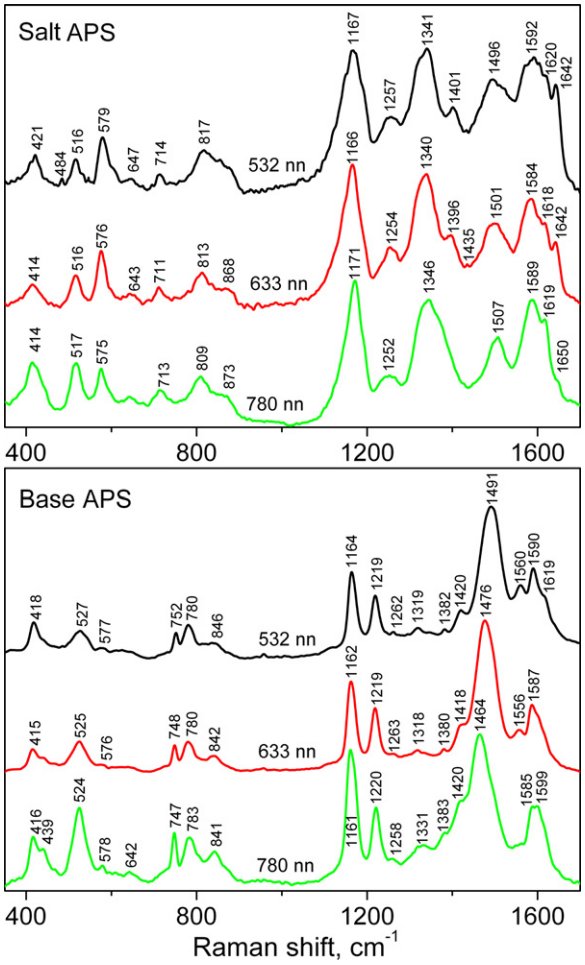

Fig. 7. Raman spectra of ES and EB forms of PANI(APS) measured using λ_{exc} = 532, 633 and 780 nm, respectively.

H_3O^+ ions are: 0.38 M, 0.48 M and 0.51 M. Considering the activity coefficient of 1 M-HCl: $\gamma_{\pm} = 0.76$ [39], respective concentrations are: $[H_3O^+]_0 = 0.5$ M, $[H_3O^+]_{infl} = 0.63$ M and $[H_3O^+]_{\infty} = 0.67$ M. Transformation of four anilinium ions into an ideal PANI ES tetrad requires a release of two protons (Scheme 2). As the reaction started with $[ANI{\cdot}HCl]_0 = 0.5$ M and reached conversion of 60%, theoretical increase in $[H_3O^+]$ is: $\Delta[H_3O^+]_{theor} = 0.15$ mol/dm^3. The found values $\Delta[H_3O^+]_{infl} = 0.13$ mol/dm^3 (at t_{infl}) and $\Delta[H_3O^+]_{\infty} = 0.17$ mol/dm^3 (at the end of measurement) are close to $\Delta[H_3O^+]_{theor}$.

The reaction-time profiles of E_{OC} each showed an inflection at nearly constant $E_{OC,infl} = 515 \pm 5$ mV (vs. SCE) for r up to 1.75; $E_{OC,infl}$ was slightly increasing for higher r (Fig. 2a, inset). By contrast, the reaction-time coordinate of the inflection point, t_{infl}, is a complicated function of r (Fig. 2b). In order to recognize a rationale lying behind the inflection, we carried out the polymerization ($r = 0.75$), at which one half of the reaction mixture that has reacted for 20 h (i.e., before reaching the limiting α_{ANI}) was sampled and the rest was allowed to react on to pass the inflection point and complete the drop in E_{OC}. The sampled mixture was immediately centrifuged to remove PANI and so gained supernatant was heated up to 70 °C. A vigorous reaction giving a significant amount of grey-brown PANI precipitate occurred. On the contrary, the supernatant gained from the mixture that had passed t_{infl} did not give PANI upon heating to 70 °C though it contained enough of ANI (ca. 40% of supplied dose). As H_2O_2 by itself polymerizes ANI at $T \geq 60$ °C [10], these results prove the presence of H_2O_2 in the reaction mixture before t_{infl} and the absence of H_2O_2 in the mixture that had passed inflection. Thus the inflection on the reaction-time profile of E_{OC} should be related to the total depletion of H_2O_2 from polymerization mixture; the inflection does not indicate depletion of ANI!

In the studied system, H_2O_2 is consumed in part on ANI polymerization and in part on self-decomposition by the redox system Fe^{3+}/Fe^{2+}. Relatively fast H_2O_2 consumption on ANI polymerization should predominate at low values r. At high values $r > 1.8$ ANI is consumed earlier than H_2O_2 and a surplus H_2O_2 then undergoes slower decomposition with the redox system Fe^{3+}/Fe^{2+}, as it is indicated by a break at $r \cong 1.8$ at the t_{infl} vs. r dependence shown in Fig. 2b. The fact that the break occurs at r exceeding the ideal ratio $r = 1.25$ indicates that a significant portion of supplied H_2O_2 decays non-productively during ANI polymerization at high values of r. At moderate r values, both modes of H_2O_2 decay are important. Increase in r implicates that more ANI must be transformed to PANI (due to improved stoichiometry of the system) and more H_2O_2 must be decomposed with the system Fe^{3+}/Fe^{2+} before the inflection is achieved. However, also rates of both modes of the H_2O_2 decay should increase at increased $[H_2O_2]_0$. This qualitatively explains the observed concave course of the t_{infl} vs. r dependence in the region of moderate values of r (Fig. 2b).

3.2. Molecular weight, morphology and conductivity of PANIs

Unimodal SEC records indicating unimodal distribution of molecular weights were found for all isolated PANIs. The number-average, M_n, and weight-average, M_w, molecular weights of PANIs and MW value pertaining to the SEC peak apex, M_p, slightly decreased while the molar-mass dispersity $Đ = M_w/M_n$ [40] slightly increased with increasing r (Fig. 3b).

SEM images show granular morphology of catalytically prepared PANIs (Fig. 4) and its dependence on the ratio r applied in PANI synthesis. PANIs prepared at under-stoichiometric values of r showed a cauliflower-like morphology typical of PANI(APS) [41,42] and an increase in the size of nanostructures with increasing r. PANIs prepared at a highly over-stoichiometric ratio r show significantly agglomerated nanostructures of micron dimensions. PANI chains start to grow in solution, and precipitate after they become insoluble in the reaction mixture. Afterwards, new nuclei can form in the presence of the oxidant not only in the solution but also at the precipitated PANI chains. Thus the polymerization can continue also at these newly formed "anchored" nuclei, which produces agglomerated nanostructure species. The observation that the size of the agglomerates increases with increased r can be correlated to the higher number of the nuclei formed at precipitated PANI chains.

Conductivity of PANI ESs prepared at low H_2O_2/ANI ratios to ca. 1.5 is close to but smaller than 1 S cm^{-1} and rather steeply decreases for $r > 2$ (Table 1).

3.3. UV/vis spectra

A PANI base can acquire any oxidation state from a series of discrete states with the increment corresponding to a single two-electron redox process (Scheme 3). There are three notable regular PANI bases: (i) totally reduced base, called leucoemeraldine base, LB, (ii) regular, exactly half-oxidized base, named emeraldine base, EB, and (iii) fully oxidized base, called pernigraniline base, PB (Scheme 3). EB and PB can be easily protonized to give respective salts: emeraldine salt, ES, and pernigraniline salt, PS; this protonization is currently referred to as a proton doping as it transforms an insulating EB into high-conductive ES.

Each PANI base shows a characteristic UV/vis absorption band [3,43,44]. The band typical of LB occurs at 330 nm, it is contributed with the $\pi \rightarrow \pi^*$ transitions in benzene units; therefore,

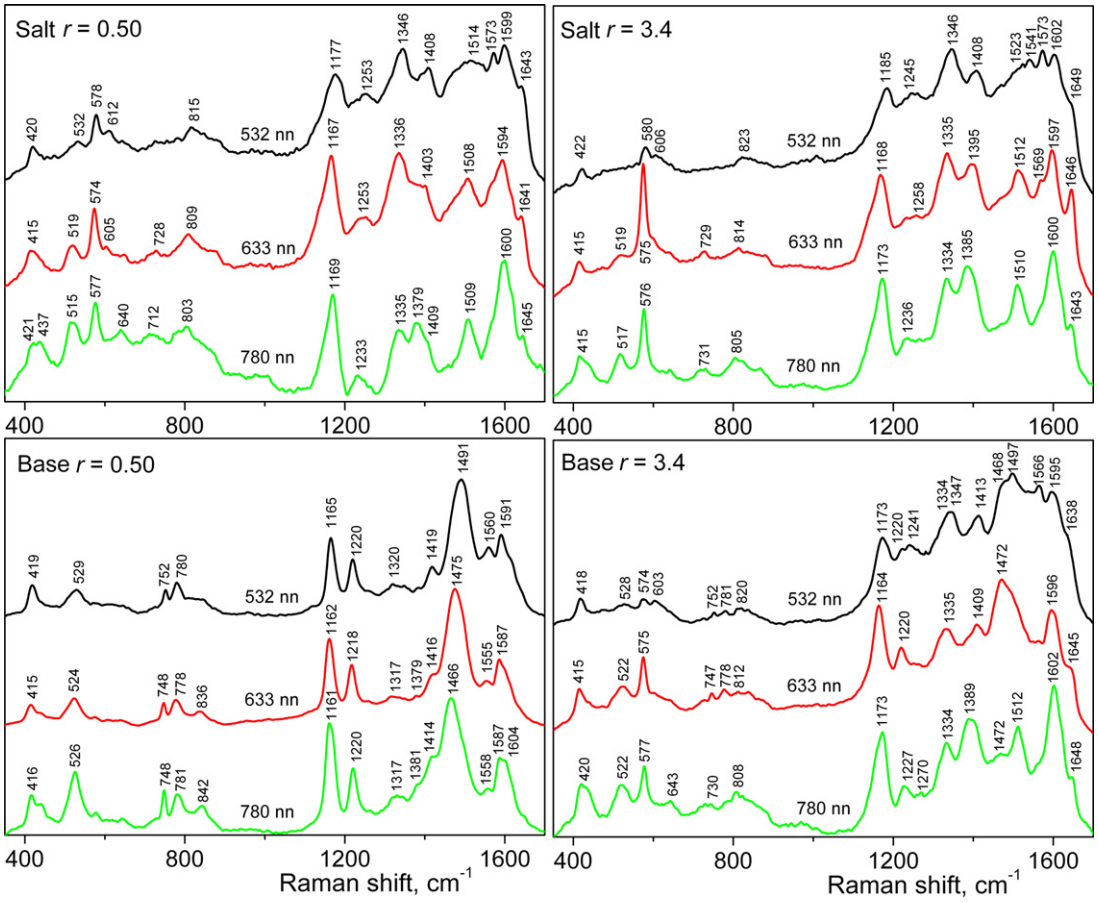

Fig. 8. Raman spectra of ES and EB forms of PANIs prepared with the Fe^{3+}/H_2O_2 catalyst system (r = 0.50 and 3.4) measured using λ_{exc} = 532, 633 and 780 nm, respectively.

it is referred to as the B-band. The band typical of EB occurs at ca. 630 nm, it is mainly contributed with exciton-like transitions in quinoid diimino units [44] and hence it is currently called the Q-band. As EB also comprises benzenoid units (Scheme 3), its spectrum contains both B-band and Q-band. The band typical of PB occurs at ca. 535 nm; it is also attributed to quinoid units and spectrum of PB also contains the B-band.

A real PANI base is mostly irregular as its chains usually include tetrads of two types (EB and LB or PB). If EB is stepwise oxidized to PB, the Q-band position gradually shifts to blue region (toward 535 nm) and, simultaneously, its intensity decreases. Origin of this shift and intensity decrease is ascribed to the Peierls gap effect [36,37,44]. Reduction of PANI EB to LB also decreases the Q-band intensity but, by contrast, the Q-band position is preserved. The absorbance ratio of the B- and Q-bands, A_B/A_Q, is regarded as a measure of the oxidation state of given PANI sample; $A_B/A_Q \cong 1.2–1.4$ for a close-to-regular PANI EB [44].

UV/vis spectra of deprotonized PANIs prepared with the $FeCl_3/H_2O_2$ system using various ratios r are shown in Fig. 5a. The absorbance ratio A_B/A_Q = 1.45–1.50 found for PANIs (r = 0.063 and 0.125) is close to the value of 1.39 found for PANI(APS) EB, which indicates well near structure of all these PANIs. However, the A_B/A_Q ratio is increasing function of r (Fig. 5a, inset) which suggests increasing difference in the structure and/or oxidation-state between PANI(APS) and catalytically prepared PANIs. Insufficient oxidation of PANI (mixed LB and EB states) can be excluded since the difference increases with increasing r. Just opposite, over-oxidation of PANI toward PB form comes into consideration. In order to examine this possibility we did stepwise reduction of PANIs (r = 2.5 and 3.4) with ascorbic acid. No increase in the Q-band intensity has been observed, as it should be expected for an over-oxidized PANI upon treatment with reducing agent. By contrast, gradual decrease in A_Q and increase in A_B occurred (Fig. 6), which indicates reduction of EB sequences contained in PANIs to the LB ones. Thus the difference in the A_B/A_Q ratio between PANI(APS) and catalytically prepared PANIs should be ascribed to some structure defects present in the latter ones. In addition, these results indicate that neither high stoichiometric excess H_2O_2 cause an over-oxidation of PANI EB toward PB form.

Optical spectra of PANI EBs (r = 3.4 and 4.6) show suppression of Q-band to a shoulder, an increase in the absorption in the region from 400 to 500 nm and blue-broadening of the B-band indicating emergence of a new band at 270 nm (Fig. 5a). Similar features were observed in the spectra of self-doped PANIs: binary copolymers of 2-methoxyaniline or aniline and various anilinic acids [33–35,45]. This of course suggests partial self-doping of catalytically prepared PANIs. Therefore, we examined solubility of PANI(r = 4.6) and its oligomeric fraction in aqueous NaOH (0.2 M) in which a weak-acid type polyelectrolyte [46] should be soluble. The PANI was insoluble but its low-MW fraction was soluble in aqueous NaOH. Spectrum of this fraction taken from NaOH solution (Fig. 5b) is similar to the spectra taken from DMSO and NMP, and to the spectrum of its parent PANI. It can be concluded that this fraction behaves like a polyacid and that this behavior support others indirect evidences on the presence of acidic groups in catalytic PANIs (Fig. 5a).

It should be noted here that the fractions obtained from supernatants upon PANI isolation, which are referred to as oligomers, became insoluble in water upon drying. Thus it they are most probably composed of solubilized low-MW PANI molecules rather than true oligomers (see also end of next section).

3.4. Raman, IR and NMR spectra

Raman spectra of PANIs (for extended survey of the spectra see Supporting Information, Figs. S1a–f and S2) have been measured on undiluted PANI samples using excitations (λ_{exc}) at 532, 633 and 780 nm and a very low energy power at the sample (typically 0.1 or 0.2 mW) to prevent a sample carbonization. Each excitation wavelength covers different parts of the optical spectrum of PANIs: λ_{exc} = 532 nm touches the Q-band and the band typical of self-doped PANIs (450–500 nm) [33–35,47]; λ_{exc} = 633 nm matches the Q-band of PANI EB and λ_{exc} = 780 nm the polaronic band of PANI ES [48]. This enables to exploit the resonance Raman effect (selective enhancement of vibrational bands pertaining to groups that show optical absorption around λ_{exc}) and the Raman dispersion effect (small shift of a spectral band position as the excitation light wavelength is varied that is observed for stretching modes of bonds constituting a π–conjugated system [49–51]) in identification of structural features of PANIs. Notation of vibrational modes used in this section is: ν – stretching, δ – in plane, γ – out of plane and τ – torsion; B stands for B-rings and Q for Q-rings.

Raman spectra of ES and EB forms of PANI(APS) are shown in Fig. 7 and the spectra of PANI(r = 0.5) and PANI(r = 3.4) in Fig. 8. Bands characteristic for PANI ES occur at 1330–1345 cm^{-1} and 1380–1400 cm^{-1} ($\nu_{C-NH^{\bullet+}}$ in polarons and bipolarons, respectively [52]); 1505–1510 cm^{-1} (ν_{C-N}, typical of ES [52]), 805 cm^{-1} ($\delta_{B\text{-ring}}$ and γ_{C-H} [53]; broad band showing Raman dispersion of 0.05 cm^{-1} per 1 nm) and 516 cm^{-1} (τ_{C-N-C} and γ_{C-N} [54]). The band at 575 cm^{-1}, which is often ascribed to an uncertain phenazine-type structure [52] should be most probably also assigned to a deformation mode in ES, since changes in its intensity are roughly harmonized with the intensities of bands at 1330 and 1505 cm^{-1}. The δ_{C-H} band occurs just below 1170 cm^{-1} for PANI ES while just above 1160 cm^{-1} for PANI EB [55]. The band most characteristic of PANI EB occurs at 1464 cm^{-1} ($\nu_{C=N}$ in Q [52]) and it shows Raman dispersion ca. 0.1 cm^{-1} per 1 nm); others bands of EB appear at: 1415–1420: (ν_{C-C} in EB [56]), 1220 cm^{-1} (ν_{C-N} in EB [56]), 750, 780 and 840 cm^{-1} (various deformation modes), 525 cm^{-1} (τ_{C-N-C} and γ_{C-N}) [53,55,56] and 415 cm^{-1} (τ_{C-N-C} and γ_{C-N} wagging) [54].

Raman spectra of PANI(APS) and PANI(r = 0.5) bases are almost the same. However, the spectra of PANI(r = 3.4) (and others PANI($r \geq 1.25$) EBs, see Supporting Info) contain almost all bands characteristic of the ES form. Even more, these ES bands predominate in the spectrum of PANI(r = 3.4) EB that was taken with λ_{exc} = 780 nm, due to high enhancement of the signal of protonized units by the resonance Raman effect; note that the main band of EBs (at ca. 1470 cm^{-1}) is almost buried in this spectrum. Opposite impact of the resonance Raman effect is seen in the spectrum of PANI(r = 3.4) EB taken with λ_{exc} = 633 nm (maximum of the Q-band), in which the bands typical of EBs unambiguously dominate (Fig. 8). Both the above resonance effects are attenuated in the spectrum taken with λ_{exc} = 532 nm, which contains all bands of both EB and ES forms but rather poorly resolved.

In summary, the Raman spectra (same as UV/vis spectra) prove that PANI EBs obtained by treatment of as-prepared PANI ES ($r \geq 1.25$) samples with aqueous ammonia are not fully deprotonized and show feature typical of self-doped PANIs [57,58].

IR spectra of EB and ES forms of PANI(APS) and selected catalytically prepared PANIs are shown in Fig. 9. Unlike Raman spectra, the IR spectra of all PANIs are much more similar to each other. Spectra of PANI ESs are almost identical and so they do not provide additional information on the structure of PANIs. Some small differences are seen only in the spectra of PANI EBs. An increase in r is reflected in the IR spectra of EBs by a decrease in the intensity of the bands at: 1380 and 1340 cm^{-1} ($\nu_{C=N}$ in Q [3,59]), 1216 cm^{-1} ($\nu_{C-N} + \delta_{C-H}$ in Q [3,59]), 1167 cm^{-1} (δ_{C-H} in Q [3,60]), 1108 cm^{-1} (δ_{Q} [3,60]), 956 cm^{-1} (probably γ_{Q}), and 852 cm^{-1} (γ_{C-H}, Q [3,59–61]). All these

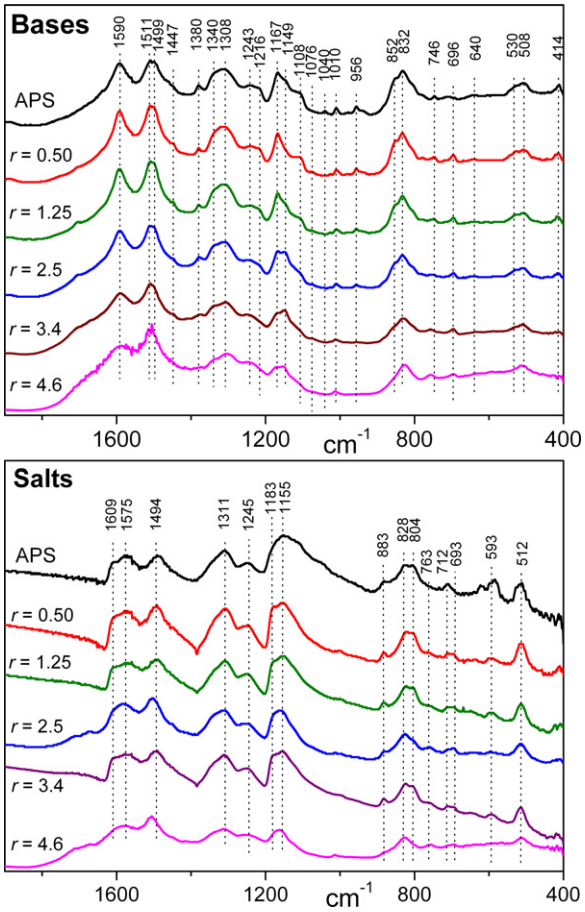

Fig. 9. IR spectra of EB and ES forms of PANI(APS) and PANIs prepared with the Fe^{3+}/H_2O_2 system using various stoichiometry r (for full range spectra see Supporting Info).

changes indicate a decrease in the content of non-protonized Q units if r increases. However, none of bands typical for PANI ES is clearly resolved in IR spectra of PANI bases. This indicates that the content of structure defects in catalytically prepared PANIs is not too high though it is important for the properties and some characteristics of these PANIs, such as for their conductivity and UV/vis and Raman spectra.

In order to reveal nature of defects in catalytically prepared PANIs we have also measured NMR spectra of oligomers (i.e., of the fraction of soluble/solubilized species obtained from the supernatant upon isolation) of PANI(r = 4.6) supposing that the concentration of defect can be high in molecules of this fraction. However, the NMR spectrum provided only signals typical of PANI without reliable evidences for the presence of others structures (see Fig. S5, Supporting Info). Thus this measurement only provided additional evidence that the concentration of defects in catalytically prepared PANIs is rather low.

4. Conclusions

The data obtained on the course of catalytic polymerization of ANI with $FeCl_3/H_2O_2$ system indicate that this reaction is disturbed by the side reaction that consumes H_2O_2, whose intensity increases with increasing H_2O_2/ANI ratio. UV/vis spectra, together with the data on conductivity of prepared PANIs show that this side reaction lowers the quality of the resulting PANI. UV/vis spectra also indicate self-doping of PANIs. Resonance Raman spectra prove the presence of protonized units in formally deprotonized PANIs (treated with

aqueous ammonia), which is the feature typical of self-doped PANIs [57,58]. In addition, Raman spectra prove an increase in the content of protonized units with increasing ratio H_2O_2/ANI applied in PANI synthesis. By contrast, IR and NMR spectra provide only feeble or no evidence proving structural differences in the samples prepared at different H_2O_2/ANI ratios, which points to rather low concentration of structure defects (self-doped ANI units) in catalytically prepared PANIs.

Considering the generic structure and partial self-doping of catalytically prepared PANIs, and the chemistry related to Fenton ($FeCl_3/H_2O_2$) system [62,63], we may speculate that the acidic groups responsible for self-doping are phenolic groups. Phenolic groups can be formed by reactions induced with HO• and/or HOO• radicals that are integral components of the Fenton system. Formation of trimers of 4-chloroanilinine comprising up to four phenolic groups induced with photo-generated HO• has been described in literature [64]. Several reaction paths to phenolic ANI units can be drawn; however, a reliable elucidation of them requires new large experimental material, and it is far beyond the scope of this paper.

Acknowledgements

Financial supports of the Ministry of Education of the Czech Republic (MSM0021620857), the Czech Science Foundation (project nos. 104/09/1435 and 203/08/H032) and the Slovenian Research Agency (bilateral Slovenian-Czech project BI-CZ/07-08/003) are greatly acknowledged. We would like to acknowledge Dr. Jan Prokeš (Charles University in Prague, Faculty of Mathematics and Physics) for conductivity measurements.

Appendix A. Supplementary data

Supplementary data associated with this article can be found, in the online version, at doi:10.1016/j.synthmet.2011.04.008.

References

[1] M. Baron, K.H. Hellwich, M. Hess, K. Horie, A.D. Jenkins, R.G. Jones, J. Kahovec, P. Kratochvíl, W.V. Metanomski, W. Mormann, R.F.T. Stepto, J. Vohlídal, E.S. Wilks, Pure Appl. Chem. 81 (2009) 1131–1183.
[2] K. Horie, M. Baron, R.B. Fox, J. He, M. Hess, J. Kahovec, T. Kitayama, P. Kubisa, E. Marechal, W. Mormann, R.F.T. Stepto, D. Tabak, J. Vohlídal, E.S. Wilks, W.J. Work, Pure Appl. Chem. 76 (2004) 889–906.
[3] E.T. Kang, K.G. Neoh, K.L. Tan, Prog. Polym. Sci. 23 (1998) 277–324.
[4] J. Stejskal, P. Kratochvíl, A.D. Jenkins, Collect. Czech. Chem. Commun. 60 (1995) 1747–1755.
[5] A.G. MacDiarmid, Angew. Chem. Int. Ed. 40 (2001) 2581–2590.
[6] J. Stejskal, R.G. Gilbert, Pure Appl. Chem. 74 (2002) 857–867.
[7] N. Toshima, S. Hara, Prog. Polym. Sci. 20 (1995) 155–183.
[8] A. Pron, F. Genoud, C. Menardo, M. Nechtschein, Synth. Met. 24 (1988) 193–201.
[9] J. Svoboda, M. Bláha, J. Sedláček, J. Vohlídal, H. Balcar, I. Mav-Golež, M. Žigon, Acta Chim. Slov. 53 (2006) 407–416.
[10] Z.C. Sun, Y.H. Geng, J. Li, X.H. Wang, X.B. Jing, F.S. Wang, J. Appl. Polym. Sci. 72 (1999) 1077–1084.
[11] S.P. Surwade, S.R. Agnihotra, V. Dua, N. Manohar, S. Jain, S. Ammu, S.K. Manohar, J. Am. Chem. Soc. 131 (2009) 12528–12529.
[12] C. Della Pina, E. Falletta, M. Rossi, Catal. Today 160 (2011) 11–27.
[13] N. Bicak, B. Karagoz, J. Polym. Sci., Part A: Polym. Chem. 44 (2006) 6025–6031.
[14] N. Toshima, H. Yan, M. Kajita, Y. Honda, N. Ohno, Chem. Lett. (2000) 1428–1429.
[15] H. Yan, M. Kajita, N. Toshima, Macromol. Mater. Eng. 287 (2002) 503–508.
[16] Z.C. Sun, Y.H. Geng, J. Li, X.B. Jing, F.S. Wang, Synth. Met. 84 (1997) 99–100.
[17] D.K. Moon, K. Osakada, T. Maruyama, T. Yamamoto, Macromol. Chem. Phys. 193 (1992) 1723–1728.
[18] H. Innoue, Y. Kida, E. Imoto, Bull. Chem. Soc. Jpn. 39 (1966) 551–555.
[19] C.F. Liu, D.K. Moon, T. Maruyama, T. Yamamoto, Polym. J. 25 (1993) 775–779.
[20] H.P. Zhu, S.L. Mu, Synth. Met. 123 (2001) 293–297.
[21] M.M. Ayad, E.A. Zaki, J. Appl. Polym. Sci. 110 (2008) 3410–3419.
[22] P.K. Tandon, R. Baboo, A.K. Singh, G. Purwar, M. Purwar, Appl. Organomet. Chem. 19 (2005) 1079–1082.
[23] H.V.R. Dias, R.M.G. Rajapakse, D.M.M. Krishantha, M. Fianchini, X.Y. Wang, R.L. Elsenbaumer, J. Mater. Chem. 17 (2007) 1762–1768.
[24] H.V.R. Dias, X.Y. Wang, R.M.G. Rajapakse, R.L. Elsenbaumer, Chem. Commun. (2006) 976–978.
[25] W. Liu, J. Kumar, S. Tripathy, K.J. Senecal, L. Samuelson, J. Am. Chem. Soc. 121 (1999) 71–78.
[26] R. Nagarajan, S. Tripathy, J. Kumar, F.F. Bruno, L. Samuelson, Macromolecules 33 (2000) 9542–9547.
[27] I.Y. Sakharov, A.C. Vorobiev, J.J.C. Leon, Enzyme Microb. Technol. 33 (2003) 661–667.
[28] A.V. Caramyshev, E.G. Evtushenko, V.F. Ivanov, A.R. Barcel, M.G. Roig, V.L. Shnyrov, R.B. van Huystee, I.N. Kurochkin, A.K. Vorobiev, I.Y. Sakharov, Biomacromolecules 6 (2005) 1360–1366.
[29] Z. Jin, Y.X. Su, Y.X. Duan, Synth. Met. 122 (2001) 237–242.
[30] S. Alvarez, S. Manolache, F. Denes, J. Appl. Polym. Sci. 88 (2003) 369–379.
[31] S. Takamuku, Y. Takeoka, M. Rikukawa, Synth. Met. 135 (2003) 331–332.
[32] A. Kausaite-Minkstimiene, V. Mazeiko, A. Ramanaviciene, A. Ramanavicius, Biosens. Bioelectron. 26 (2010) 790–797.
[33] I. Mav, M. Žigon, J. Vohlídal, Macromol. Symp. 212 (2004) 307–314.
[34] I. Mav-Golež, D. Pahovnik, M. Bláha, M. Žigon, J. Vohlídal, Synth. Met., submitted for publication.
[35] I. Mav, M. Žigon, A. Šebenik, J. Vohlídal, J. Polym. Sci., Part A: Polym. Chem. 38 (2000) 3390–3398.
[36] J.E. de Albuquerque, L.H.C. Mattoso, D.T. Balogh, R.M. Faria, J.G. Masters, A.G. MacDiarmid, Synth. Met. 113 (2000) 19–22.
[37] J.E. de Albuquerque, L.H.C. Mattoso, R.M. Faria, J.G. Masters, A.G. MacDiarmid, Synth. Met. 146 (2004) 1–10.
[38] J.G. Masters, Y. Sun, A.G. MacDiarmid, A.J. Epstein, Synth. Met. 41 (1991) 715–718.
[39] J. Vohlídal, A. Julák, K. Štulík, Chemické a analytické tabulky (Chemical and Analytical Tables), Grada Publishing, Prague, 1999.
[40] R.G. Gilbert, M. Hess, A.D. Jenkins, R.G. Jones, R. Kratochvil, R.F.T. Stepto, Pure Appl. Chem. 81 (2009) 779.
[41] I. Sapurina, J. Stejskal, Polym. Int. 57 (2008) 1295–1325.
[42] D. Pahovnik, E. Žagar, J. Vohlídal, M. Žigon, Synth. Met. 160 (2010) 1761–1766.
[43] E. Erdem, M. Sacak, M. Karakisla, Polym. Int. 39 (1996) 153–159.
[44] A.R. Hopkins, P.G. Rasmussen, R.A. Basheer, Macromolecules 29 (1996) 7838–7846.
[45] I. Mav, M. Žigon, Polym. Bull. 45 (2000) 61–68.
[46] M. Hess, R.G. Jones, J. Kahovec, T. Kitayama, P. Kratochvíl, P. Kubisa, W. Mormann, R.F.T. Stepto, D. Tabak, J. Vohlídal, E.S. Wilks, Pure Appl. Chem. 78 (2006) 2067–2074.
[47] M.M. Ayad, N.A. Salahuddin, A.K. Abou-Seif, M.O. Alghaysh, Eur. Polym. J. 44 (2008) 426–435.
[48] J.M. Ginder, A.J. Epstein, Phys. Rev. B 41 (1990) 10674–10685.
[49] M. Gussoni, C. Castiglioni, G. Zerbi, in: R.J.H. Clark, R.E. Hester (Eds.), Spectroscopy of Advanced Materials, Wiley, New York, 1991, p. 251.
[50] G. Zerbi, M. Gussoni, C. Castiglioni, in: J.L. Bredas, R. Silbey (Eds.), Conjugated Polymers, Kluwer Academic Publishers, Dortrecht, 1991, p. 435.
[51] J. Vohlídal, J. Sedláček, N. Patev, M. Pacovská, O. Lavastre, S. Cabioch, P.H. Dixneuf, V. Blechta, P. Matějka, H. Balcar, Collect. Czech. Chem. Commun. 63 (1998) 1815–1838.
[52] M.C. Bernard, A. Hugot-Le Goff, Electrochim. Acta 52 (2006) 728–735.
[53] S. Quillard, G. Louarn, S. Lefrant, A.G. MacDiarmid, Phys. Rev. B 50 (1994) 12496–12508.
[54] M.C. Bernard, A. Hugot-Le Goff, H. Arkoub, B. Saidani, Electrochim. Acta 52 (2007) 5030–5038.
[55] J.X. Zhang, C. Liu, G.Q. Shi, J. Appl. Polym. Sci. 96 (2005) 732–739.
[56] K. Berrada, S. Quillard, G. Louarn, S. Lefrant, Synth. Met. 69 (1995) 201–204.
[57] X.L. Wei, A.J. Epstein, Synth. Met. 74 (1995) 123–125.
[58] X.L. Wei, Y.Z. Wang, S.M. Long, C. Bobeczko, A.J. Epstein, J. Am. Chem. Soc. 118 (1996) 2545–2555.
[59] M.I. Boyer, S. Quillard, E. Rebourt, G. Louarn, J.P. Buisson, A. Monkman, S. Lefrant, J. Phys. Chem. B 102 (1998) 7382–7392.
[60] G. Socrates, Infrared and Raman Characteristic Group Frequencies, Wiley, New York, 2001.
[61] I. Šeděnková, M. Trchová, N.V. Blinova, J. Stejskal, Thin Solid Films 515 (2006) 1640–1646.
[62] J.J. Pignatello, E. Oliveros, A. MacKay, Crit. Rev. Environ. Sci. Technol. 36 (2006) 1–84.
[63] P. Bautista, A.F. Mohedano, J.A. Casas, J.A. Zazo, J.J. Rodriguez, J. Chem. Technol. Biotechnol. 83 (2008) 1323–1338.
[64] G. Mailhot, L. Hykrdová, J. Jirkovský, K. Lemr, G. Grabner, M.B. Bolte, Appl. Catal. B 50 (2004) 25–35.

Supporting Info to

Polyaniline Synthesis with Iron(III) Chloride - Hydrogen Peroxide Catalyst System: Reaction Course and Polymer Structure Study

Michal Bláha[a], Martina Riesová[a], Jiří Zedník[a], Alojz Anžlovar[b], Majda Žigon[b], Jiří Vohlídal[a]

[a] *Charles University in Prague, Faculty of Science, Department of Physical and Macromolecular Chemistry, Hlavova 2030, CZ-128 40 Prague, Czech Republic*

[b] *National Institute of Chemistry, Laboratory of Polymer Chemistry and Technology, Hajdrihova 19, SI-1000 Ljubljana, Slovenia*

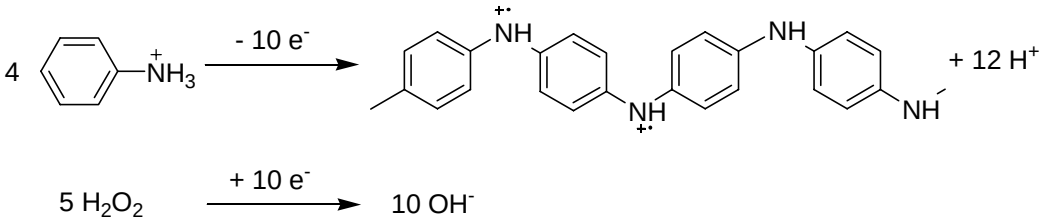

To scheme 2: Formal half-reactions of aniline oxidation and H_2O_2 reduction

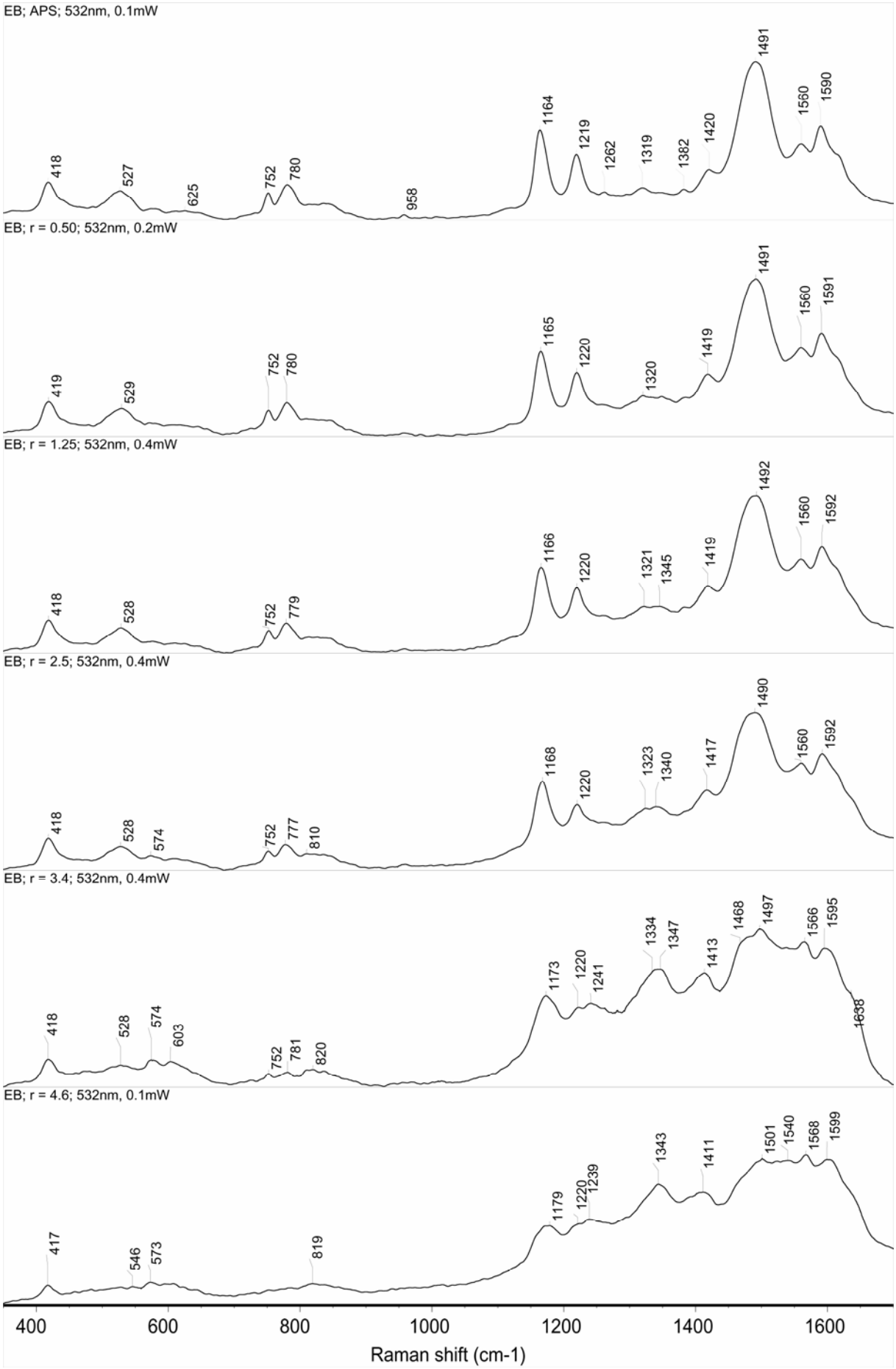

Fig. S1a. Raman spectra of EB forms of PANIs prepared with the Fe^{3+}/H_2O_2 catalyst system at various H_2O_2–to–aniline mole ratio *r*; measured at 532 nm excitation wavelength. Spectrum of PANI (APS) is shown for a comparison.

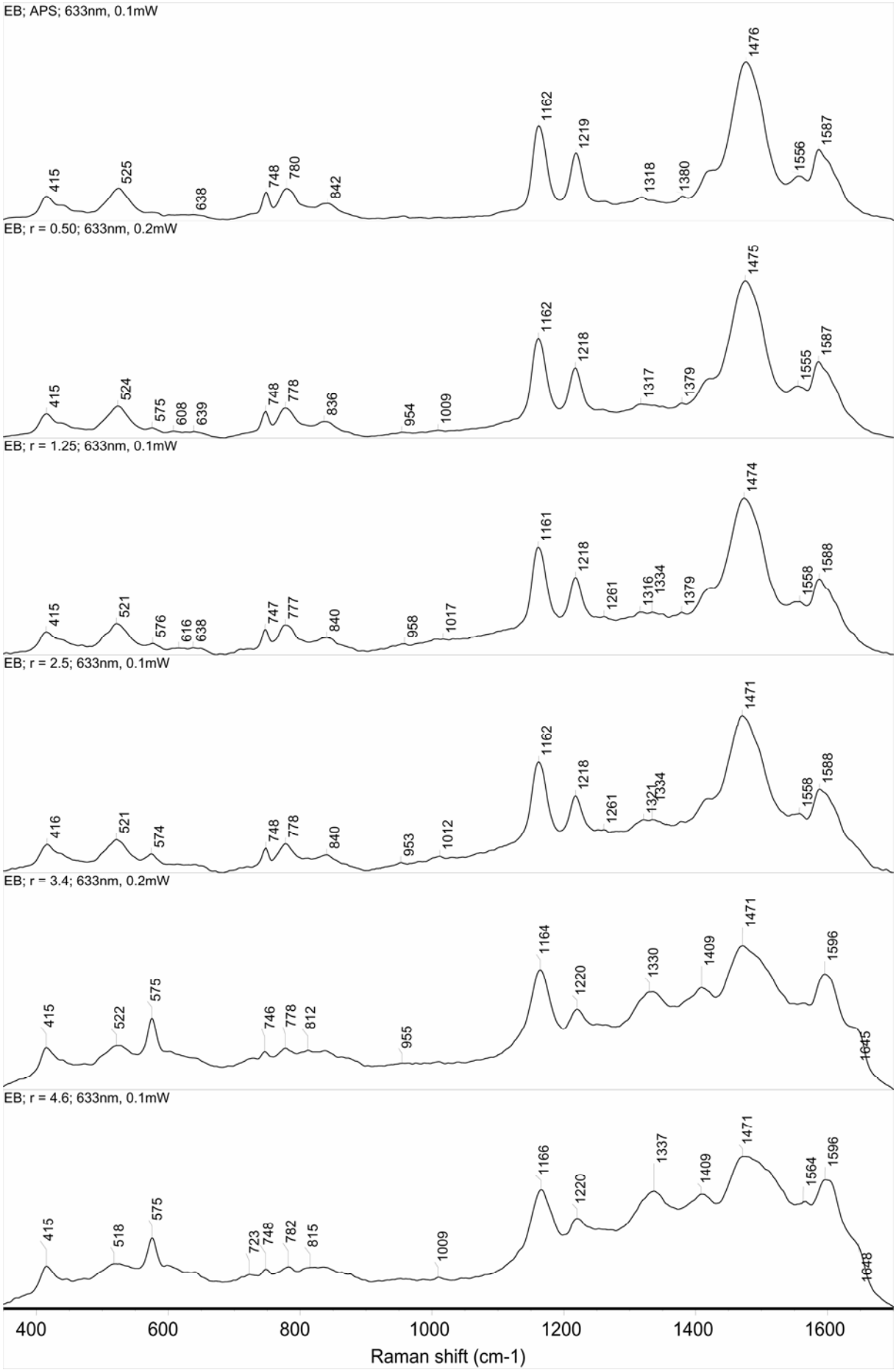

Fig. S1b. Raman spectra of EB forms of PANIs prepared with the Fe^{3+}/H_2O_2 catalyst system at various H_2O_2–to–aniline mole ratio *r*; measured at 633 nm excitation wavelength. Spectrum of PANI (APS) is shown for a comparison.

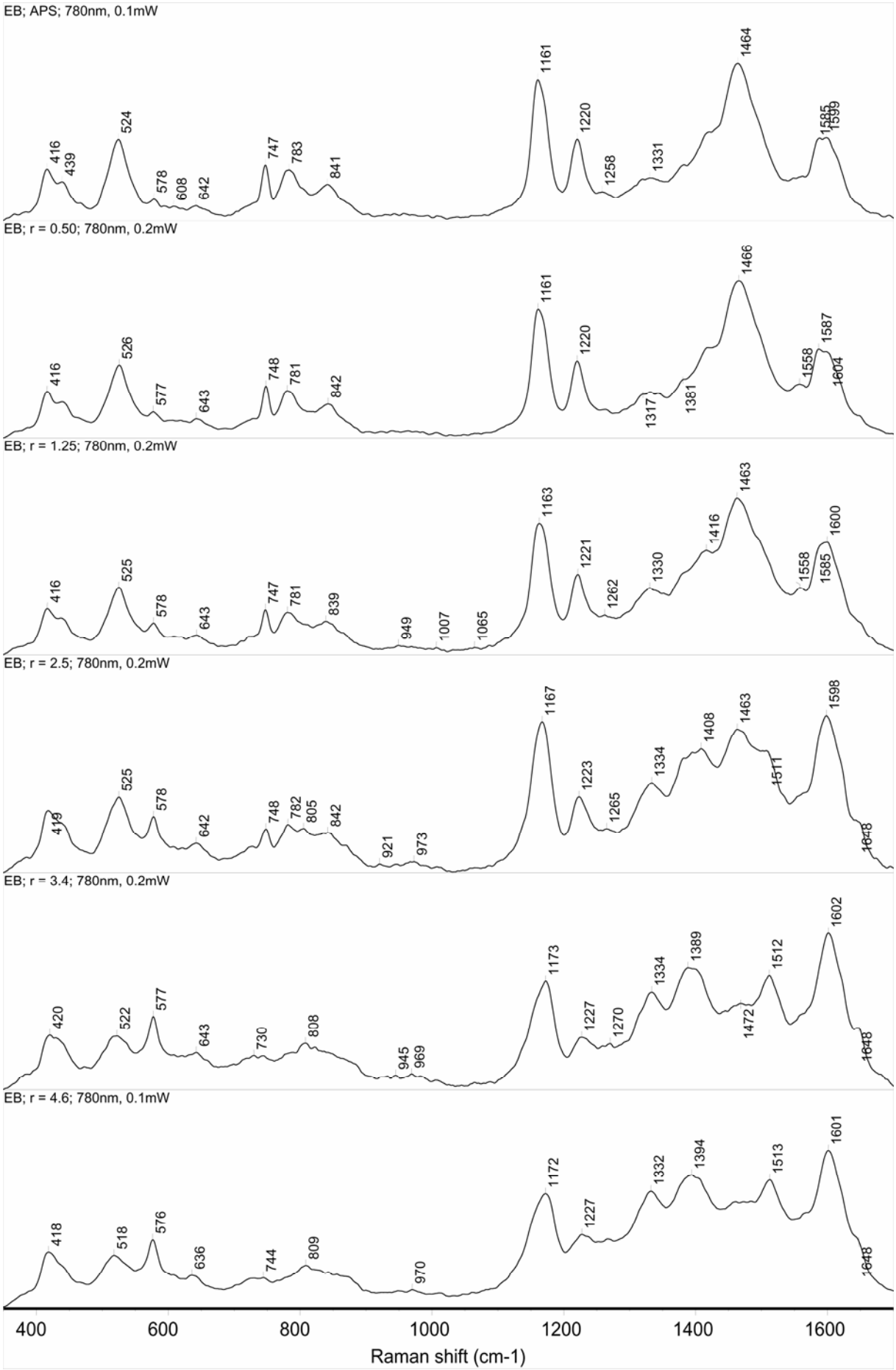

Fig. S1c. Raman spectra of EB forms of PANIs prepared with the Fe^{3+}/H_2O_2 catalyst system at various H_2O_2–to–aniline mole ratio *r*; measured at 780 nm excitation wavelength. Spectrum of PANI (APS) is shown for a comparison.

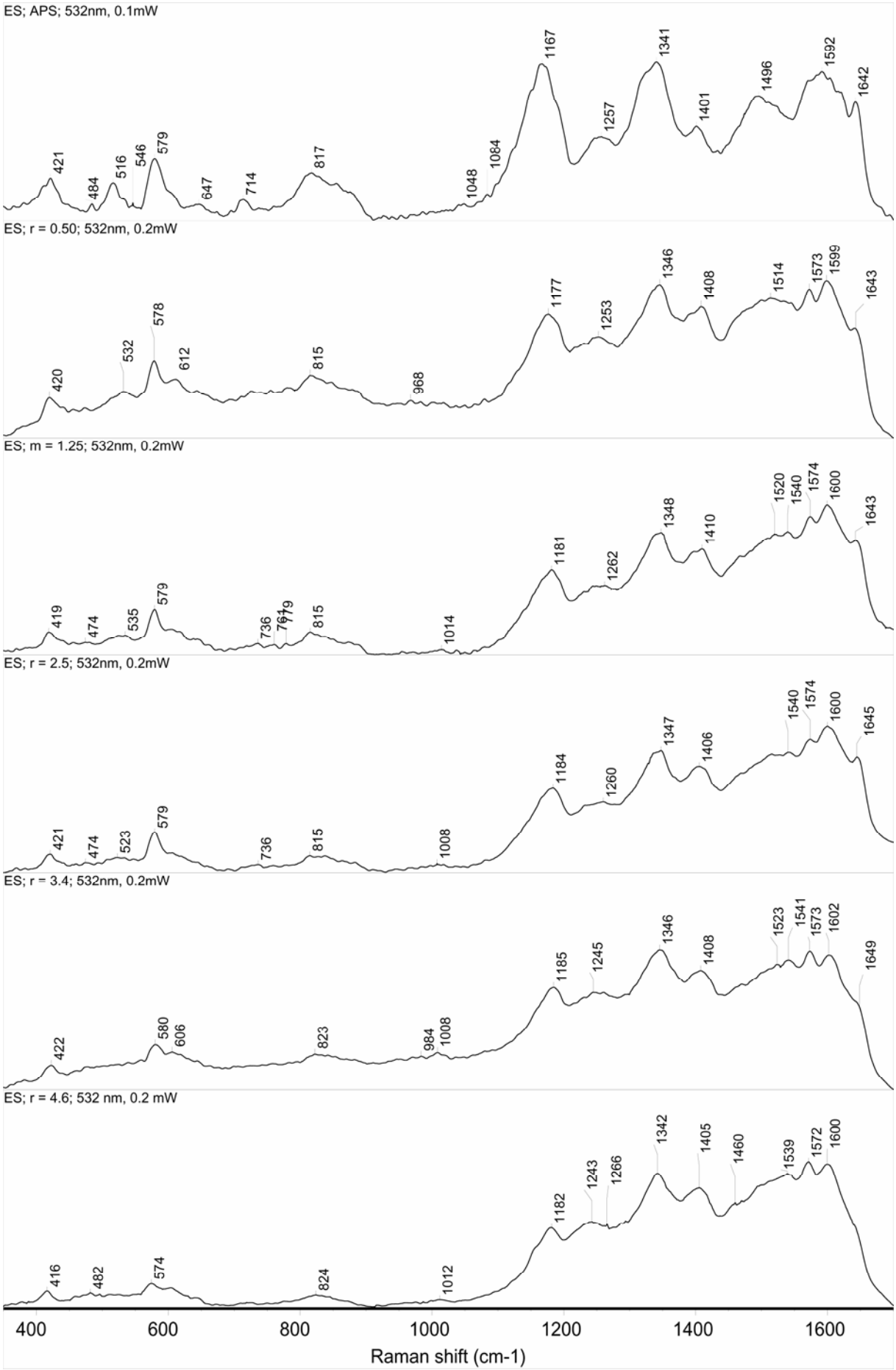

Fig. S1d. Raman spectra of ES forms of PANIs prepared with the Fe^{3+}/H_2O_2 catalyst system at various H_2O_2–to–aniline mole ratio *r*; measured at 532 nm excitation wavelength. Spectrum of PANI (APS) is shown for a comparison.

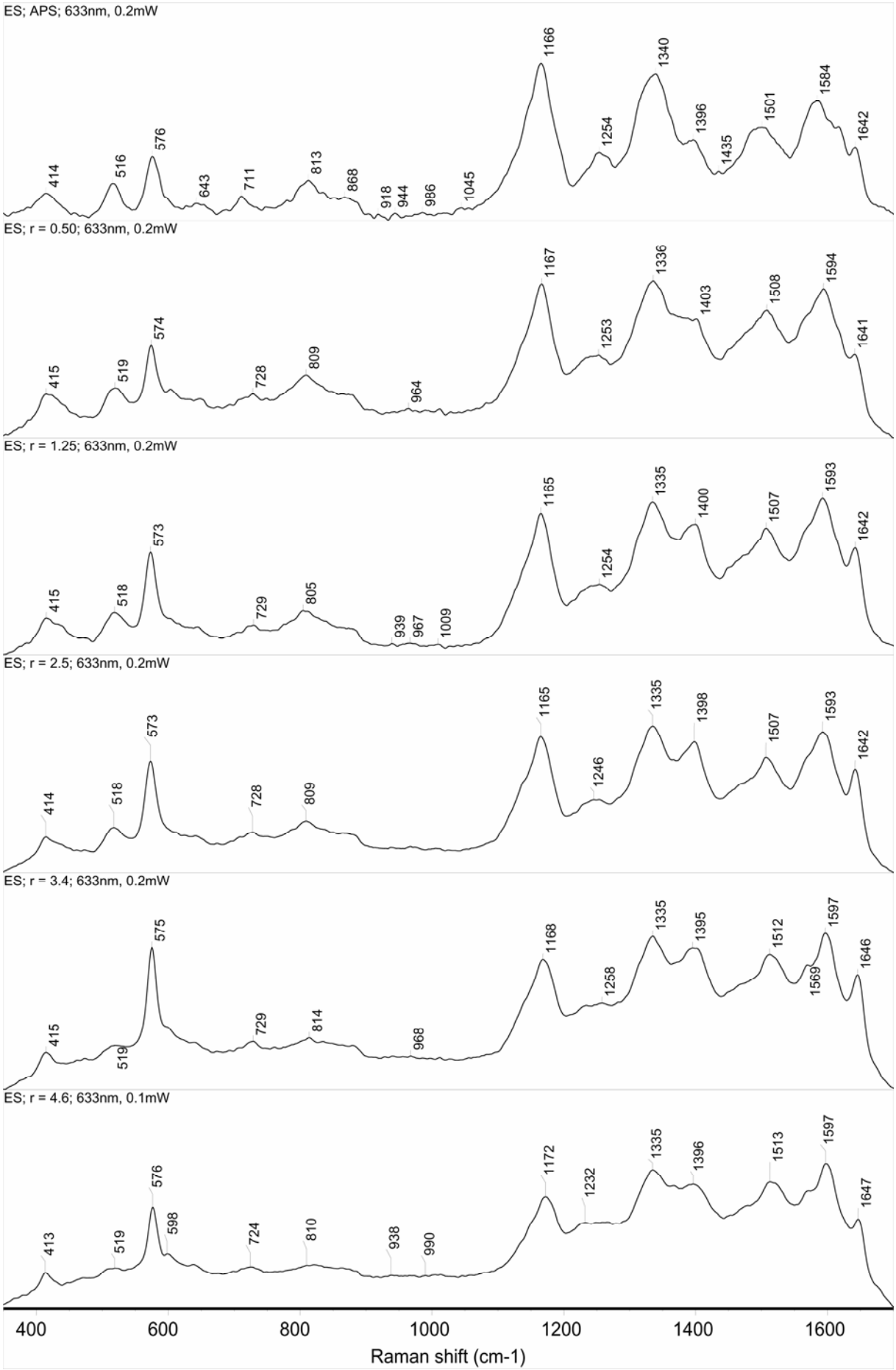

Fig. S1e. Raman spectra of ES forms of PANIs prepared with the Fe^{3+}/H_2O_2 catalyst system at various H_2O_2–to–aniline mole ratio *r*; measured at 633 nm excitation wavelength. Spectrum of PANI (APS) is shown for a comparison.

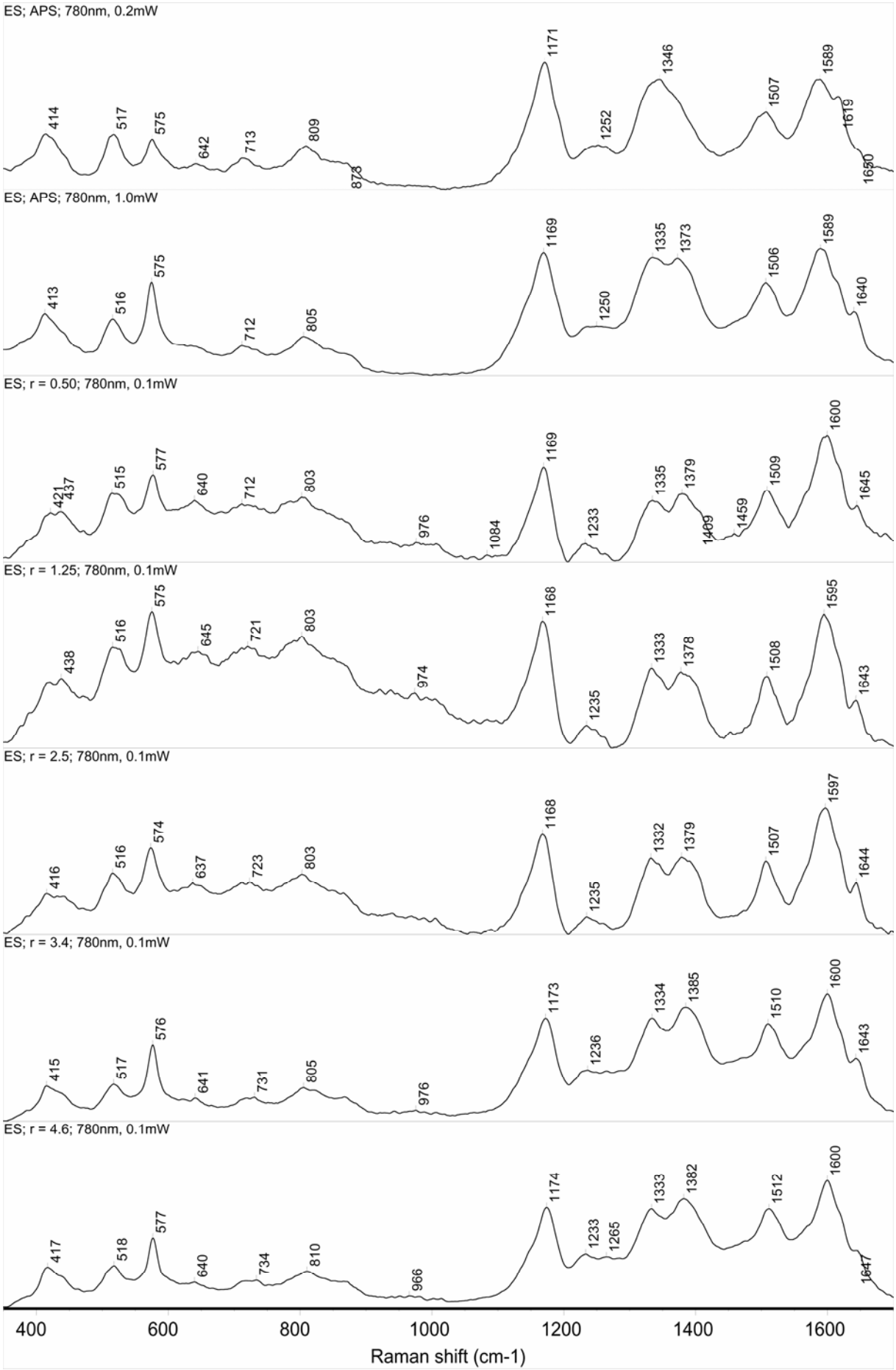

Fig. S1f. Raman spectra of ES forms of PANIs prepared with the Fe^{3+}/H_2O_2 catalyst system at various H_2O_2–to–aniline mole ratio *r*; measured at 780 nm excitation wavelength. Spectrum of PANI (APS) is shown for a comparison.

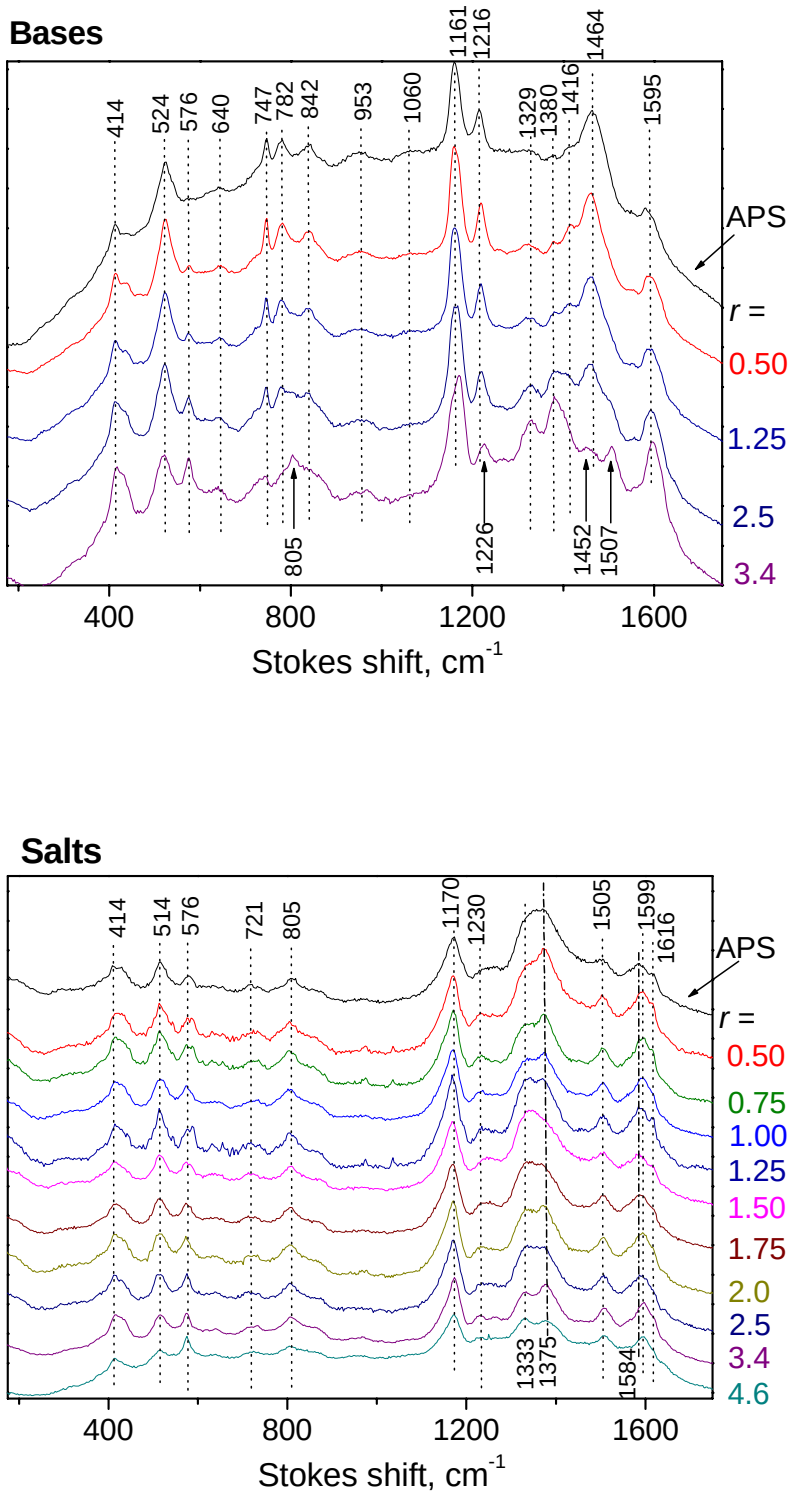

Fig. S2. Raman spectra of EB and ES forms of PANIs prepared with Fe^{3+}/H_2O_2 catalytic system at various H_2O_2–to–aniline mole ratio *r*; spectrum of PANI (APS) is shown for a comparison.

Raman spectra at 785 nm measured using λ_{exc} = 785 nm (7 mW at the sample) and KBr diluted solid samples to prevent carbonization. The spectra measured with λ_{exc} = 785 nm and 780 nm are similar to each other, however, the former ones are less resolved and contain (mainly in spectra of salts), though poorly resolved, bands at 1375 and 1584 cm^{-1} that might be assigned to structures present in carbonized PANIs (ref. M. Trchová, P. Matějka, J. Brodinová, A. Kalendová, J. Prokeš, J. Stejskal, *Polym. Degrad. Stabil.* 91 (2006) 114-121).

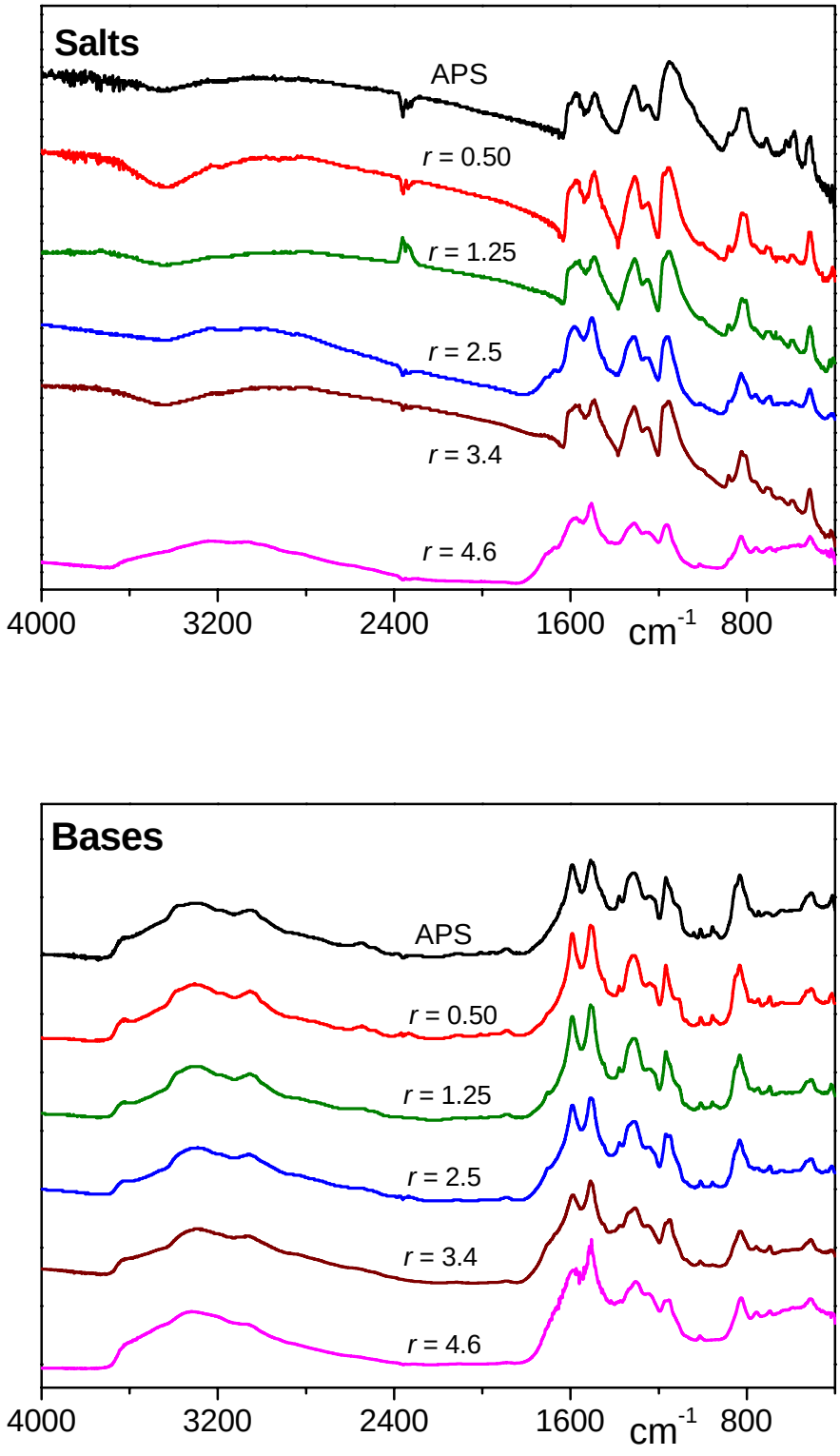

Fig. S3. Full range IR spectra of ES and EB forms of PANI prepared with Fe^{3+}/H_2O_2 catalytic system at various H_2O_2–to–aniline mole ratio *r*; spectrum of PANI prepared with APS as oxidant is shown for a comparison.

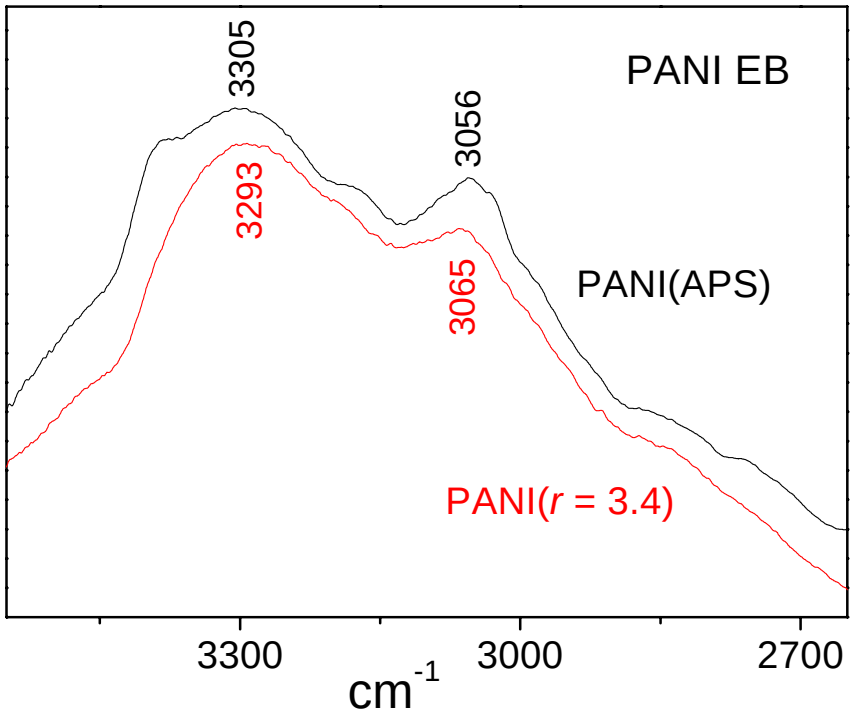

Fig. S4. Comparison of FTIR spectra of EB forms of PANI APS and PANI prepared catalytically with high over-stoichiometric ratio (r = 3.4) in the range 2650 – 3550 cm^{-1}.

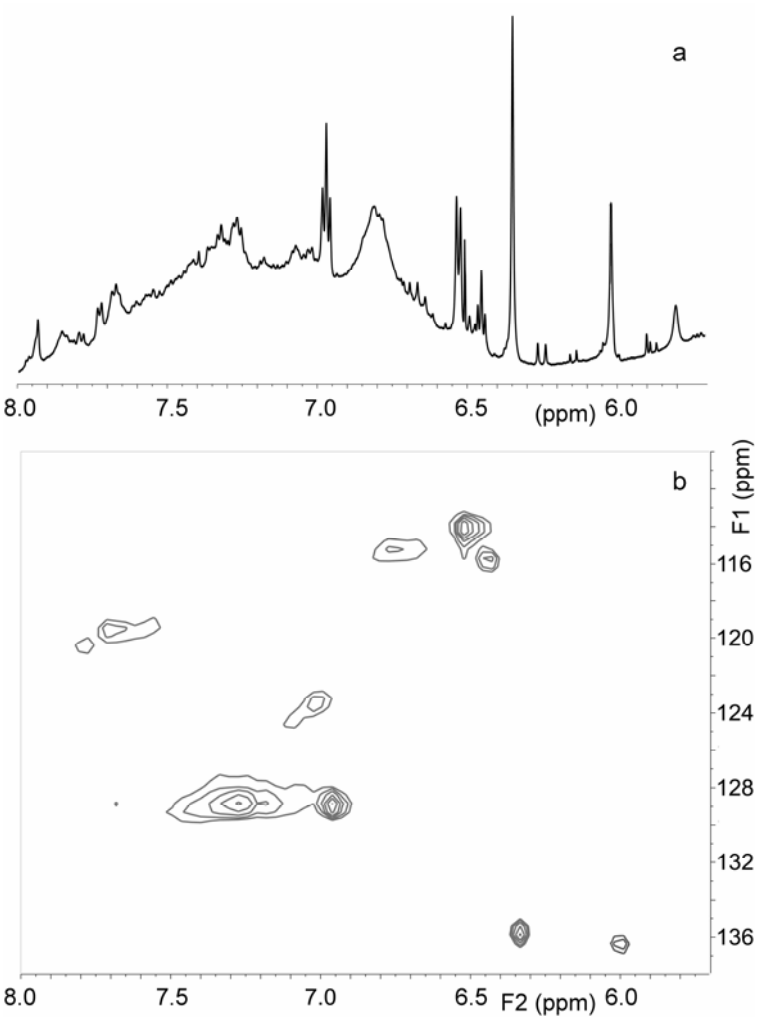

Fig. S5. ^{1}H (a) and HSQC (b) NMR spectra of oligomeric fraction resulting from polymerization with high over-stoichiometric H_2O_2-to-ANI ratio (r = 4.6).

^{1}H NMR (400 MHz) and ^{13}C NMR (100 MHz) in d^6-DMSO with 15 molar % of triethylamine spectroscopy were done using Varian ^{UNITY}INOVA and Bruker Avance III 600 MHz. Spectra were referenced to the solvent signal, 2.50 ppm for ^{1}H NMR and 39.51 ppm for ^{13}C NMR. HSQC and HMBC were performed as gradient experiments in same solvent. All 2D experiments were recorded with spectral windows 5 000 Hz for ^{1}H and 25 000 Hz for ^{13}C. Character of ^{1}H NMR spectra, in spectral region 6 – 8 ppm (see Figure S5a), also showed PANI character of this chemical moiety comparable to spectra of "as-synthesized" copolymer of 2-methoxyaniline with 3-aminobenzenesulfonic acid literature (I. Mav, M. Zigon, *Polym. Bull.* 45 (2000) 61-68.). In ^{13}C NMR we observed sharp signals (100 MHz, d^6-DMSO with 15 (mol.) % of triethylamine, δ, ppm: 114.0, 115.5, 119.4, 128.8, 135.7, 136.2, 165.2, 167.3, 167.5, 168.9, 169.7, 172.6 and 174.3). According to HSQC spectrum (Figure S5b) we can assign carbons in spectral area 113 - 137 ppm to C-H groups in polymer main chain. Signals in the spectral region 165 – 175 ppm could be ascribed to the quaternary carbons belonging to either C-N groups in the polymer main chain or maybe to C-OH groups pendant on the

polymer main chain or maybe to C-O-C groups in polymer main chain. Unfortunately, it is not possible to prove a presence of self-doping groups attached to the polymer main chain due to the complexity of HMBC spectrum, which didn't allow detailed assignment.

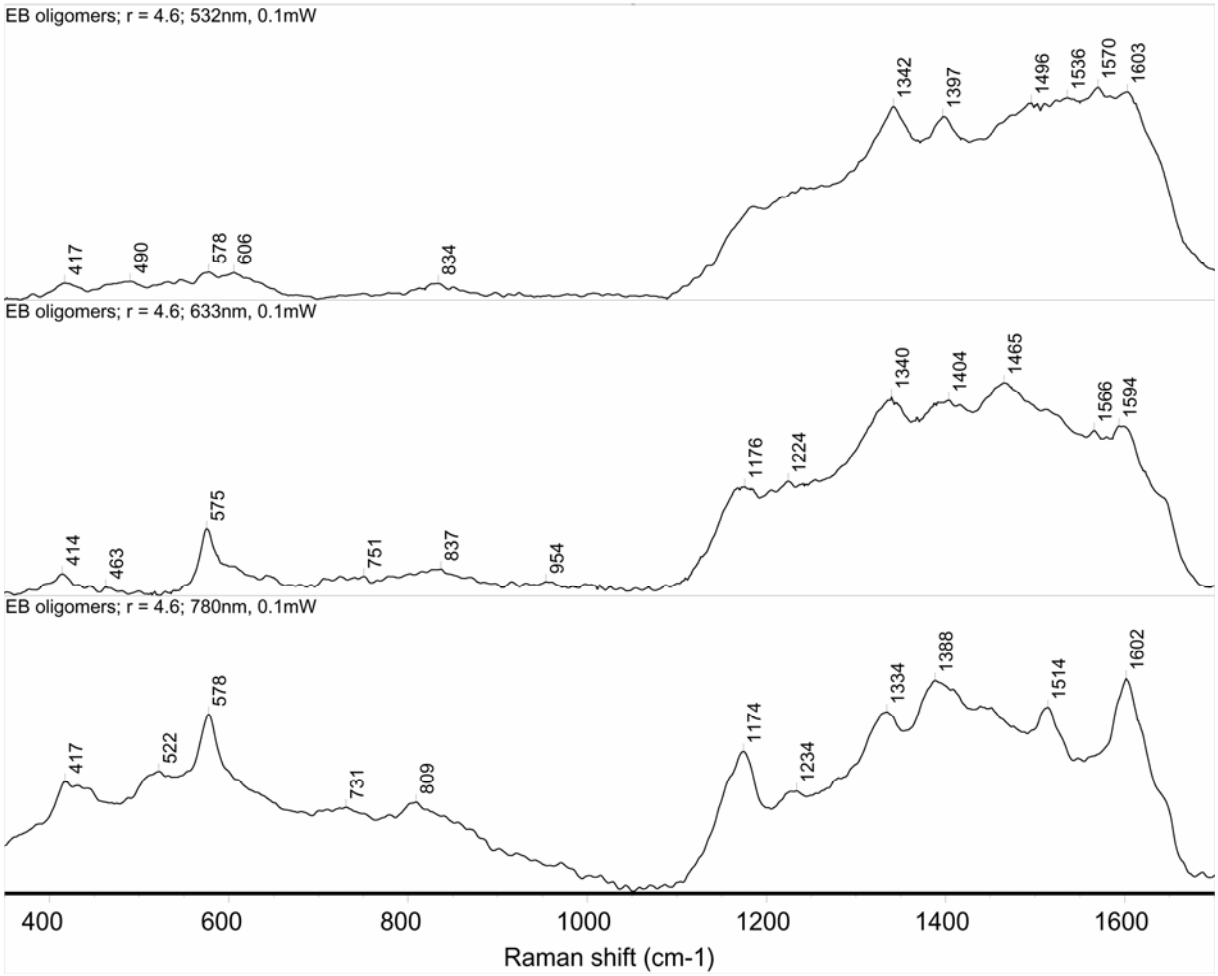

Fig. S6. Raman spectra of EB form (gained by treatment of ES form with sixfold stoichiometric excess of 0.2 M aqueous ammonia) of PANI oligomers prepared with the Fe^{3+}/H_2O_2 catalyst system at r = 4.6; measured at 532, 633 and 780 nm excitation wavelength.

Příloha C:

Mav-Golež I., Pahovnik D., Bláha M., Žigon M., Vohlídal J.: *Copolymers of 2-methoxyaniline with 2- and 3-aminobenzenesulfonic and 2- and 3-aminobenzoic acids: Relationships between the polymerization conditions, structure, spectroscopic characteristics and conductivity*, Synthetic Metals 161 (17-18): 1845-1855, **2011**.

Synthetic Metals 161 (2011) 1845–1855

Contents lists available at ScienceDirect

Synthetic Metals

journal homepage: www.elsevier.com/locate/synmet

Copolymers of 2-methoxyaniline with 2- and 3-aminobenzenesulfonic and 2- and 3-aminobenzoic acids: Relationships between the polymerization conditions, structure, spectroscopic characteristics and conductivity

Ida Mav-Golež[a], David Pahovnik[a], Michal Bláha[b], Majda Žigon[a,*], Jiří Vohlídal[b,**]

[a] Laboratory for Polymer Chemistry and Technology, National Institute of Chemistry, Hajdrihova 19, 1000 Ljubljana, Slovenia
[b] Charles University in Prague, Faculty of Science, Department of Physical and Macromolecular Chemistry, Hlavova 2030, CZ-128 40, Prague 2, Czech Republic

ARTICLE INFO

Article history:
Received 13 April 2011
Received in revised form 10 June 2011
Accepted 17 June 2011
Available online 16 July 2011

Keywords:
Conjugated polymers
Copolymerization
Electrical conductivity
Self-doped polyanilines

ABSTRACT

The effect of the reaction conditions – feed monomer ratio, oxidant/monomers ratio, reaction time, reaction temperature, T, and HCl concentration – on the structure, conductivity and spectra of partly self-doped copolymers of 2-methoxyaniline (OMA) with the anilinic acids (ANIA) 2- and 3-aminobenzoic and the 2- and 3-aminobenzenesulfonic acids was studied using ICP-AES/elemental analysis, size exclusion chromatography, NMR, FT-IR, UV–vis and impedance spectroscopy. The molar fraction of the OMA units, F_1, in a P(OMA/ANIA) copolymer always exceeded the OMA fraction, f_1, in the feed monomer mixture since the OMA is much more reactive than any ANIA due to the electron-donating effect of the methoxy group. Increasing f_1 consistently increased the yield and the molecular weight (MW) of the P(OMA/ANIA), and with an under-stoichiometric amount of oxidant or a shortened reaction time this favored the incorporation of the OMA into the copolymer chains. Increasing the acidity of the reaction mixture increased the yield, MW and F_1 of the P(OMA/ANIA)s, while increasing T gave just the opposite effects. The unusual decrease in the yield (reaction rate) with an increase in the T was related to the increased population of low-reactivity ANIA units at the growing-chain-end positions. The electrical conductivity, σ, of the P(OMA/ANIA)s lies in the region typical for semiconductors (0.05–2.5 mS/cm) and is roughly an exponential growth function of F_1 that differs significantly for P(OMA/ANIA)s with sulfonic and carboxylic groups. In contrast, a conjoint correlation for all P(OMA/ANIA)s was found between σ and the relative intensity of the UV/vis Q-band. The decrease in σ with the increasing fraction of ANIA units in the P(OMA/ANIA) is in accord with the electrostatic binding of positive polarons and bipolarons (electronic charge carries) with immobilized counter-anions.

1. Introduction

Polyaniline (PANI) is an environmentally stable conducting functional polymer [1,2] with excellent electric, magnetic, and optical properties that has attracted considerable attention because of its high application potential. The oxidation state and the proton doping level (Scheme 1) are key factors affecting the electrical conductivity, σ, and other functional properties that are important for the practical applications of PANI [3–5]. The unsubstituted PANI is insoluble or sparingly soluble in almost all solvents and neither can it be processed thermally. Therefore, there is a widespread interest in the development of a more easily processable substituted PANI based on substituents attached to the main chains, which are known to decrease the conductivity of the PANI [6].

One of the most commonly prepared substituted PANIs is polymer of 2-methoxyaniline (OMA) since this monomer is more reactive than aniline in oxidative polymerization and its homopolymer shows good solubility in organic solvents and a good electrical conductivity [7–14]. Besides OMA, anilines carrying acidic side groups are of particular interest as these groups can also act as internal proton-doping agents; therefore, PANIs of this class are called self-doped PANIs. The emeraldine salt (ES) form (Scheme 1) of a self-doped PANI is usually doped internally by the acidic side groups linked to PANI chains, as well as externally by an added acid (mostly the one used in the preparation of the PANI). The electrical conductivity, σ, of a self-doped PANI-ES is lower than that of externally doped PANIs; however, it does not drop so dramatically with an increase in the pH, as is typical of externally doped PANIs. A drop in σ from $\sim 10^0$ to $\sim 10^{-10}$ S/cm is usually observed for PANI with the ES to emeraldine base (EB) transfor-

* Corresponding author. Tel.: +386 1 4760 205; fax: +386 1 4760 300.
** Corresponding author. Tel.: +420 2 2195 1310; fax: +420 2 2491 9752.
E-mail addresses: majda.zigon@ki.si (M. Žigon), vohlidal@natur.cuni.cz (J. Vohlídal).

0379-6779/$ – see front matter © 2011 Elsevier B.V. All rights reserved.
doi:10.1016/j.synthmet.2011.06.023

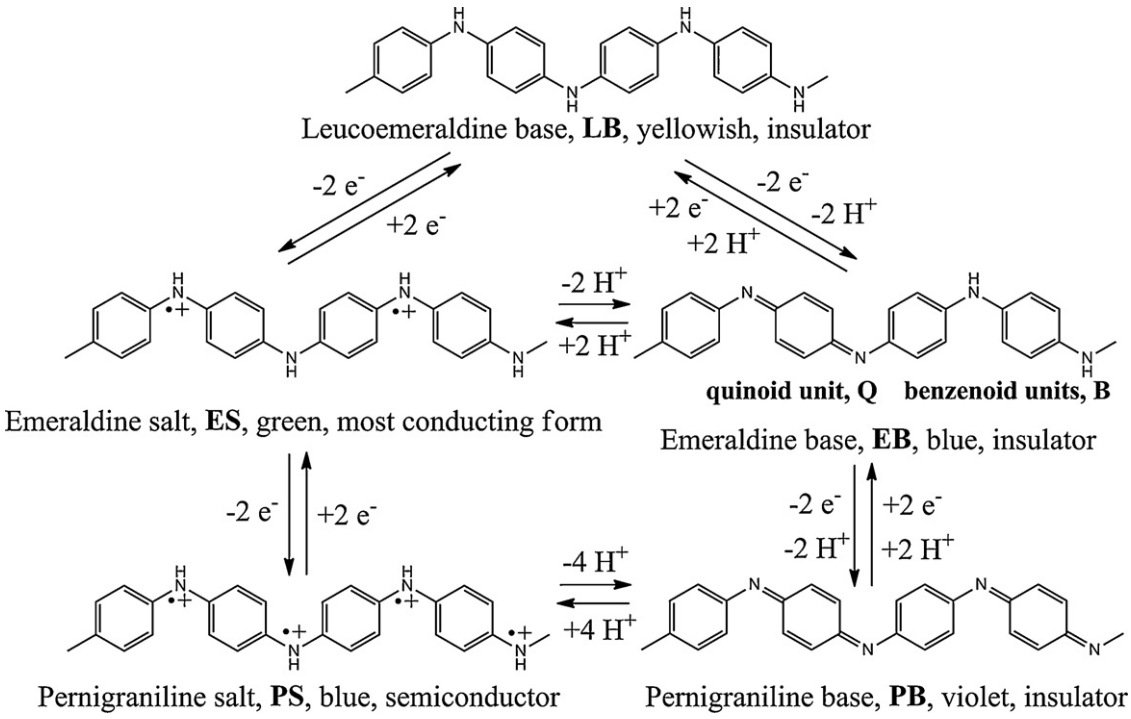

Scheme 1. Distinctive redox and protonic states of a regular PANI chain.

mation, while, for example, the σ of PANI sulfonated to 50% is independent of the external protonation carried out at pH values from 1 to 7 [6,15–18] and PANI sulfonated to approximately 75% shows an almost constant conductivity over the entire pH range of 1–14 [19,20]. The internal proton-doping by acidic groups linked to PANI chains is responsible for this property, which represents a key advantage of self-doped PANIs that opens the way to novel applications for which the leaching of a corrosion-promoting acid is not allowed.

A self-doped PANI can be prepared by a post-polymerization modification of PANI, such as by its sulfonation [6,19–24], or by the homopolymerization of an anilinic acid (ANIA), or the copolymerization of an ANIA with aniline (ANI) or a substituted ANI without an acidic group [25,26]. Unfortunately, the homopolymerization of ANIAs almost never gives a polymer, but only oligomers, owing to the electron-withdrawing effect of the acidic groups [27,28]. A few strategies have been examined to overcome this obstacle. Shimizu et al. used an ANI monomer carrying both the electron-withdrawing and the electron-donating group, 2-methoxyaniline-5-sulfonic acid, which homopolymerized easily [29]. In contrast, Prevost et al. tried to homopolymerize ANIAs with acidic groups linked to benzene rings through an alkoxy spacer, 3-(2-aminophenoxy)propane-1-sulfonic and 4-(2-aminophenoxy)butane-4-sulfonic acids; however, without success [30]. So far the most effective preparative pathway to self-doped PANIs is the copolymerization of a commercially available ANIA with aniline (ANI) [27,28,31–41] or its derivative, such as alkyl- or alkoxy-aniline [42–49] or both [50].

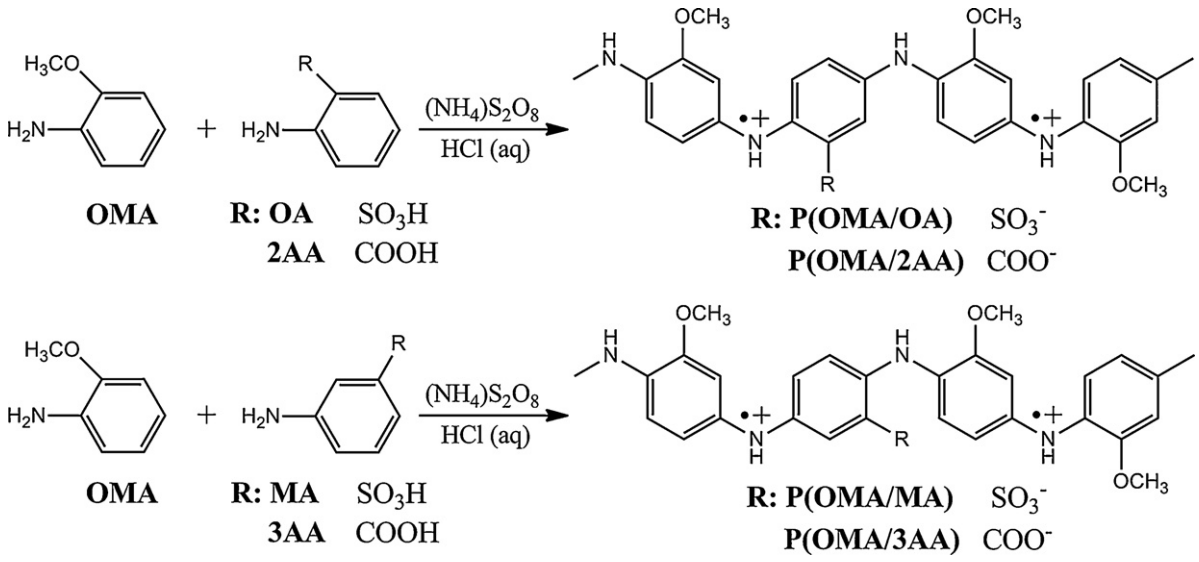

Scheme 2. Studied copolymerizations of OMA and ANIAs; statistical order of monomeric units along copolymer chains is anticipated.

Rao and Sathyanarayana [42] reported an inverse emulsion copolymerization of 3-aminobenzenesulfonic acid (MA) with 2- and 3-methylaniline, giving copolymers that were more conducting than the homopolymers of methylanilines. They also prepared soluble conducting terpolymers of ANI, toluidines and ANIAs – 2-aminobenzoic acid (2AA) or MA – which exhibited a thermostability that is greater than PANI. Lee et al. [34] prepared copolymers of ANI and 2-aminobenzenesulfonic acid (OA) that showed a high degree of crystallinity, a morphology ranging from nanospheres via nanotubes to coral-reef like structures, and a σ from approximately 1 μS/cm to 1 mS/cm. Mav et al. [44–46] copolymerized OMA and various ANIAs with a peroxodisulfate oxidant and exploited the NMR monitoring of the depletion of monomers from the reaction mixture to determine the reactivity ratios of OMA and ANIAs (OA, MA, 2AA and 3AA) (3AA stands for 3-aminobenzoic acid) [47,48]. The reactivity ratios of the ANIAs were found to be about two-to-three orders of magnitude lower than that of OMA.

In the present paper we also report on the chemical copolymerizations of OMA with OA, MA, 2AA and 3AA; however, the reactivity of the monomers is evaluated here on the basis of the composition of the corresponding copolymers – P(OMA/OA), P(OMA/MA), P(OMA/2AA) and P(OMA/3AA) (Scheme 2) – and on the effect of the reaction conditions (OMA/ANIA monomer ratio, oxidant/monomers ratio, concentration of HCl, reaction temperature, reaction time) on the copolymer yield, the molecular weight, the composition, the structure, the electrical conductivity and the spectroscopic characteristics.

2. Experimental

2.1. Synthesis of copolymers, variation of the reaction conditions

All the chemicals were of AR grade and used as supplied. The copolymerizations of the OMA (2-methoxyaniline, Aldrich) with the OA (2-aminobenzenesulfonic acid, Fluka), the MA (3-aminobenzenesulfonic acid, Aldrich), the 2AA (2-aminobenzoic acid, Fluka), and the 3AA (3-aminobenzoic acid, Fluka) were carried out in aqueous hydrochloric acid (HCl, Merck) using ammonium peroxodisulfate ($(NH_4)_2S_2O_8$, Fluka) as an oxidant. A weighed amount of the oxidant was dissolved in aqueous HCl (1 mol/l, 100 ml) and the solution formed was added to a stirred aqueous HCl solution (700 ml) of the OMA and the particular ANIA monomer (0.1 mol in total) of a chosen composition (Tables 1 and 2). The resulting reaction mixture was allowed to react under stirring for 2–20 h (Tables 1 and 2). After an induction period (10–15 min) the light-orange starting mixture turned dark-red to purple and a precipitate started to form. After a certain time the polymer precipitate was filtered off, extensively washed, first with aqueous HCl (1 mol/l, 1 l in total) and then with methanol (up to 250 ml in total), until the filtrate obtained was colorless, to remove all the unreacted monomers and oligomers. The purified dark-green (color typical of ES) polymer was dried in a vacuum oven at 40 °C for 48 h.

The reference reaction conditions were set as follows: total concentration of monomers, 0.1 mol/l; molar fraction of OMA in feed monomer mixture, $f_1 = 0.5$; oxidant/monomer(s) ratio, ox/mon = 1; aqueous HCl (1 mol/l); reaction temperature, $T = 20$ °C; and polymerization time, 20 h. When studying the effect of particular reaction conditions, all the other conditions were kept at the reference values. The value of f_1 was varied from $f_1 = 0$ (homopolymerization of particular ANIA) to $f_1 = 1$ (homopolymerization of OMA) in six steps (Table 2). The other parameters were examined using only two additional values: ox/mon = 0.25 and 2; [HCl] = 0.5 and 1.5 mol/l; reaction temperature $T = 10$ °C and 30 °C and the polymerization time $t = 2$ and 5 h.

Table 1
Comparison of characteristics of ANI/ANIA and OMA/ANIA copolymers and PANI, POMA, P2AA homopolymers; Y is isolated polymer yield, M_w weight-average molecular weight, $Đ = M_w/M_n$ dispersity and σ electric conductivity. All polymers were prepared under reference reaction conditions: ox/mon = 1, $T = 20$ °C, $t_r = 20$ h, [HCl] = 1 mol/dm^3; for copolymers: $f_1 = 0.5$.

Polymer	Y %	M_w g/mol	D	σ mS/cm
PANI	93	31 800	3.2	67
P(ANI/OA)	54	12 000	2.8	6.5
P(ANI/MA)	48	8600	2.1	8.5
P(ANI/2AA)	59	6600	4.0	2.4
P(ANI/3AA)	55	3700	2.0	4.4
POMA	84	6250	2.3	2.5
P(OMA/OA)	33	4100	1.7	0.18
P(OMA/MA)	30	3600	1.6	0.22
P(OMA/2AA)	53	2350	1.8	0.22
P(OMA/3AA)	50	2150	1.7	0.15
P2AA	2	1450	1.4	0.05

2.2. Preparation of the emeraldine and leucoemeraldine bases

PANI EB was prepared by deprotonization of the corresponding as-prepared PANI ES by treating it with aqueous ammonia (1 mol/l) for 20 h. The formed PANI EB was filtered and then dried under vacuum at 40 °C. PANI LB was prepared by reduction of the corresponding PANI ES (1 g) with hydrazine hydrate (20 g) under argon. PANI ES was dispersed in hydrazine hydrate in an ultrasound bath (for 15 min) and the resulting suspension was stirred under argon for 20 h. Next, the volatile components of the suspension were evaporated in a vacuum rotary evaporator at 40 °C, and the PANI LB was washed with acetone under argon, dried under vacuum at room temperature and stored under argon prior to measurements.

2.3. Measurements

Size-exclusion chromatography (SEC) was used to determine the apparent (with respect to polyvinylpyridine, PVP, standards) weight-average, M_w, and number-average, M_n, molecular weights and the dispersity [51], $Đ = M_w/M_n$, of the polymers prepared (Tables 1 and 2). The measurements were made on a modular chromatograph composed of a Waters 510 pump and a UV diode-array detector (Perkin Elmer LC 235) using two μ-Styragel (Waters Associates) columns with a nominal pore size of 10^4 Å and 10^3 Å covering the molecular-weight ranges 5000–600,000 and 200–30,000, respectively, and *N,N*-dimethylacetamide (DMA, Aldrich) with added LiCl (Kemika Zagreb, 0.5%, w/w) as a mobile phase (flow rate 1 ml/min). The system was calibrated with PVP standards (2900–240,000, Polymer Laboratories, Ltd.). The SEC records were taken at a wavelength of 320 nm for the PANIs and 270 nm for the PVP. An analyzed solution was prepared by dissolving the as-prepared copolymer sample (1 mg) in the mobile phase (4 ml) (mixing for 20 h was applied) and filtering the solution through a 0.2-μm Teflon filter. The injection volume was 10 μl.

The FTIR spectra of the PANIs were recorded on a Perkin-Elmer FTIR 1725X spectrometer using KBr-diluted samples pressed into pellets; 5 scans and resolution of 8 cm^{-1} were used. The UV/vis absorption spectra of the polymer solutions (0.02%) were recorded on a Hewlett Packard 8452 diode-array instrument using quartz cuvettes with an optical path of 0.2 cm. A mixture of 1-methylpyrrolidin-2-one (NMP) and triethylamine (TEA) (0.5%) was used as the solvent in which PANIs are in the EB state, while DMSO was used as a solvent in which the ES forms of PANIs are preserved [46]. The spectra were measured using as-prepared samples and so their oxidation state corresponds to that one resulting from the synthesis procedure.

Table 2
Characteristics of P(OMA/ANIA)s prepared under various conditions; f_1 is the feed molar fraction of OMA; ox/mon molar ration oxidant-to-monomer(s), t_r reaction time; T reaction temperature; Y isolated yield; S/N molar ratio of sulfur and nitrogen atoms in the copolymer; F_1 mole fraction of OMA units in the copolymer as obtained by the ICP-AES and NMR analyses; M_w weight-average molecular weight; $Đ = M_w/M_n$ dispersity and σ electrical conductivity.

Sample	Polymerization conditions						Composition and characersitics					
	f_1	$\frac{ox}{mon}$	t_r h	T °C	[HCl] mol/dm^3	Y %	S/N ICP-AES	F_1	F_1 NMR	M_w	$Đ$	σ mS/cm
(a) P(OMA/OA)												
POA	0	1	20	20	1	0	–	–	–	–	–	–
P(OMA/OA)-1	0.20	1	20	20	1	6	0.53	0.47	0.50	3400	1.7	0.077
P(OMA/OA)-2	0.33	1	20	20	1	24	0.36	0.64	0.65	3850	1.7	0.076
P(OMA/OA)-3*	0.5	1	20	20	1	33	0.28	0.72	0.71	4100	1.7	0.18
P(OMA/OA)-4	0.66	1	20	20	1	40	0.19	0.81	0.80	4200	1.9	0.60
P(OMA/OA)-5	0.8	1	20	20	1	53	0.11	0.89	0.90	5200	2.1	2.00
POMA	1.0	1	20	20	1	84	<0.006	>0.994	1	6250	2.3	2.5
P(OMA/OA)-6	0.5	0.25	20	20	1	14	0.15	0.85	0.85	5750	2.8	0.71
P(OMA/OA)-7	0.5	2	20	20	1	30	0.29	0.71	0.70	4050	1.6	0.16
P(OMA/OA)-8	0.5	1	20	10	1	45	0.17	0.83	0.81	4300	1.7	0.61
P(OMA/OA)-9	0.5	1	20	30	1	19	0.29	0.71	0.73	2750	1.6	0.15
P(OMA/OA)-10	0.5	1	2	20	1	21	0.25	0.75	0.76	2350	1.6	0.11
P(OMA/OA)-11	0.5	1	5	20	1	25	0.26	0.74	0.74	3550	1.6	0.18
P(OMA/OA)-12	0.5	1	20	20	0.5	18	0.30	0.70	0.69	4000	1.7	0.18
P(OMA/OA)-13	0.5	1	20	20	1.5	38	0.22	0.78	0.77	4050	1.7	0.31

Sample	Polymerization conditions						Composition and characersitics					
	f_1	$\frac{ox}{mon}$	t_r h	T °C	[HCl] mol/dm^3	Y %	S/N ICP-AES	F_1	F_1 NMR	M_w	$Đ$	σ mS/cm
(b) P(OMA/MA)												
PMA	0	1	20	20	1	0	–	–	–	–	–	–
P(OMA/MA)-1	0.20	1	20	20	1	3	0.32	0.68	0.67	2450	2.0	0.084
P(OMA/MA)-2	0.33	1	20	20	1	15	0.27	0.73	0.77	3500	1.5	0.15
P(OMA/MA)-3*	0.5	1	20	20	1	30	0.20	0.80	0.80	3600	1.6	0.22
P(OMA/MA)-4	0.66	1	20	20	1	36	0.12	0.88	0.87	4000	1.8	0.72
P(OMA/MA)-5	0.8	1	20	20	1	39	0.06	0.94	0.92	4100	1.7	2.5
POMA	1.0	1	20	20	1	84	<0.006	>0.994	1	6250	2.3	2.5
P(OMA/MA)-6	0.5	0.25	20	20	1	12	0.11	0.89	0.88	3800	1.5	1.1
P(OMA/MA)-7	0.5	2	20	20	1	29	0.32	0.68	0.65	3450	1.6	0.10
P(OMA/MA)-8	0.5	1	20	10	1	44	0.10	0.90	0.91	3650	1.6	0.33
P(OMA/MA)-9	0.5	1	20	30	1	25	0.23	0.77	0.76	3000	1.7	0.11
P(OMA/MA)-10	0.5	1	2	20	1	20	0.19	0.81	0.85	2150	1.6	0.20
P(OMA/MA)-11	0.5	1	5	20	1	24	0.21	0.79	0.76	3600	1.7	0.23
P(OMA/MA)-12	0.5	1	20	20	0.5	20	0.23	0.77	0.76	3500	1.5	0.20
P(OMA/MA)-13	0.5	1	20	20	1.5	37	0.13	0.87	0.87	4000	1.6	0.39

Sample	Polymerization conditions						Composition and characersitics			
	f_1	$\frac{ox}{mon}$	t_r h	T °C	[HCl] mol/dm^3	Yield %	F_1 NMR	M_w	$Đ$	σ mS/cm
(c) P(OMA/2AA)										
P2AA	0	1	20	20	1	2	0	1450	1.4	0.050
P(OMA/2AA)-1	0.20	1	20	20	1	27	0.45	1550	1.5	0.065
P(OMA/2AA)-2	0.33	1	20	20	1	35	0.54	1750	1.6	0.16
P(OMA/2AA)-3*	0.5	1	20	20	1	53	0.65	2350	1.8	0.22
P(OMA/2AA)-4	0.66	1	20	20	1	58	0.76	3200	1.8	1.1
P(OMA/2AA)-5	0.8	1	20	20	1	72	0.86	3750	1.8	1.4
POMA	1.0	1	20	20	1	84	1	6250	2.3	2.5
P(OMA/2AA)-6	0.5	0.25	20	20	1	18	0.81	3500	1.7	1.8
P(OMA/2AA)-7	0.5	2	20	20	1	56	0.51	1700	1.5	0.095
P(OMA/2AA)-8	0.5	1	20	10	1	67	0.87	3050	1.8	0.55
P(OMA/2AA)-9	0.5	1	20	30	1	29	0.6	2300	1.7	0.20
P(OMA/2AA)-10	0.5	1	2	20	1	45	0.7	1850	1.6	0.090
P(OMA/2AA)-11	0.5	1	5	20	1	48	0.68	2350	1.8	0.16
P(OMA/2AA)-12	0.5	1	20	20	0.5	44	0.6	2150	1.7	0.14
P(OMA/2AA)-13	0.5	1	20	20	1.5	58	0.77	2500	1.8	0.35

Sample	Polymerization conditions						Composition and characersitics			
	f_1	$\frac{ox}{mon}$	t_r h	T °C	[HCl] mol/dm^3	Yield %	F_1 NMR	M_w	$Đ$	σ mS/cm
(d) P(OMA/3AA)										
P3AA	0	1	20	20	1	0	–	–	–	–
P(OMA/3AA)-1	0.20	1	20	20	1	20	0.5	1250	1.4	0.063
P(OMA/3AA)-2	0.33	1	20	20	1	30	0.59	1350	1.4	0.060
P(OMA/3AA)-3*	0.5	1	20	20	1	50	0.75	2150	1.7	0.15
P(OMA/3AA)-4	0.66	1	20	20	1	55	0.84	3100	1.7	0.56
P(OMA/3AA)-5	0.8	1	20	20	1	60	0.9	3800	1.7	1.7

Table 2 (*Continued*)

Sample	Polymerization conditions						Composition and charactersitics			
	f_1	$\frac{ox}{mon}$	t_r h	T °C	[HCl] mol/dm^3	Yield %	F_1 NMR	M_w	Đ	σ mS/cm
POMA	1.0	1	20	20	1	84	1	6250	2.3	2.5
P(OMA/3AA)-6	0.5	0.25	20	20	1	19	0.88	3100	1.8	1.2
P(OMA/3AA)-7	0.5	2	20	20	1	60	0.52	1400	1.5	0.080
P(OMA/3AA)-8	0.5	1	20	10	1	57	0.90	2850	1.6	0.54
P(OMA/3AA)-9	0.5	1	20	30	1	24	0.71	1700	1.6	0.11
P(OMA/3AA)-10	0.5	1	2	20	1	35	0.78	1350	1.4	0.09
P(OMA/3AA)-11	0.5	1		20	1	44	0.775	1900	1.7	0.13
P(OMA/3AA)-12	0.5	1	7.0	20	0.5	42	0.65	1750	1.6	0.14
P(OMA/3AA)-13	0.5	1	20	20	1.5	61	0.775	2200	1.7	0.34

* Reference copolymerization conditions.

The NMR spectra were recorded on a Varian VXR 300-MHz spectrometer at 25 °C using the following parameters: (for ^{1}H NMR spectra) 45° pulse, relaxation delay 3 s, acquisition time 4 s, 500 repetitions (1 h); and (for ^{13}C NMR spectra) 90° pulse, relaxation delay of 2 s, acquisition time 1.637 s, up to 45,000 repetitions (45 h). Polymer solutions (10%, w/v) in the mixture of NMP, TEA and dimethylsulfoxide (DMSO-d_6) of volume ratios 70:10:20 were used; they were prepared under argon in the case of the LB forms. TEA was added to increase the polymer solubility by transforming the ES into the EB form. The ^{1}H NMR spectra were referenced to tetramethylsilane, while the ^{13}C NMR spectra were referenced to the DMSO signal.

The electrical conductance measurements were made on as-prepared PANIs ES samples pressed into pellets (diameter 13 mm, thickness 1–5 mm) that were coated with a carbon paste and placed between two copper wires connected to the Electrochemical Interface 1286 of a Solarton system equipped with a Frequency Response Analyzer 1250. The conductance of a sample was determined from the impedance response measured at excitation frequencies in the range from 20 to 10^7 Hz at room temperature.

2.4. Determination of the compositions of copolymers

The molar fraction of OMA units built into the particular copolymer, F_1, was determined from the ratio of the integral intensities of the ^{1}H NMR signals of the aromatic (around 7 ppm) and methoxy protons (around 3.7 ppm). In addition, we determined the content of nitrogen and sulfur in the P(OMA/OA) and P(OMA/MA) copolymers using a current analyzer CE440 LeemanLabs (CHN) for nitrogen and the ICP-AES method on an Atomcsan 25 (Thermo Jarrell Ash) instrument for sulfur. These data provided us with a value for the sulfur-to-nitrogen mole ratio (S/N) in a given copolymer, from which the value of F_1 was easily calculated. Good agreement was obtained for the F_1 values determined from the S/N ratios and those obtained from the NMR measurements (Table 2a and b).

3. Results and discussion

3.1. IR spectra and composition of the P(OMA/ANIA) copolymers

The fingerprint regions of the selected IR spectra of the P(OMA/OA) and P(OMA/2AA) ES forms prepared using different feed molar fractions of the OMA, f_1, are shown in Fig. 1. The presence of OA units in the P(OMA/OA) copolymers is documented in their IR spectra, mainly by the presence of the bands of deformation modes at 615, 705 and 770 cm^{-1}; the corresponding bands of the MA units in the P(OMA/MA) copolymers occur at 625, 682, 705 and 805 cm^{-1} (all these bands are also present in the IR spectra of OA and MA). In addition, the spectra of the OA- and MA-rich copolymers show a shoulder at approximately 1640 cm^{-1}, which broadens the band of the benzenoid-ring stretching modes. The presence of the 2AA and 3AA units in the P(OMA/2AA) and P(OMA/3AA) is evidenced by the presence of IR bands at 1695–1660 cm^{-1} ($\nu_{C=O}$ in COOH), 1520 cm^{-1} (ν_{C-CO}), 1375 (2AA) to 1400 cm^{-1} (3AA) (ν_{C-N}), and bands of the deformation modes at approximately 770–750 cm^{-1}. The increased content of OMA units in a copolymer is reflected in a decrease in the intensity of the IR bands typical of ANIA units and the enhancement of bands at 1494 cm^{-1} (typical of ν_{C-N} in PANI-ES), 1296 (ν_{C-N}), 1258 ($\nu_{C-NH^{\bullet}+}$), 1175 (δ_{C-H}) and 1125 cm^{-1} (typical of PANIs with delocalized electrons) [52–55]. In the case of P(OMA/2AA) and P(OMA/3AA) the bands at 1210 and 1017 cm^{-1} are also enhanced. The IR spectra of the copolymers prepared using various ox/mon ratios (Fig. 2) only reflect the changes in the composition of the copolymers; no additional structural feature is apparent from them. The same is true for the spectra of the polymers prepared using various reaction times, T, and $[HCl]_0$. In general, the IR spectra provide plausible semi-quantitative information on the structure of the as-prepared P(OMA/ANIA)s that can be utilized for a rapid, reliable assessment of the composition of these copolymers.

3.2. Reactivity of OMA and ANIAs in oxidative polymerization

The homopolymerization of the OMA was relatively fast and gave only a slightly lower yield (Y = 84%) of POMA with a markedly lower molecular weight (M_w = 6250) than the homopolymerization of ANI (93%, M_w = 31,800) under the same reference conditions: ox/mon = 1; $[HCl]_0$ = 1 mol/l; T = 20 °C; and t_r = 20 h (Table 1). The POMA formed contained traces of sulfur (S/N ≅ 0.5%), obviously due to the partial external doping and/or sulfonation of the main-chain benzene rings with H_2SO_4 (formed as byproduct) [56]. Of all the ANIAs tested, only 2AA homopolymerized under reference conditions, but the yield (Y = 2%), as well as the molecular weight (M_w = 1450) of the isolated P2AA was low. Only a slight, or no, coloration of the reaction mixture appeared during attempts to homopolymerize the 3AA, OA and MA.

All the ANIAs copolymerized with OMA and ANI to give the corresponding copolymers for which better solubility, higher thermal stability and lower pH dependency of the conductivity is expected compared to externally doped homopolymers [15,18,22,27]. The Y and M_w values obtained for the P(OMA/ANIA)s were always lower than the values found for their P(ANI/ANIA) counterparts (Table 1), obviously due to the steric effects of the CH_3O group in the OMA (Table 1). The difference in Y is mainly given by the type of acidic group: it is remarkable for copolymers of sulfonic ANIAs, ANI-SO_3H (OA and MA): $Y \sim 50\%$ (ANI copolymers); $Y \sim 30\%$ (OMA copolymers) but low for copolymers of carboxylic ANIAs, ANI-COOH (2AA and 3AA): $Y \sim 55\%$ (ANI copolymers); $Y \sim 50\%$ (OMA copolymers). In contrast, the copolymer M_w value is mainly controlled by the non-acidic co-monomer ($M_{w,ANI} > M_{w,OMA}$) and only secondarily by the

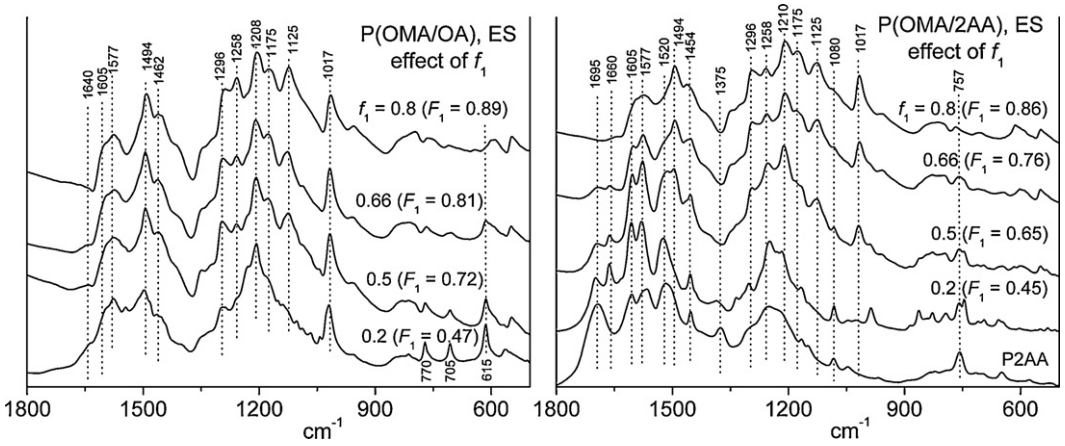

Fig. 1. IR spectra of selected P(OMA/OA) and P(OMA/2AA) copolymers prepared at various feed molar fractions of OMA, f_1; F_1 is the fraction of OMA units in the resulting copolymer.

type and position of the ANIA acidic group: (i) $M_{w,SO3H} > M_{w,COOH}$, and (ii) $M_{w,2\text{-deriv}} > M_{w,3\text{-deriv}}$.

3.3. Effect of the OMA feed molar fraction f_1

One cannot construct copolymerization diagrams using the F_1 and f_1 values listed in Table 2 as the F_1 values were obtained on a too-broad range of copolymer yields (from 3% to 72%). Therefore, the values of Y must also be taken into account to analyze these data correctly. Such an analysis is performed in the diagram in Fig. 3a, which shows that: (i) the molar fraction of OMA units in the copolymer chains, F_1, is roughly directly proportional to Y; (ii) increasing the OMA feeding fraction f_1 increases both Y and F_1, and (iii) for each f_1 applied, the extent of the enchainment of the ANIA molecules to the copolymer chains decreases in the sequence 2AA > 3AA > OA > MA. This sequence is more plausibly apparent from Fig. 3b where the amount of substance of ANIA units, N_2, built into the copolymer is correlated with f_1 and Y. The extent of the enchainment of the monomer molecules to copolymer chains reflects the monomer reactivity in the particular copolymerization. Hence, this sequence shows that in the copolymerization with OMA (the most reactive monomer in our systems): (a) ANI-COOH acids are more reactive than ANI-SO_3H acids, which can be attributed to the lower electro-withdrawing effect of the COOH compared with the SO_3H groups; and (b) the *o*-acids are more reactive than the *m*-acids, which can be explained by the lower steric hindrances of the OMA to *o*-acid linkages compared with the OMA to *m*-acid linkages (see Scheme 2). It should be noted that the monomer reactivity sequence observed does not obey the order of the monomer reactivity ratios determined from the kinetic measurements that were based on the ^{1}H NMR monitoring of the monomersĭ depletion from the reaction mixture [47]. This discrepancy might be ascribed to the formation of the oligomers that we washed out during the isolation of our copolymers, while the monomer consumption during the formation of oligomers was attributed to the copolymers in earlier NMR measurements.

The effect of f_1 on the M_w of the formed copolymers should also be analyzed with regard to the copolymer yield. The correlation diagram (Fig. 3c) shows that: (i) the M_w values of ANI-SO_3H copolymers are systematically higher than the values for the corresponding ANI-COOH copolymers, and (ii) that the position of the acidic group has a negligible effect on M_w. This indicates that the nature of the ANIA acidic group strongly influences the growth of the copolymer chains (see below).

3.4. Effects of the reaction time, ox/mon ratio, acidity and temperature of the reaction mixture

The effects of the reaction time, ox/mon ratio, acidity and temperature of the reaction mixture on the isolated yield Y and the characteristics of the P(OMA/ANIA)s (F_1, M_w and σ) are indicated in Fig. 4. With respect to the effect of the reaction time (the first column) it is clear that the major part of a copolymerization (65–85% of the final conversion after 20 h) is always achieved during the first 2 h of the reaction. The next 18 h of the reaction are characterized by a slow decrease in F_1 (about 0.03–0.05) and an increase in M_w

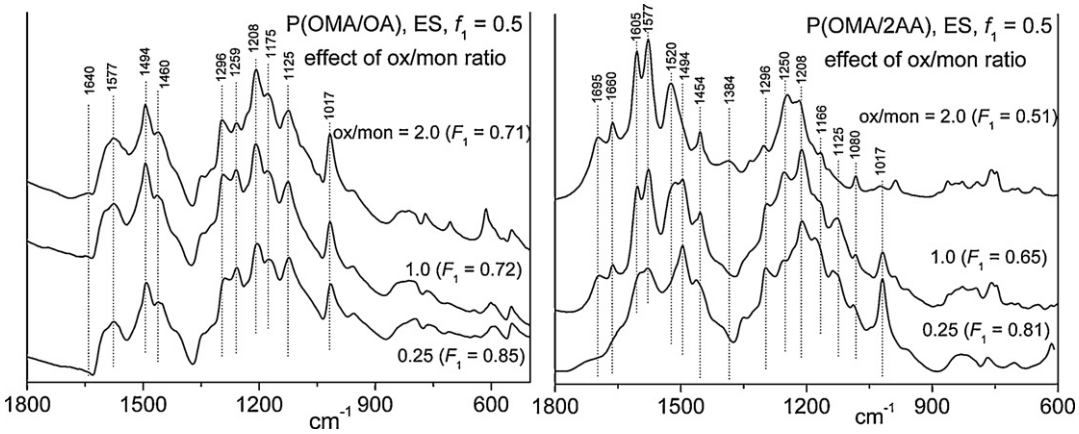

Fig. 2. IR spectra of P(OMA/OA) and P(OMA/2AA) copolymers prepared using various ox/mon ratios; F_1 is the fraction of OMA units in the resulting copolymer.

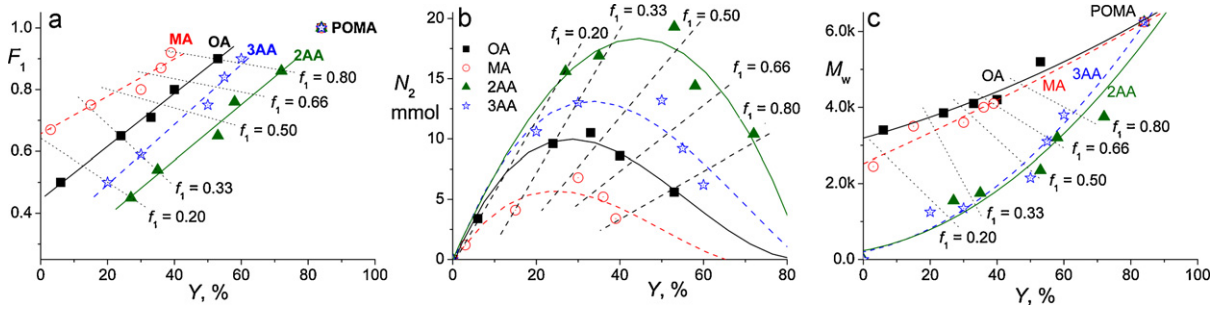

Fig. 3. Correlations among (a) molar fraction of OMA units, F_1, in the copolymer, feed molar fraction of OMA, f_1, and isolated copolymer yield, Y; (b) amount of substance of ANIA units, N_2, built in the isolated copolymer, fraction f_1 and Y; and (c) the weight-average molecular weight, M_w, f_1 and Y for P(OMA/ANIA)s prepared under reference others conditions.

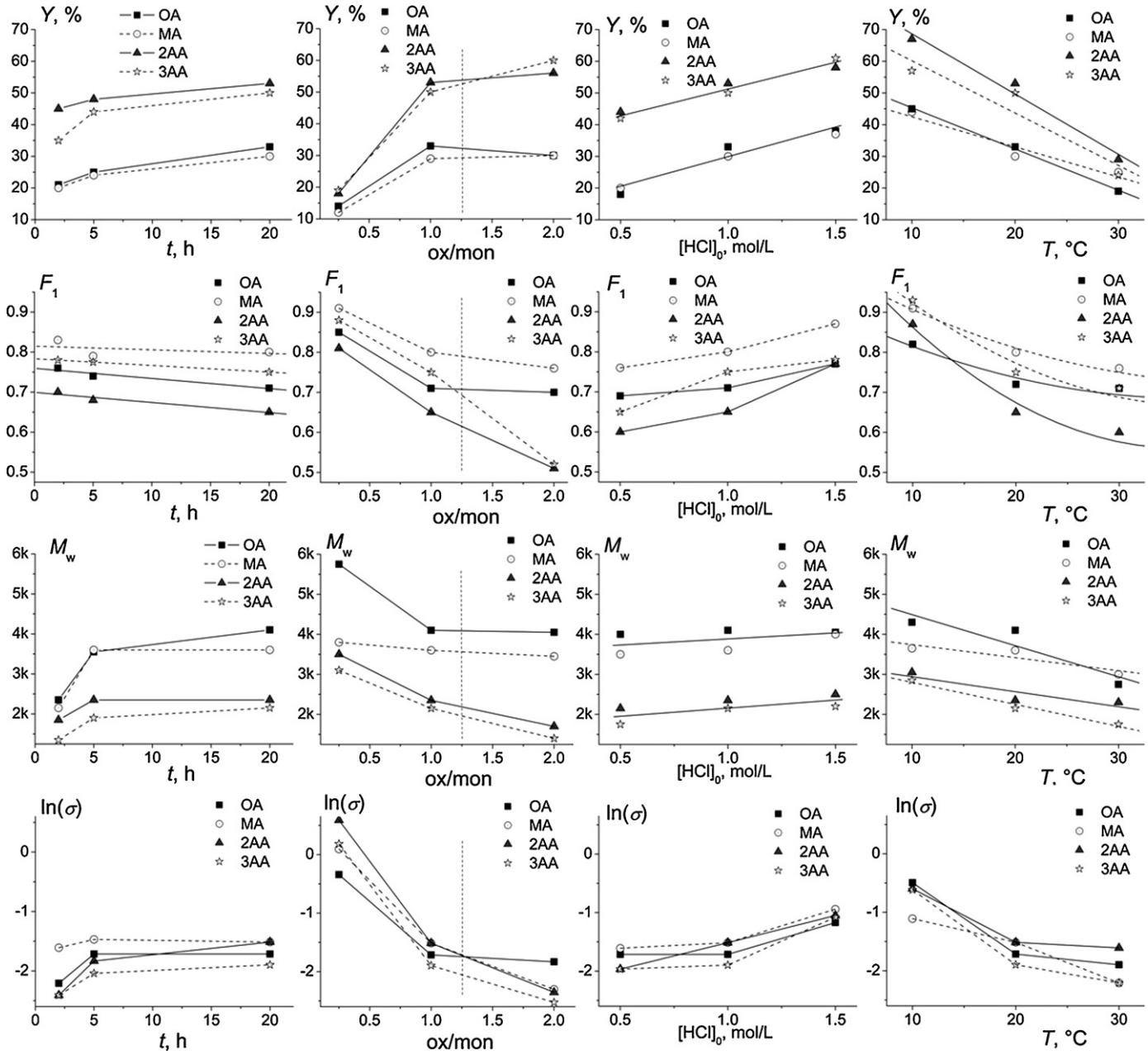

Fig. 4. Effects of the reaction time (1st col.), ox/mon ratio (2nd col.), $[HCl]_0$ (3rd col.), and temperature (4th col.) on the isolated yield Y (1st row), copolymer composition parameter F_1 (2nd row), weight-average molecular weight, M_w, (3rd row), and electrical conductivity, σ in mS/cm, (4th row) of the P(OMA/ANIA) copolymers. Dashed lines in the 2nd column indicate the ideal stoichiometric ratio ox/mon = 1.25.

(about 60% to 75%, except for the 2AA copolymer, $\Delta M_w = 27\%$, for which Y only slightly increased in the second reaction stage). This indicates that any further growth of already-existing chains dominates, while the formation of new ones (initiation) is of marginal importance in the second stage of the polymerization. The observed decreases in the F_1 values are rather low; however, they are related to total samples. The chains or sub-chains created in the second reaction stage are enriched with ANIA units by approximately 15%, which points to the axial composition gradient of the P(OMA/ANIA) chains.

The effects of the ox/mon ratio are shown in the second column in Fig. 4. The changes caused by the increase in the ox/mon ratio from 0.25 to 1.0 are mainly of a stoichiometric origin. The large increase in Y is due to the better stoichiometric balance between the monomers and the oxidant; the decrease in F_1 is due to the necessity of including more ANIA molecules into the copolymer at increased Y, and the decrease in M_w is caused by an increased rate of initiation due to the increased total concentration of the activated monomer species for an increased concentration of the oxidant. The increase in the ox/mon ratio far above the stoichiometric optimum 1.25, to a value of 2.0, only slightly increased the yields of P(OMA/ANIA)s and, interestingly, affected the F_1 and M_w values of the sulfonic and carboxylic copolymers in different ways. Compared to the respective copolymers prepared under reference conditions, the values of F_1 and M_w remained nearly preserved for the P(OMA/ANI-SO_3H)s, but significantly decreased for the P(OMA/ANI-COOH)s. This means that the high ox/mon ratio significantly enhanced the enchainment of the ANIA-COOH, whereas it did not affect the enchainment of the ANI-SO_3H molecules. This observation also proves the higher reactivity of the carboxylic ANIAs compared with the sulfonic ANIAs.

The increasing acidity of the reaction mixture increased the values of all the studied parameters except for the M_w of P(OMA/OA), which remains nearly constant (Fig. 4, third column). A remarkable feature is the simultaneous increases in Y and F_1, which shows that a higher Y is obtained due to the reduced incorporation of ANIA molecules into the copolymer chains. Note that the increase in Y with an increase in the ox/mon ratio is caused by an enhanced enchainment of the ANIA molecules into the copolymer chains.

Increasing the reaction temperature caused changes (Fig. 4, last column) opposite to those caused by increasing $[HCl]_0$: a continuous decrease of all monitored quantities. In other words, a decrease in T has a similar impact to an increase in $[HCl]_0$. Note that also in this case the increase in Y with a decrease in T is caused by an enhanced enchainment of the ANIA molecules into copolymer chains. Perhaps the most interesting effect of T is the relatively sharp decrease in Y (which reflects a decrease in the rate of polymerization) with an increase in T from 10 °C to 30 °C, which strongly contradicts the generally observed increase in the reaction rate with increasing T. A simultaneous decrease in F_1 and M_w (with increasing T) (i) proves the increased enchainment of the ANIA molecules, and (ii) the decreased growth capability of the individual chains. Hence, this unusual behavior appears to be a result of the synergic effect of: (i) an increased enchainment probability of the ANIA molecules at higher T, and (ii) a low propagation activity of the ANIA units occupying the end positions of the growing chains. The low propagation activity of the ANIA units appears to be due to the attached electron-withdrawing acidic groups.

3.5. Electrical conductivity of P(OMA/ANIA)s

The electrical conductivity of POMA ($\sim 10^{-3}$ S/cm) is about three orders of magnitude lower than the σ of PANI ($\sim 10^{0}$ S/cm) due to the steric effects of the methoxy groups. The inclusion of the ANIA units into the POMA chains decreases the conductivity of the copolymers by up to two orders of magnitude (Table 2). The data in Fig. 4 (rows 2 and 4) suggest the existence of a correlation between σ and the fraction of OMA (resp. ANIA) units in the P(OMA/ANIA) chains. An analysis of all the measured σ values revealed a roughly linear dependence of $\ln(\sigma)$ on $(1 - F_1)$, which is significantly different for the ANI-SO_3H and ANI-COOH copolymers (Fig. 5).

PANI ES (Scheme 1) is considered as a mixed electronic and protonic conductor. The electronic charge carriers are positive polarons and bipolarons, and the protonic conductivity is supposed to proceed by a proton-hopping mechanism (the conducting protons are classified as free protons since their binding to imine nitrogens is weak [57,58]). The contribution of the counter-anions to the ionic conductivity of PANI is mostly neglected, though it is important in other ionic conjugated polymers [59,60]; the counter-anions are believed to be closely associated with the doped PANI [57,61] chains. Nevertheless, the counter-anions cannot be immobilized completely; they should diffuse and/or migrate, at least in a restricted volume element, and so be temporarily absent from the positive charge carriers of the PANI chains. This assumption makes it possible to explain the decrease in the conductivity of partly self-doped PANIs with the increasing content of self-doped units. Unlike the free counter-anions in externally doped PANIs, the covalently bound counter-anions in a self-doped PANI cannot move far enough off the positive polarons to make them, temporarily, almost free. Therefore, the anchored counter-anions progressively decrease the mobility of the polarons and, as a consequence, the conductivity of the self-doped PANIs. Moreover, the interactions of the counter-anions with the polarons can enforce the main chain distortions that further reduce the conductivity of partly self-doped PANIs. Both these effects can significantly contribute to the observed decrease in σ due to an increasing fraction of ANIA units in the P(OMA/ANIA)s.

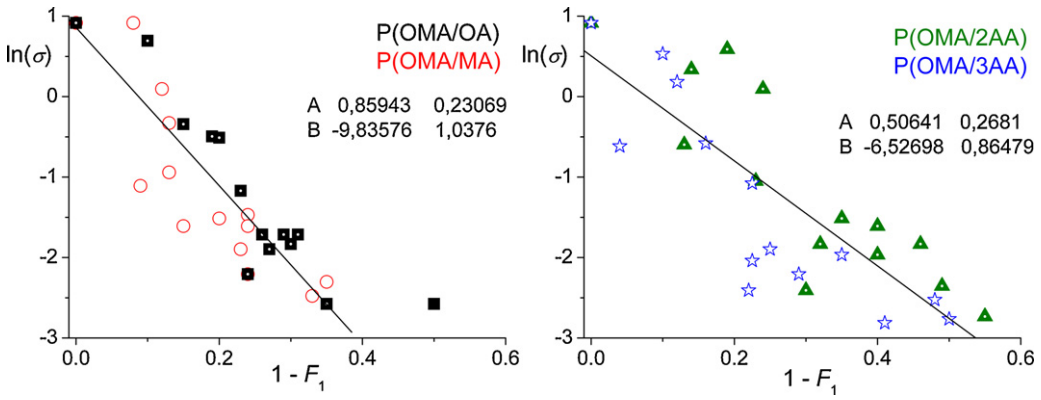

Fig. 5. Electrical conductivity, σ (mS/cm), of P(OMA/ANIA)s as a function of the molar fraction of ANIA units, $(1 - F_1)$, in the copolymer.

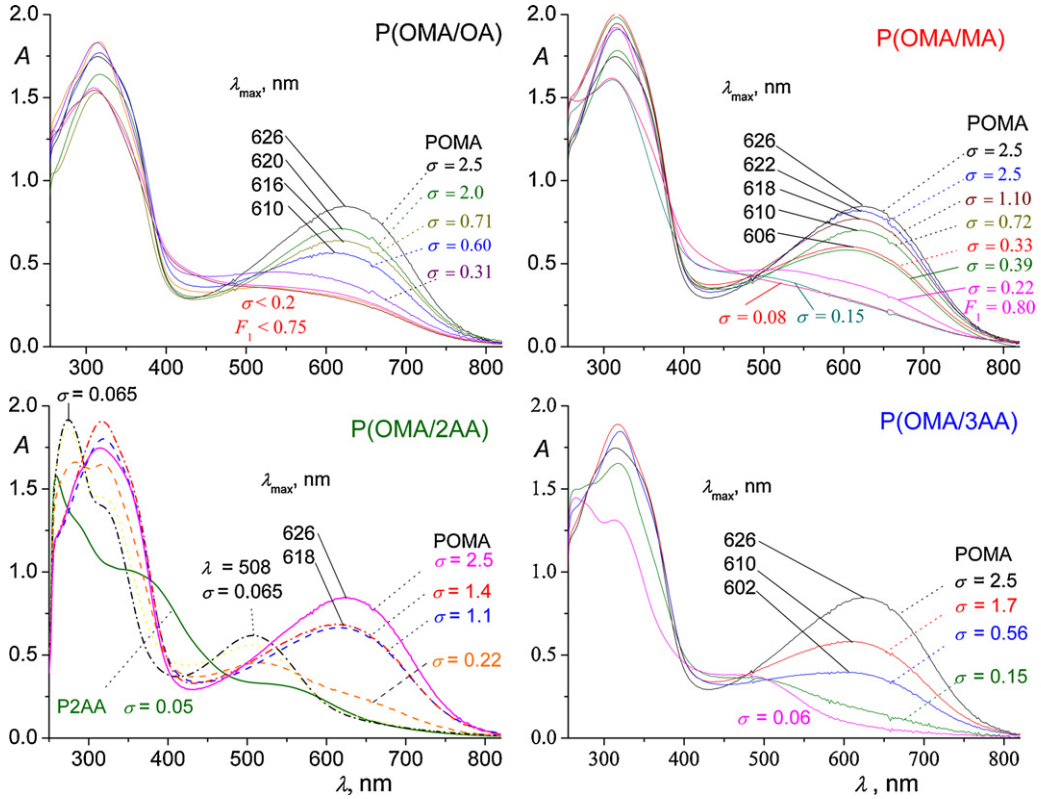

Fig. 6. UV–vis spectra of selected P(OMA/ANIA) copolymers with inserted values of σ (mS/cm).

The steric effects of side groups are also important, since the lowered symmetry reduces the ability of the chains to create crystalline domains, dubbed metallic islands [61–65]. These effects explain the lowered conductivity of the POMA and other not-self-doped ring-substituted PANIs compared to PANI (the decrease factor is typically 10^{-3}). Steric effects should not be that important within our series of copolymers composed exclusively of single-substituted monomeric units. Nevertheless, these effects may lie behind the minor differences in the dependence $\ln\sigma$ vs $(1-F_1)$ for copolymers of different ANIAs. Compared with P(OMA/ANI-COOH), P(OMA/ANI-SO_3H) copolymers exhibit a sharper decrease in $\ln\sigma$ that might be ascribed to the greater bulkiness of the SO_3H compared to the COOH groups. Another possible explanation is that the external doping agent, HCl, partly protonizes the ANIA counter-anions and so weakens their electrostatic binding with positive polarons/bipolarons, which makes the charge carriers more mobile. Compared to sulfonic groups, carboxy groups can be more easily protonized; therefore, the positive charge carriers should be more mobile in the P(OMA/ANI-COOH) compared to the P(OMA/ANI-SO_3H) of the corresponding composition $(1-F_1)$.

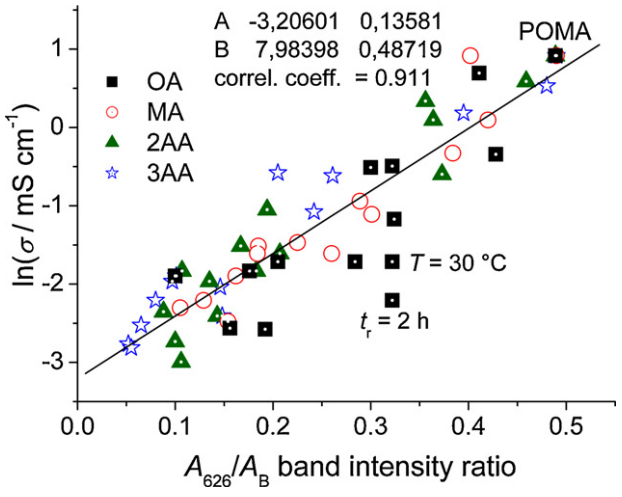

Fig. 7. Semi-logarithmic dependence of the electrical conductivity σ (mS/cm) of P(OMA/ANIA) copolymers on the absorbance ratio of the bands at 602–626 nm (Q-band) and at about 315 nm (B-band).

3.6. UV–vis spectra of P(OMA/ANIA)s

The UV–vis spectrum of POMA EB (Fig. 6) contains the so-called B-band at 315 nm, contributed by the π–π^* transitions in the benzenoid rings, and the Q-band at 626 nm contributed by the transitions in quinone diimine units. For the ideal POMA EB (50% oxidized form), the B/Q band absorbance ratio (A_B/A_Q) is 1.6 [5]. The reduction of POMA from the EB to the LB form does not change the position (λ_{max}) but decreases the Q band intensity; this decrease is usually expressed as an increase in the A_B/A_Q ratio, e.g., $A_B/A_Q \cong 3.5$ for POMA oxidized from 40%. On the other hand, the A_B/A_Q ratio only slightly increases (up to 1.75) if POMA EB is oxidized toward the PB (pernigraniline base) form and, simultaneously, the Q-band shifts toward 560 nm (the band typical of the PB form, which is ascribed to the Peierls gap [5]). Similar spectral changes accompany analogous transformations of the forms of other PANIs.

We found that $A_B/A_Q \cong 2.05$ for our POMA sample, which indicates a slightly under-oxidized EB form (from approximately 48%, which is consistent with a slightly under-stoichiometric amount of oxidant used in our syntheses). An increasing content of ANIA units decreases the intensity and causes a blue shift of the Q-band of the P(OMA/ANIA) (Fig. 6). The observed high values of the A_B/A_Q ratio (up to 8) practically exclude the possibility that our copolymers are

in the PB form ($A_B/A_Q = 1.75$). Besides, there is no band that could be ascribed to the PB form, even in the spectra of copolymers prepared with the largely over-stoichiometric ratio ox/mon = 2. Hence the observed blue shift of the Q-band can be ascribed to the increasing intensity of the band at 500 nm, which is best developed in the spectrum of P(OMA/2AA) ($F_1 = 0.45$). Note that this band is not present in the spectrum of P2AA and so it is not due to long sequences of 2AA units. This band might be ascribed to transitions in self-doped, nearly alternating OMA/ANIA sequences [46]. Accordingly, the observed increase in the A_B/A_Q ratio, as well as the blue shift of Q-band, can be attributed to the self-doping effect of the acidic groups.

UV–vis spectra prove that the P(OMA/ANIA) chains are not in the base form but in a partly protonized form, even in the NMP solution containing TEA. The most striking self-doping effect is observed for P2AA, for which the spectrum in NMP/TEA is almost identical with the spectrum of the as-prepared sample in DMSO [46]. Similar spectral features have been observed for PANIs prepared with a $FeCl_3/H_2O_2$ catalyst system in which the partial self-doping is supposed to originate from phenolic groups formed in side reactions [66]. In summary, the UV–vis spectra indicate that our P(OMA/ANIA) copolymers are in a close-to-emeraldine state and that their chains are permanently partly protonized due to the self-doping effect of the acidic groups anchored on the main-chain benzene rings.

3.7. Correlation between UV–vis spectra and the conductivity of P(OMA/ANIA)s

The values of σ indicated in the spectra shown in Fig. 6 show the existence of a correlation between the copolymer conductivity and its optical absorbance in the Q-band region. Therefore, we have examined a few correlations of this kind and found that the most significant is the correlation between ln σ and the absorbance ratio A_{626}/A_B (Fig. 7) ($\lambda = 626$ nm is the position of the POMA Q-band). Separate dependences for individual P(OMA/ANIA) gave nearly equal values of the linear-fit parameters and the regression coefficients: $R > 0.95$ (except for P(OMA/OA)s, $R = 0.81$, for which some outlying points were found, which are specified in Fig. 7). This correlation suggests that the conductivity of P(OMA/ANIA)s is to a large extent controlled by the content of quinoidal OMA units. This seems reasonable since just quinoid OMA units can be easily externally doped to give ES units of much greater ability to transport polarons than the self-doped ANIA units.

4. Conclusions

We copolymerized OA, MA, 2AA and 3AA with OMA to corresponding copolymers for which a better solubility, higher thermal stability and lower pH dependency of the conductivity compared to externally doped homopolymers is expected. Copolymerizations of OMA with aniline-sulfonic and aniline-carboxylic acids were found to be robust reactions during which all the examined changes of the reaction conditions have a strong impact only on the composition of the formed copolymers. The ability of ANIAs to copolymerize with OMA, as ascertained from the extent of the incorporation of ANIA molecules into copolymer chains, decreases in the order 2AA > 3AA > OA > MA, which is consistent with the electronic and steric effects of the acidic substituents. The large reactivity difference between the OMA and the ANIAs unambiguously favors the enchainment of the OMA over the ANIA molecules. The enchainment of ANIA molecules can be enhanced by: (i) an increase in the ANIA fraction in the feed monomer mixture, (ii) an increase in the reaction temperature, or (iii) a decrease in the acidity of the reaction mixture; in all cases to the detriment of the copolymer yield. The enchainment of the ANIA-COOH molecules is also markedly enhanced by an increase in the ox/mon ratio above the optimum stoichiometric ratio, without a loss in the copolymer yield in this case.

The OMA/ANIA copolymerizations surprisingly exhibit a decrease in the reaction rate (based on the copolymer yield) with an increase in the reaction temperature. This unusual behavior is supposed to be the result of the following two effects: (i) an increased incorporation of ANIA molecules into the copolymer chains (due to increased T), and (ii) a low propagation activity of the ANIA end-units.

The third main output of this work is the identification of a generalized correlation between the electrical conductivity and the absorbance ratio A_{626}/A_B for P(OMA/ANIA) copolymers, which can be potentially exploited for rapid estimates of σ for P(OMA/ANIA)s. In addition, this correlation, together with the σ vs F_1 dependences, points to the importance of the local mobility (diffusion) of counterions for the conductivity of PANIs.

Acknowledgements

The authors gratefully acknowledge the financial support of the Ministry of Higher Education, Science and Technology of the Republic Slovenia and the Slovenian Research Agency (project P2-0145 and bilateral Slovenian-Czech project BI-CZ/07-08/003), Czech Science Foundation (project 104/09/1435 and 203/08/H032) and the Ministry of Education, Youth and Sport of the Czech Republic (project MSM0021620857). The authors thank Prof. Dr. Miran Gaberšček for discussion on the conductivity measurements.

References

[1] M. Baron, K.-H. Hellwich, M. Hess, K. Horie, A.D. Jenkins, R.G. Jones, J. Kahovec, P. Kratochvil, W.V. Metanomski, W. Mormann, R.F.T. Stepto, J. Vohlidal, E.S. Wilks, Pure Appl. Chem. 81 (2009) 1131–1183.
[2] K. Horie, M. Baron, R.B. Fox, J. He, M. Hess, J. Kahovec, T. Kitayama, P. Kubisa, E. Marechal, W. Mormann, R.F.T. Stepto, D. Tabak, J. Vohlidal, E.S. Wilks, W.J. Work, Pure Appl. Chem. 76 (2004) 889–906.
[3] E. Erdem, M. Sacak, M. Karakisla, Polym. Int. 39 (1996) 153–159.
[4] A.R. Hopkins, P.G. Rasmussen, R.A. Basheer, Macromolecules 29 (1996) 7838–7846.
[5] J.E. Albuquerque, L.H.C. Mattoso, D.T. Balogh, R.M. Faria, J.G. Masters, A.G. McDiarmid, Synth. Met. 113 (2000) 19–22.
[6] J. Yue, Z.H. Wang, K.R. Cromack, A.J. Epstein, A.G. MacDiarmid, J. Am. Chem. Soc. 113 (1991) 2665–2671.
[7] M.C. Gupta, S.S. Umare, Macromolecules 25 (1992) 138–142.
[8] L.H.C. Mattoso, R.M. Faria, L.O.S. Bulhoes, A.G. MacDiarmid, J. Polym. Sci. Part A: Polym. Chem. 32 (1994) 2147–2153.
[9] L.H.C. Mattoso, A.G. MacDiarmid, A.J. Epstein, Synth. Met. 68 (1994) 1–11.
[10] L.H.C. Mattoso, S.K. Manohar, A.G. MacDiarmid, A.J. Epstein, J. Polym. Sci. Part A: Polym. Chem. 33 (1995) 1227–1234.
[11] W.A. Gazotti Jr., R. Faez, M.-A. De Paoli, J. Electroanal. Chem. 1–2 (1996) 107–113.
[12] W.A. Gazotti Jr., T. Matencio, M.-A. De Paoli, Electrochim. Acta 43 (1997) 457–464.
[13] J. Han, G. Song, R. Guo, Chem. Mater. 19 (2007) 973–975.
[14] L. Zhang, H. Peng, J. Sui, C. Soeller, P.A. Kilmartin, J. Travas-Sejdic, J. Phys. Chem. C 133 (2009) 9128–9134.
[15] P.A. Kilmartin, G.A. Wright, Synth. Met. 88 (1997) 153–162.
[16] P.A. Kilmartin, G.A. Wright, Synth. Met. 88 (1997) 163–170.
[17] J. Yue, A.J. Epstein, J. Am. Chem. Soc. 112 (1990) 2800–2801.
[18] A. Kitani, K. Satoguchi, H.Q. Tang, S. Ito, K. Sasaki, Synth. Met. 69 (1995) 129–130.
[19] X.L. Wei, Y.Z. Wang, S.M. Long, C. Bobeczko, A.J. Epstein, J. Am. Chem. Soc. 118 (1996) 2545–2555.
[20] X.L. Wei, A.J. Epstein, Synth. Met. 74 (1995) 123–125.
[21] X.L. Wei, M. Fahlman, A.J. Epstein, Macromolecules 32 (1999) 3114–3117.
[22] Q.J. Wu, Z.N. Qi, F.S. Wang, Synth. Met. 105 (1999) 191–194.
[23] J. Yue, G. Gordon, A.J. Epstein, Polymer 33 (1992) 4410–4418.
[24] S. Ho, K. Murata, S. Teshima, R. Aizawa, Y. Asako, K. Takahashi, B.M. Hoffman, Synth. Met. 96 (1998) 161–163.
[25] H.S.O. Chan, A.J. Neuendorf, S.C. Ng, P.M.L. Wong, D.J. Young, Chem. Commun. 13 (1998) 1327–1328.
[26] J.H. Fan, M.X. Wan, D.B. Zhu, J. Polym. Sci. Part B: Polym. Chem. 36 (1998) 3013–3019.
[27] K.G. Neoh, E.T. Kang, K.L. Tan, Synth. Met. 60 (1993) 13–21.
[28] I. Mav, M. Žigon, A. Šebenik, Synth. Met. 101 (1999) 717–718.

[29] S. Shimizu, T. Saitoh, M. Uzawa, M. Yuasa, K. Yano, T. Maruyama, K. Watanabe, Synth. Met. 85 (1997) 1337–1338.
[30] V. Prevost, A. Petit, F. Pla, Synth. Met. 104 (1999) 79–87.
[31] N.A. Rahman, M. Gizdavic-Nikolaidis, S. Ray, A.J. Easteal, J. Travas-Sejdic, Synth. Met. 160 (2010) 2015–2022.
[32] I. Mav, M. Žigon, A. Šebenik, J. Vohlidal, J. Polym. Sci. Part A: Polym. Chem. 38 (2000) 3390–3398.
[33] C.H. Yang, L.R. Huang, Y.K. Chih, W.C. Lin, F.J. Liu, T.L. Wang, Polymer 48 (2007) 3237–3247.
[34] R.H. Lee, H.H. Lai, J.J. Wang, R.J. Jeng, J.J. Lin, Thin Solid Films 517 (2008) 500–505.
[35] G. Li, C. Zhang, H. Peng, K. Chen, Z. Zhang, Macromol. Rapid. Commun. 29 (2008) 1954–1958.
[36] M.T. Nguyen, A.F. Diaz, Macromolecules 28 (1995) 3411–3415.
[37] H.J. Salavagione, D.F. Acevedo, M.C. Miras, A.J. Motheo, C.A. Barbero, J. Polym. Sci. Part A: Polym. Chem. 42 (2004) 5587–5599.
[38] J. Arias-Pardilla, H.J. Salavagione, C.A. Barbero, E. Morallon, J.L. Vazquez, Eur. Polym. J. 42 (2006) 1521–1532.
[39] S.C. Ng, H.S.O. Chan, H.H. Huang, P.K.H. Ho, J. Chem. Soc. Chem. Commun. (1995) 1327–1328.
[40] M.R. Gizdavic-Nikolaidis, Z.D. Zujovic, S. Ray, A.J. Easteal, G.A. Bowmaker, J. Polym. Sci. Part A: Polym. Chem. 48 (2010) 1339–1347.
[41] J.C. Fatuch, M.A. Soto-Oviedo, C.O. Avellaneda, M.F. Franco, W. Romao, M.-A. De Paoli, A.F. Nogueira, Synth. Met. 159 (2009) 2348–2354.
[42] P.S. Rao, D.N. Sathyanarayana, J. Polym. Sci. Part A: Polym. Chem. 40 (2002) 4065–4076.
[43] B.C. Roy, M.D. Gupta, L. Bhoumik, J.K. Ray, Synth. Met. 130 (2002) 27–33.
[44] I. Mav, M. Žigon, Synth. Met. 119 (2001) 145–146.
[45] I. Mav, M. Žigon, Polym. Bull. 45 (2000) 61–68.
[46] I. Mav, M. Žigon, J. Vohlidal, Macromol. Symp. 212 (2004) 307–314.
[47] I. Mav, M. Žigon, Polym. Int. 51 (2002) 1072–1078.
[48] I. Mav, M. Žigon, J. Polym. Sci. Part A: Polym. Chem. 39 (2001) 2482–2493.
[49] P.S. Rao, D.N. Sathyanarayana, Synth. Met. 138 (2003) 519–527.
[50] P. Savitha, D.N. Sathyanarayana, J. Polym. Sci. Part A: Polym. Chem. 43 (2005) 3040–3048.
[51] R.G. Gilbert, M. Hess, A.D. Jenkins, R.G. Jones, R. Kratochvil, R.F.T. Stepto, Pure Appl. Chem. 81 (2009) 351–353.
[52] Y. Furukawa, F. Ueda, Y. Hyodo, I. Harada, T. Nakajima, T. Kawagoe, Macromolecules 21 (1988) 1297–1305.
[53] Z. Ping, J. Chem. Soc. Faraday Trans. 92 (1996) 3063–3067.
[54] W. Zheng, M. Angelopoulos, A.J. Epstein, A.G. MacDiarmid, Macromolecules 30 (1997) 2953–2955.
[55] I. Šeděnková, M. Trchová, N.V. Blinova, J. Stejskal, Thin Solid Films 515 (2006) 1640–1646.
[56] J. Stejskal, D. Hlavata, P. Holler, M. Trchova, J. Prokes, I. Sapurina, Polym. Int. 53 (2004) 294–300.
[57] J. Stejskal, O.E. Bogomolova, N.V. Blinova, M. Trchova, I. Sedenkova, J. Prokes, I. Sapurina, Polym. Int. 58 (2009) 872–879.
[58] A. El Khalki, Ph. Colomban, B. Hennion, Macromolecules 35 (2002) 5203–5211.
[59] D. Bondarev, J. Zedník, I. Šloufová, A. Sharf, M. Procházka, J. Pfleger, J. Vohlídal, J. Polym. Sci. Part A: Polym. Chem. 48 (2010) 3073–3081.
[60] M. Hess, R.G. Jones, J. Kahovec, T. Kitayama, P. Kratochvíl, P. Kubisa, W. Mormann, R.F.T. Stepto, D. Tabak, J. Vohlídal, E.S. Wilks, Pure Appl. Chem. 78 (2006) 2067–2074.
[61] J. Epstein, J.M. Ginder, F. Zuo, R.W. Bigelow, H.S. Woo, D.B. Tanner, A.F. Richter, W.S. Huang, A.G. MacDiarmid, Synth. Met. 18 (1987) 303–309.
[62] J.M. Ginder, A.F. Richter, A.G. MacDiarmid, A.J. Epstein, Solid State Commun. 63 (1987) 97–101.
[63] P.K. Kahol, A.J. Dyakonov, B.J. McCormick, Synth. Met. 84 (1997) 691–694.
[64] A. Raghunathan, P.K. Kahol, B.J. McCormick, Solid State Commun. 108 (1998) 817–822.
[65] F.L. Leite, W.F. Alves, M. Mir, Y.P. Mascarenhas, P.S.P. Herrmann, L.H.C. Mattoso, O.N. Oliviera Jr., Appl. Phys. A 93 (2008) 537–542.
[66] M. Bláha, M. Riesová, J. Zedník, A. Anžlovar, M. Žigon, J. Vohlídal, Synth. Met. 161 (2011) 1217–1225.